

**Quantifying gas phase chlorine compounds in
sewer system headspaces**

by

Xiaoyu Sun

A thesis

presented to the University of Waterloo

in fulfillment of the

thesis requirement for the degree of

Master of Applied Science

in

Civil Engineering

Waterloo, Ontario, Canada, 2024

© Xiaoyu Sun 2024

Author's Declaration

I hereby declare that I am the sole author of this thesis. This is a true copy of the thesis, including any required final revisions, as accepted by my examiners.

I understand that my thesis may be made electronically available to the public.

Abstract

Municipal sewers may receive industrial discharges that contain high levels of sodium hypochlorite (NaOCl). However, most municipalities do not include NaOCl in sewer-use bylaws as the risks associated with these discharges have not been evaluated. In the current study, elevated chlorine gas concentrations were reported by a municipality in the headspace of the wet well of a pumping station when using a commercial chlorine gas sensor. These reports led to concerns about the potential for corrosion and unsafe work environment. This study investigated and modelled chlorine compounds in the headspace of a batch reactor that simulated the discharge of NaOCl to sewer environments. The temporal responses in the gas concentrations were monitored by the same chlorine gas sensor that was subject to cross-detection of substances other than chlorine gas. Three phases of experiments were designed and conducted with water matrices of increasing complexity to identify the gas phase compounds and to gather data on factors that influence the levels present in sewer headspaces. Since there was no analytical instrument for direct identification or quantification of the gas-phase substances, the aqueous solutions were analysed for chlorine species, including free chlorine, monochloramine (NH_2Cl), dichloramine (NHCl_2) and trichloramine (NCl_3) as they were potentially volatile and present in the headspaces. A mass balance model that incorporated the liquid-gas mass transfer process and the decay of the chlorine compounds in both aqueous and gas phases was developed to assist with data analysis and to understand the mechanism that led to the gas-phase responses.

Analysis of the time series data reported by the sensor and corresponding aqueous concentrations of chlorine species revealed that the reported gas signals were from NCl_3 when ammonia was present in the water and the chlorine to ammonia-nitrogen (Cl:N) mass ratios ranged from 10:1 to 14:1 at neutral pH. The reported peak gas concentrations ranged from 2.8 to 13.8 ppm at pH 6.5 and 20°C. In contrast, in the absence of ammonia, the sensor reported measurable gas concentrations with peak values ranging from 0.8 to 5.3 ppm at neutral pH, which was attributed to the presence of free chlorine species (HOCl). The effects of pH and temperature on gas-phase responses were observed either with or without ammonia present in the solution. When wastewater was employed with ammonia present at a Cl:N ratio of ~11.6:1, the magnitudes of the gas-phase responses were relatively low with peak concentrations ranging from 0.6 to 3.1 ppm. This was attributed to the reduction in mass transfer rates, which

was evidenced when lowering the mass transfer coefficients for NCl_3 in the model by a factor of 0.2. By fitting the experimental data to the model, a gas-phase decay process was found to be active and a first-order decay rate constant of 4.0 hr^{-1} at 20°C was estimated. In solutions, first-order decay rate constants for NCl_3 were found to range between $3.0\text{-}6.0 \text{ hr}^{-1}$ in a simple water matrix and were less than 1.0 hr^{-1} in a wastewater matrix at 20°C . Overall, this study produced experimental evidence and developed a mechanistic model that helped understand the fate of reactive chlorine compounds in sewer systems.

Acknowledgements

I would like to first thank my supervisor, Dr. Wayne Parker for his timely and comprehensive feedback and his guidance throughout the project and thesis. Thanks for providing this fantastic opportunity for me to learn and grow.

I would like to thank the Municipality for providing assistance and comments along the way.

Thanks to our Department staff: Peter Volcic, Mark Sobon, and Mark Merlau for helping me set up apparatus and troubleshoot my experimental work.

Thanks to all my peers and friends for supporting me emotionally. It is my pleasure to meet them and have their company during my journey at University of Waterloo.

Thanks to my family for financially supporting me. Without them, I will not be able to achieve where I am now.

Table of Contents

Author's Declaration.....	i
Abstract.....	ii
Acknowledgements.....	iv
List of Figures.....	vii
List of Tables.....	viii
Chapter 1: Introduction.....	1
Chapter 2: Literature Review.....	4
2.1 Physico-chemistry of chlorine compounds.....	4
2.1.1 Henry's law constants for inorganic chlorine compounds.....	4
2.2 Aqueous chemistry of inorganic chlorine compounds.....	7
2.2.1 Equilibria and stability of aqueous free chlorine solutions.....	7
2.2.2 Equilibria of inorganic chloramines in aqueous solutions.....	11
2.2.3 Decomposition of inorganic chloramines in aqueous solutions.....	12
2.3 Characterisation of aqueous chemistry in chlorinated waters.....	15
2.3.1 Chlorination of wastewater.....	16
2.3.2 Chlorination of swimming pool water.....	19
2.3.3 Summary.....	20
2.4 Models for liquid-gas partitioning of volatile compounds.....	21
2.5 Summary.....	23
Chapter 3: Methodology.....	24
3.1 Experimental plan.....	24
3.2 Reactor setup and operation.....	24
3.3 Experimental procedures.....	26
3.3.1 Phase I.....	26
3.3.2 Phase II.....	27
3.3.3 Phase III.....	28
3.4 Analytical methods.....	28
3.5 Model description.....	29
3.6 Calculation of Henry's law constants (H).....	30
3.6.1 Unit conversion.....	30
3.6.2 pH dependency for effective H	31
3.6.3 Temperature correction.....	31
3.7 Estimation of overall mass transfer coefficients (K_L).....	31
3.7.1 K_L estimation for oxygen.....	31
3.7.2 K_L estimation for chlorine compounds.....	33

Chapter 4: Results and Discussion.....	35
4.1 Model parameters.....	35
4.1.1 Henry’s law constants (H).....	35
4.1.2 Mass transfer coefficients (K_L)	37
4.2 Experimental and model results.....	39
4.2.1 Phase I.....	39
4.2.2 Phase II.....	47
4.2.3 Phase III	55
4.3 Sensitivity analysis.....	61
Chapter 5: Conclusions and Recommendations.....	64
References.....	67
Appendices.....	73
A. 1. Procedures for preparing stock solutions	73
A. 2. Calibration curve development	75
A. 3. Unit conversions	76
A. 4. Parameter estimation.....	77
A. 5. Test results for Phase I.....	80
A. 6. Test results for Phase II.....	83
A. 7. Test results for Phase III	87
A. 8 Wastewater characterization in Phase III.....	88
A. 9 Sensor cross-sensitivity data	89
A. 10 References.....	90

List of Figures

- Figure 1** Schematics of the batch reactor.....25
- Figure 2** Effective Henry’s law constant (H_{xx}) for free chlorine (HOCl) vs pH. The line is the predicted result. The points are measured data reported in Holzwarth et al. (1984a).....37
- Figure 3** Time series plot for a chlorine-alone test with a NaOCl dose of 400 mg/L as Cl₂ at pH 6.5 and 20 °C. Line represents gas concentration reported by sensor. Filled circles are free chlorine concentrations.....41
- Figure 4** Time series plot for aqueous free chlorine concentrations from chlorine-alone tests at a NaOCl dose of 400 mg/L as Cl₂, 20 °C and pH 6.5 (green), 7.0 (orange) and 7.5 (purple).....43
- Figure 5** Model results for the temporal change of free chlorine concentrations in the headspace of the reactor and in the solution at 20°C and (a) pH 6.5, (b) pH 7.0, and (c) pH 7.5. Lines are modelled gas-phase concentration. Dashed lines are modelled aqueous concentration. Filled circles are observed aqueous free chlorine concentration from three replicates at each condition. Detection limit (DL) for the gas sensor is indicated as a horizontal line in each plot.....46
- Figure 6** Time series plot for a chlorine-ammonia test with a NaOCl dose of 400 mg/L as Cl₂ at 20 °C, pH 6.5, and Cl:N mass ratio of 12:1. Open circles are total chlorine; squares are monochloramine; triangles are dichloramine; diamonds are trichloramine; filled circles are free chlorine.....48
- Figure 7** Model results for the temporal change of trichloramine concentrations in the headspace of the reactor and in the solution at Cl:N mass ratios of 14:1 (a), 12:1 (b, d) and 10:1 (c). Plots (a), (b) and (c) are at pH 6.5 20°C; (d) at pH 6.5 15°C. Lines are modelled gas-phase concentration. Dashed lines are modelled aqueous concentration. Diamonds are observed aqueous trichloramine concentration. Detection limit (DL) for the gas sensor is indicated as a horizontal line in each plot.....54
- Figure 8** Time series plot for a chlorine-wastewater test with a NaOCl dose of 400 mg/L as Cl₂ to yield a Cl:N mass ratio of ~11.6:1 at pH 6.5 and 20°C. Open circles are total chlorine; squares are monochloramine; triangles are dichloramine; diamonds are trichloramine; filled circles are free chlorine.....56
- Figure 9** Model results for the temporal change of trichloramine concentrations in the headspace of the reactor and in the solution at a Cl:N mass ratio of ~11.6:1 at (a) pH 6.5 20°C, (b) pH 6.5 15°C, and (c) pH 7.5 20°C. Lines are modelled gas-phase concentration. Dashed lines are modelled aqueous concentration. Diamonds are observed aqueous trichloramine concentration. Detection limit (DL) for the gas sensor is indicated as a horizontal line in each plot.....60

List of Tables

Table 1 Values of Henry’s law constant at 20°C (other temperature as indicated) for inorganic chlorine compounds. The dimensionless values were calculated following the method described in Chapter 3.....	6
Table 2 Summary of major equilibrium reactions and their kinetics in aqueous chlorinating systems.....	10
Table 3 Chlorine to ammonia ratios used in Phase II experiments.....	27
Table 4 HACH methods used for determination of free chlorine, total chlorine and ammonia-N. (Retrieved from HACH manuals accessed at https://www.hach.com/resources/water-analysis-handbook#C).....	29
Table 5 Values of dimensionless effective Henry’s law constant and corresponding mass transfer coefficient for HOCl at 20°C used for modeling.....	37
Table 6 Values of dimensionless Henry’s law constant calculated at 15°C for HOCl and NCl ₃ according to Sander (2023), along with values at 20°C for comparison.....	37
Table 7 Values of mass transfer coefficients ($K_L a$, h ⁻¹) at 15°C and 20°C for HOCl and NCl ₃	38
Table 8 Fit model parameters along with observed and predicted gas-phase response characteristics at chlorine dose of 400 mg/L as Cl ₂ and 20°C at pH 6.5, 7.0 and 7.5.....	44
Table 9 Fit model parameters along with observed and predicted gas-phase response characteristics at pH 6.5 and 20°C with Cl:N mass ratios 10:1, 12:1, 14:1 and 16:1 applied.....	49
Table 10 Fit model parameters along with observed and predicted gas-phase response characteristics at pH 6.5 20°C, pH 7.5 20°C, and pH 6.5 15°C.....	57
Table 11 Estimated values of sensitivity coefficient (S) and normalized sensitivity coefficient (S_n)...	62

Chapter 1: Introduction

Sewers in large municipalities often receive discharges of industrial wastewater that can contain elevated concentrations of specific chemicals. If it is determined that the levels of these chemicals are problematic to the sewer system itself or to downstream treatment processes, then sewer-use bylaws can be enacted. In the current case, a municipality identified a potential concern associated with the discharge of sodium hypochlorite to the sewer system. The potentially problematic situation was originally raised when a commercial chlorine gas sensor installed in a wet well reported elevated chlorine gas concentrations. The presence of chlorine gas in the sewer system posed concerns because of its potential to cause corrosion of exposed metals and unsafe work environments. There were however several aspects of the issue that were uncertain. The conventional knowledge of chlorine in aqueous systems (Snoeyink & Jenkins, 1980) indicates that there should not be significant levels of chlorine gas present under typical sewer systems. Hence, it was unclear what type of compounds might have been causing the chlorine gas sensor to report a signal. It was speculated that the sensor might have cross-detected chlorine substance(s) other than chlorine gas. Yet, the sensor had not been tested for cross-sensitivity to other chlorine compounds in previous investigations. Further, if cross-detection was occurring it was not immediately apparent which gas(es) could be responsible for causing the sensor signal. Finally, the chemistry leading to formation and liquid-gas mass transfer of the chlorine compounds was not well understood. This study sought to examine these issues in detail to support an assessment of whether a sewer use bylaw should be enacted for hypochlorite-based chemicals.

The chlorine compounds that were investigated in this study include hypochlorous acid (HOCl), monochloramine (NH₂Cl), dichloramine (NHCl₂) and trichloramine (NCl₃) as they are most likely to be formed rapidly when hypochlorite is discharged to water that contains ammonia (Deborde & von Gunten, 2008). At neutral pH, HOCl is the dominant chlorine species in free chlorine solutions (Palin, 1975). In the presence of ammonia, HOCl reacts rapidly with ammonia forming NH₂Cl, NHCl₂ and NCl₃, which are well-known reactions that occur during the practice of breakpoint chlorination (Palin, 1975). When organic compounds are present in the solution, HOCl and chloramines may react with them and produce chlorinated organic compounds (Deborde & von Gunten, 2008; Soltermann et

al., 2015). However, the reactions with organic compounds are slow relative to the reactions between HOCl and ammonia at environmental conditions (Deborde & von Gunten, 2008). Hence, chlorinated organic compounds were not included in the scope of the current study.

The rate of mass transfer at the liquid-gas interface was assumed to be an important process determining the levels of chlorine compounds in the headspaces since it was assumed that they originated from the reactions in the liquid phase. This process is affected by the physico-chemical properties of the compounds as well as the physical characteristics of the system such as temperature, mixing intensity and air speed (Rittmann et al., 1983; Munz & Roberts, 1989; Deacon, 1977). Henry's law constant is employed as a measure of the volatility of the chlorine compounds relative to their solubility, and its values indicate the tendency of the compounds to transfer into the gas phase. The values of Henry's law constant have been reported for the chlorine compounds mentioned previously, where NCl_3 is most volatile, followed by NHCl_2 , NH_2Cl , and HOCl (Holzwarth et al., 1984a). However, the mass transfer rates, characterised by the mass transfer coefficients, of those compounds have been barely reported, and their values are dependent on system-specific properties. Thus, the values of mass transfer coefficients for the chlorine compounds were quantified in this study by a combination of experimental testing and empirical correlations.

It was anticipated that liquid and gas-phase decay process would influence the concentrations of the compounds in headspaces. A few studies have reported the decay rates of chlorine compounds in aqueous solutions, but there was little relevance to wastewater conditions. The gas-phase decay of the compounds under sewer conditions has not been reported, though the photolytic decomposition of gaseous NCl_3 has been observed (Gérardin et al., 2013). Hence, the decay of the chlorine compounds in the liquid and gas phase was investigated in this study by a combination of testing and modeling.

The objectives of this study were to (1) investigate the chlorine compounds that might be present in sewer headspaces when hypochlorite is discharged and their potential detection by the chlorine gas sensor, and (2) quantify the gas-phase chlorine compounds by developing and employing a mass balance model to provide information for the development of the sewer-use bylaw. To achieve these goals, a series of experiments were conducted in a batch system to evaluate the responses of the gas sensor under different solution conditions and water matrices. The effects of pH and temperature were assessed as they were considered to affect reaction rates. Three different water matrices were designed with increasing complexity

that resembled wastewater. A model was developed to describe the temporal responses of a chlorine compound in both gas and liquid phases due to both chemical and liquid-gas mass transfer processes. The model parameters were either independently estimated or calibrated from experimental results. The current study extends the knowledge of the fate and transport of chlorine substances in sewer systems.

The main body of the thesis is structured in five chapters, titled:

- Chapter 1 Introduction, where problem statements, a brief review of knowledge gaps and objectives of the current study are included;
- Chapter 2 Literature Review, where the existing knowledge relevant to the current work is critically reviewed and discussed in detail;
- Chapter 3 Methodology, where experimental setups, general procedures, and procedures for model development and parameter estimation are described;
- Chapter 4 Results and Discussion, where experimental results and model results are analysed and discussed;
- Chapter 5 Conclusions and Recommendations, where the key findings from the current study are summarised and recommendations for future studies are proposed.

Chapter 2: Literature Review

A literature review was conducted to identify knowledge gaps, inform methodologies and provide references for the results of this study to compare with. In the following sections of the literature review:

- volatile chlorine compounds are identified according to their physico-chemical properties reported in the literature;
- equilibrium and oxidation-reduction reactions of the identified compounds and the kinetics of these reactions are reviewed to understand their formation and decomposition pathways in aqueous systems;
- the applications of the chemistry theories to the chlorination of real waters under conditions that are relevant to wastewater are reviewed and discussed;
- models of the kinetics and liquid-gas mass transfer of volatile compounds in relevant systems are reviewed to provide insights in modeling the fate and transport of the chlorine compounds in sewer systems.

2.1 Physico-chemistry of chlorine compounds

To investigate the potential chlorine compounds that might exist in the headspace of a sewer system receiving chlorine bleach discharge, the physico-chemistry of common chlorine compounds was reviewed. In this regard, information on the volatility and solubility of these compounds was deemed particularly important as they both affect the partitioning of the compounds in water-air systems. This process can be characterised using Henry's law constant (H) as discussed subsequently.

2.1.1 Henry's law constants for inorganic chlorine compounds

Henry's law constant (H) has been used to represent the ratio between the partial pressure of a volatile species and the concentration of the species in water that is in contact with the gas phase at equilibrium (Sander, 2023). It is also referred to as the liquid-gas partition coefficient (Schwarzenbach et al., 2017). The Henry's law constant for substances that react with water in a rapid and reversible manner can be reported as effective H , to be distinguished by the

intrinsic H as defined above (Sander, 2023). The values of effective H vary with pH, aqueous chloride concentration and temperature in the chlorine-water systems (Holzwarth et al., 1984a; Lin & Pehkonen, 1998; Blatchley III et al., 1992).

Henry's law constants have been reported for chlorine gas (Cl_2) and hypochlorous acid (HOCl). An intrinsic H value of $7.61 \times 10^{-4} \text{ mol L}^{-1} \text{ atm}^{-1}$ at 25°C has been determined for Cl_2 as it hydrolyses when being absorbed in water (Lin & Pehkonen, 1998). Other H values for Cl_2 have reported, presumably the effective ones, as summarised in **Table 1**. For HOCl , an intrinsic H value was found to be 0.0600 atm (Blatchley III et al., 1992). Effective H s for HOCl have been reported at specific pH values and are 4 orders of magnitude lower than those for Cl_2 (**Table 1**; Holzwarth et al., 1984a; Blatchley III et al., 1992). This suggests that, at similar concentrations in the solution, HOCl is much less likely to volatilise than Cl_2 . Moreover, as HOCl exhibits equilibrium with dichlorine monoxide (Cl_2O) in both liquid and gas phases (Wojtowicz, 2004; Sivey et al., 2010), Cl_2O may coexist with HOCl and be potentially volatile. However, as the volatility of Cl_2O is unknown and its solubility is high in water (143.6 g/100 g H_2O ; Wojtowicz, 2004), Henry's law constant for Cl_2O has not been determined. In summary, Henry's law constants for Cl_2 and HOCl have been reported in various sources but there is a knowledge gap on the properties of Cl_2O , which has been considered as an important chlorine species converted from HOCl .

Values of Henry's law constants have been reported for inorganic chloramines, including monochloramine (NH_2Cl), dichloramine (NHCl_2) and trichloramine (NCl_3), which are higher than the reported values for HOCl (Holzwarth et al., 1984a). Among the chloramines, NCl_3 has been reported to be most volatile and the value of Henry's law constant is at similar magnitude as Cl_2 's (**Table 1**). Similar to Cl_2 , NCl_3 exhibits a penetrating chlorine odor, which makes it receive great attentions as a volatile chlorination by-product in swimming pool water (Kumar et al., 1987; Li & Blatchley, 2007; Chu et al., 2013; Devi & Dalai, 2021). Although there is no other source that has reported Henry's law constants for NH_2Cl , NHCl_2 and NCl_3 , the reported value for NCl_3 from Holzwarth et al. (1984a) has been adopted in later studies (Judd & Black, 2000; Schmalz et al., 2011). In summary, NCl_3 is the most volatile chloramine species, so in conditions where chloramines are produced, NCl_3 could be the dominant chlorine compound present in gas phase.

Table 1 Values of Henry’s law constant at 20°C (other temperature as indicated) for inorganic chlorine compounds. The dimensionless values were calculated following the method described in Chapter 3.

Substance	Henry’s law constant at 20°C		Reference(s)
	(original unit)	(dimensionless C_G/C_L)	
Cl ₂	7.6×10^{-4} (mol L ⁻¹ atm ⁻¹)	0.54 (at 25°C)	Lin & Pehkonen (1998)
	6.1×10^{-4} (mol m ⁻³ Pa ⁻¹)	0.68 (at 25°C)	Aieta & Roberts (1986) as cited in Sander (2023)
	5.9×10^{-4} (mol m ⁻³ Pa ⁻¹)	0.66 (at 25°C)	Leaist (1986) as cited in Sander (2023)
HOCl	0.076 ^a	5.69×10^{-5}	Holzwarth et al. (1984)
	0.0600 ^b (atm)	4.52×10^{-5} ^b	Blatchley III et al. (1992)
NH ₂ Cl	0.45	3.37×10^{-4}	Holzwarth et al. (1984)
NHCl ₂	1.52	1.14×10^{-3}	Holzwarth et al. (1984)
NCl ₃	435	0.326	Holzwarth et al. (1984)

^a Value was calculated at pH = 5.5 assuming equilibrium condition

^b Intrinsic Henry’s law constant. The value was calculated at pH = 5.4 assuming equilibrium condition

Uncertainties in the reported values of Henry’s law constants (H) for the identified volatile chlorine compounds were reviewed as H is an important parameter in mass transfer models of volatile compounds. Although the Henry’s law constant has been well characterised for Cl₂, there are a limited number of studies that have reported Henry’s law constants for HOCl (Holzwarth et al., 1984a; Blatchley III et al., 1992). In these studies, the effective Henry’s law constants for HOCl were determined by quantifying the loss of free chlorine (Cl₂ + HOCl + OCl⁻) in solution via volatilisation, then H was calculated by applying equilibrium data to the system under specific conditions (e.g. pH, chloride concentration, etc.). Hence, the HOCl concentration in the gas phase was not directly quantified, which potentially contributed to the uncertainty of reported Henry’s law constants for HOCl. Furthermore, as Henry’s law constants have been reported in a variety of units (Sander, 2023), accurate conversion of reported Henry’s law constants to dimensionless concentration-based values requires thermodynamic data specific to each study, which was typically unavailable. In summary, variation in reported effective Henry’s law constants has been observed. Thus, this may contribute to the uncertainty in modelling the liquid-gas mass transfer of volatile chlorine substances in aqueous systems.

In summary, Cl_2 and NCl_3 were identified as the most volatile inorganic chlorine species that can potentially exist in the gas phase of an aqueous system at concerning levels because of their relatively high Henry's law constants compared to other compounds reviewed. Yet, uncertainty in the reported values of Henry's law constants exists due to analytical limitations. In addition, since NCl_3 is a product of rapid reaction between chlorine and ammonia, it is believed that it will more likely be observed in the headspace of a sewer system as wastewater contains ammonia which will react with the chlorine discharge. Thus, literature on NCl_3 in chlorinated ammoniacal waters was discussed in subsequent sections.

2.2 Aqueous chemistry of inorganic chlorine compounds

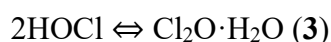
Chlorine-based disinfectants have been used in water and wastewater disinfection for over a century (Sondossi, 2000). The common form of chlorine disinfectant is sodium hypochlorite (NaOCl), commonly known in a dilute aqueous solution as chlorine bleach, which is the sodium salt of hypochlorous acid (HOCl). In practice, HOCl and OCl^- both have disinfection efficacy, thus, together with aqueous chlorine (Cl_2), are referred to as "free chlorine". In water that contains ammonia/ammonium ($\text{NH}_3/\text{NH}_4^+$), free chlorine reacts rapidly and produces monochloramine (NH_2Cl), dichloramine (NHCl_2) and trichloramine (NCl_3), which together are referred as "combined chlorine". The sum of combined chlorine and free chlorine are referred to as "total chlorine". These terms will be used throughout this work.

2.2.1 Equilibria and stability of aqueous free chlorine solutions

Chlorine gas (Cl_2), hypochlorous acid (HOCl), and hypochlorite (OCl^-) are oxidizing agents that have been studied extensively in applications of water disinfection. Knowledge of chlorine equilibrium reactions and decomposition mechanisms in aqueous solutions is important in understanding the fate of chlorine compounds in sewer systems where wastewater containing oxidizing chlorine species might be discharged.

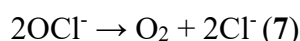
Free chlorine solutions contain several species, including molecular chlorine (Cl_2), hypochlorous acid (HOCl), and hypochlorite (OCl^-), and less-known species, such as dichlorine monoxide (Cl_2O), which are in equilibria with one another in the aqueous solution. Such solutions can be obtained by dissolving chlorine gas (Cl_2) into water. When dissolved in water, Cl_2 is rapidly hydrolysed and undergoes disproportionation (**Eq. 1**) forming hypochlorous acid (HOCl) and hydrochloric acid (HCl). The reverse reaction of chlorine

hydrolysis produces Cl_2 which is favored at acidic conditions according to the equilibrium constant listed in **Table 2**. In aqueous solutions, HOCl dissociates into hypochlorite (OCl^-) and hydrogen ion (H^+) with a pKa of 7.5 (25 °C; Snoeyink & Jenkins, 1980; **Eq. 2; Table 2**). Hypochlorous acid can dehydrate and form dichlorine monoxide (Cl_2O) and the two compounds are interconvertible in both aqueous and gas phase (**Eq. 3; Eq. 4**; Adam et al., 1992; Wojtowicz, 2004). Hence, in dilute HOCl solutions, Cl_2O and HOCl coexist, but the former exists in lower equilibrium concentrations at most conditions as seen in Figure 1 in Sivey et al. (2010). Like other chlorine oxides, Cl_2O is highly reactive and explosive in the gas phase as it decomposes into Cl_2 and O_2 (Wojtowicz, 2004). Information on reaction rate constants and equilibrium constants for reactions mentioned in this section are summarised in **Table 2**. The reactions discussed above are the major equilibria in free chlorine solutions that have been well documented, though the reality is that these reactions share more complicated mechanisms involving many intermediate species as described by Wang & Margerum (1994) and Adam et al. (1992). In summary, the fundamental chemical equilibria of chlorine species in aqueous solutions have been well-established and they are the first step towards understanding the speciation and thus the fate of chlorine compounds in aqueous systems containing free chlorine.



Aqueous solutions of hypochlorous acid (HOCl) and hypochlorite (OCl^-) are subject to decomposition with HOCl being unstable under ultraviolet (UV) irradiation, air exposure and elevated temperatures (Nowell & Hoigné, 1992; Ishihara et al., 2017). HOCl has been reported to be less stable than OCl^- in solution and photolyzes more rapidly (Nowell & Hoigné, 1992; Ishihara et al., 2017). Even without exposure to light or air, HOCl and OCl^- decompose to produce chlorate (ClO_3^-) and chloride (Cl^-) as final products (**Eq. 5**). Different decomposition pathways have been proposed at neutral and alkaline pH values (Busch et al., 2019). At neutral pH, the decomposition of HOCl has been found to be third-order with respect to [HOCl]. The maximum decomposition rate was found to occur at pH 6.89, where the ratio of hypochlorous acid and hypochlorite is 2:1 as per **Eq. 5** (Adam et al., 1992; Adam

& Gordon, 1999; Wojtowicz, 2004; Busch et al., 2019). In alkaline conditions, hypochlorite has been found to decompose to produce oxygen (O₂) in addition to ClO₃⁻ and Cl⁻ (**Eq. 6**; **Eq. 7**). The pathway to formation of O₂ has been found to be slow compared to that of formation of ClO₃⁻, thus, is a minor decomposition pathway (Adam & Gordon, 1999). Furthermore, chloride ion has been observed to be catalytic to the decomposition of hypochlorite ion at pH 9-10 in addition to its contribution to the ionic strength (Adam & Gordon, 1999). Although the decay mechanisms of HOCl and OCl⁻ are somewhat complex, the slow disproportionation of HOCl/OCl⁻ (I) into more stable products, ClO₃⁻ (V) and Cl⁻ (-I), provides insight into the time-dependent behaviour of free chlorine species, which may help with understanding the fate of chlorine in aqueous solutions over time.



In summary, the decomposition of hypochlorous acid and hypochlorite ion has been found to be complex with various intermediate chlorine species involved (Adam et al., 1992; Adam & Gordon, 1999; Busch et al., 2019). These studies highlight the need to consider a complex system of all chlorine species when addressing the chemistry of hypochlorite solutions. The variety of decay products may impact on the ability to close mass balances of chlorine species in systems that are dosed with sodium hypochlorite, especially when they cannot be quantified by traditional analytical methods. Furthermore, the pH dependence of the chlorine speciation and reaction kinetics is important to consider when modeling the decomposition of these reactive chlorine compounds in aqueous systems that could impact the presence of volatile chlorine species under various pH conditions.

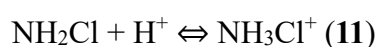
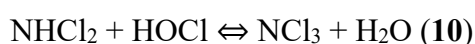
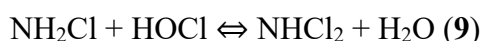
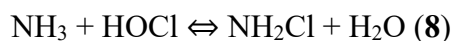
Table 2 Summary of major equilibrium reactions and their kinetics in aqueous chlorinating systems.

Reaction	Equation	Reaction order / Rate expression		Rate constant k at 25°C (otherwise as indicated)		Equilibrium constant K at 25°C, $\mu = 0.50$ M (otherwise as indicated)	Reference(s)
		Forward	Reverse	Forward k_1	Reverse k_{-1}		
Hydrolysis of chlorine gas	$\text{Cl}_2 + \text{H}_2\text{O} \rightleftharpoons \text{HOCl} + \text{H}^+ + \text{Cl}^-$	$k[\text{Cl}_2]$	$k_{-1} \frac{[\text{HOCl}][\text{Cl}^-]}{[\text{H}^+]}$	$22.3 \pm 0.6 \text{ s}^{-1}$	$21.4 \pm 0.8 \times 10^{-3} \text{ M}^{-2} \text{ s}^{-1}$	$1.04 \times 10^{-3} \text{ M}^2$	Wang & Margerum (1994)
	Base-assisted: $\text{Cl}_2 + \text{A}^- + \text{H}_2\text{O} \rightleftharpoons \text{HOCl} + \text{Cl}^- + \text{HA}$	$k[\text{Cl}_2][\text{A}^-]$	$k_{-1} \frac{[\text{HOCl}][\text{Cl}^-]}{[\text{HA}]}$	$45 \pm 3 \text{ M}^{-1} \text{ s}^{-1}$ ($\text{A}^- = \text{H}_2\text{PO}_4^-$)	$1.3 \pm 0.2 \times 10^3 \text{ M}^{-2} \text{ s}^{-1}$ ($\text{HA} = \text{H}_3\text{PO}_4$)	$3.84 \times 10^{-4} \text{ M}^2$ (20°C)	Wang & Margerum (1994)
Hypochlorous acid dissociation	$\text{HOCl} \rightleftharpoons \text{OCl}^- + \text{H}^+$					$10^{-7.54} \text{ M}$; $2.54 \times 10^{-8} \text{ M}^{-1}$ (20°C)	Snoeyink & Jenkins (1980); Blatchley III et al. (1992)
Hypochlorous acid dehydration	$2\text{HOCl} \rightleftharpoons \text{Cl}_2\text{O} \cdot \text{H}_2\text{O}$					$0.08\text{-}0.09 \text{ M}^{-1}$	Mishalanie et al. (1986)
	$2\text{HOCl} \rightleftharpoons \text{Cl}_2\text{O} + \text{H}_2\text{O}$					0.03 M^{-1} (50 °C)	Adam et al. (1992)
Monochloramine formation	$\text{NH}_3 + \text{HOCl} \rightleftharpoons \text{NH}_2\text{Cl} + \text{H}_2\text{O}$	$k[\text{HOCl}][\text{NH}_3]$	$k_{-1}[\text{NH}_2\text{Cl}]$	$1.5 \times 10^{10} \text{ M}^{-1} \text{ h}^{-1}$; $2.5 \times 10^{10} \text{ e}^{-2500/\text{RT}}$	$7.6 \times 10^{-2} \text{ h}^{-1}$	$2.4 \times 10^{11} \text{ M}^{-1}$ ($\mu = 0.45 \text{ M}$); $1.5 \times 10^{10} \text{ M}^{-1}$	Weil and Morris (1949); Morris and Isaac (1981) as cited in Jafvert & Valentine (1992) and Vikesland et al. (2001); Granstrom (1954) as cited in Gray et al. (1978) and Jafvert & Valentine (1992); Gray et al. (1978)
Dichloramine formation	$\text{NH}_2\text{Cl} + \text{HOCl} \rightleftharpoons \text{NHCl}_2 + \text{H}_2\text{O}$	$k[\text{HOCl}][\text{NH}_2\text{Cl}]$	$k_{-1}[\text{NHCl}_2]$	$1.0 \times 10^6 \text{ M}^{-1} \text{ h}^{-1}$	$2.3 \times 10^{-3} \text{ h}^{-1}$	$2.3 \times 10^8 \text{ M}^{-1}$	Margerum et al. (1978) as cited in Vikesland et al. (2001) and Jafvert & Valentine (1992); Gray et al. (1978)
Trichloramine formation	$\text{NHCl}_2 + \text{HOCl} \rightleftharpoons \text{NCl}_3 + \text{H}_2\text{O}$	$k[\text{HOCl}][\text{NHCl}_2]$	$k_{-1}[\text{NCl}_3]$			$1.6 \times 10^8 \text{ M}^{-1}$; $4.8 \times 10^4 \text{ M}^{-1}$	Kumar et al. (1987); Jafvert & Valentine (1992)
	Base-assisted: $\text{NHCl}_2 + \text{HOCl} + \text{B} \rightleftharpoons \text{NCl}_3 + \text{OH}^- + \text{HB}^+$	$k[\text{HOCl}][\text{NHCl}_2][\text{B}]$		$1.6 \times 10^4 \text{ M}^{-2} \text{ s}^{-1}$ ($\text{B} = [\text{HPO}_4^{2-}]$); $1 \times 10^5 \text{ M}^{-2} \text{ s}^{-1}$ ($\text{B} = [\text{OCl}^-]$)			Hand & Margerum (1983)
Monochloramine disproportionation	$2\text{NH}_2\text{Cl} \rightleftharpoons \text{NHCl}_2 + \text{NH}_3$	$k[\text{NH}_2\text{Cl}]^2$		Function of $[\text{H}^+]$, $[\text{H}_2\text{PO}_4^-]$ and $[\text{H}_3\text{PO}_4]$ (if present)	$2.16 \times 10^8 \text{ M}^{-2} \text{ h}^{-1}$	$1 \times 10^9 \text{ M}^{-1}$; $4.3 \times 10^6 \text{ M}^{-1}$	Valentine & Jafvert (1988); Jafvert & Valentine (1992); Vikesland et al. (2001)
	$2\text{NH}_2\text{Cl} + \text{H}^+ \rightleftharpoons \text{NHCl}_2 + \text{NH}_4^+$	$k[\text{NH}_2\text{Cl}][\text{NH}_3]$	$k_{-1} \frac{[\text{NHCl}_2][\text{H}^+]}{[\text{NH}_3]}$	$3.2 \times 10^4 \text{ M}^{-2} \text{ s}^{-1}$		$6.7 \times 10^5 \text{ M}^{-1}$	Hand & Margerum (1983); Gray et al. (1978)

2.2.2 Equilibria of inorganic chloramines in aqueous solutions

Knowledge of the rates of formation and chemical equilibria of inorganic chloramines is fundamental for understanding the fate and transformation of these compounds when chlorine is introduced to aqueous systems containing ammonia. Trichloramine (NCl₃) is the most volatile chloramine and can play an important role in systems where the gas phase concentration of chlorine compounds is of concern. Thus, the fate and transport of inorganic chloramines, particularly NCl₃, is the focal point of the following sections that address their formation and decomposition upon chlorination of ammonia-containing waters.

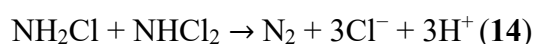
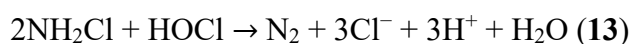
When a free chlorine solution is dosed in a solution containing ammonia/ammonium (NH₃/NH₄⁺), the free chlorine reacts rapidly with ammonia forming inorganic chloramines, namely monochloramine (NH₂Cl), dichloramine (NHCl₂) and trichloramine (NCl₃), which are in equilibria with one another (Gray et al., 1978). The stepwise formation of NH₂Cl, NHCl₂ and NCl₃ are described by **Eq. 8-10** and their reaction rates and equilibrium constants are summarised in **Table 2**. NCl₃ formation is base-catalysed, and thus, its formation rate is a function of the concentrations of HPO₄²⁻, OCl⁻, OH⁻ and CO₃²⁻ if present in the solution (Hand & Margerum, 1983; Jafvert & Valentine, 1992; **Table 2**). Other important chemical equilibria among the three chloramine species include monochloramine protonation (pK_a for NH₃Cl⁺ = 1.5 at 25 °C; **Eq. 11**; Gray et al., 1978; Jafvert & Valentine, 1992), and monochloramine disproportionation (**Eq. 12**; Gray et al., 1978; Valentine & Jafvert, 1988; **Table 2**). The review of the equilibrium chemistry reveals that the relative concentrations of chloramine species at equilibrium will be dependent on the pH and the relative concentration of free chlorine to ammonia in the solution. Thus, this section lays the foundation for further discussion on the dependency of chloramine speciation and decomposition on pH and chlorine dose in later sections. This knowledge is important in modeling the fate of volatile chlorine species under various pH and chlorine dose conditions.



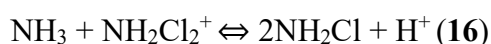
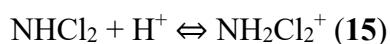
2.2.3 Decomposition of inorganic chloramines in aqueous solutions

The potential for decomposition of chloramines in water was reviewed as this would influence their availability to partition to the gas phase. In this regard, they have been reported to self-decompose in aqueous solutions via a series of reactions that are assisted by general acid or base leading to oxidation of the nitrogen (-III) and reduction of the chlorine (I) in chloramines (Jafvert & Valentine, 1987; Valentine & Jafvert, 1988; Vikesland et al., 2001). The following sections review the stability of monochloramine (NH₂Cl), dichloramine (NHCl₂) and trichloramine (NCl₃) in aqueous solutions and their decomposition pathways under different conditions.

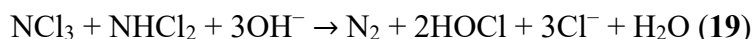
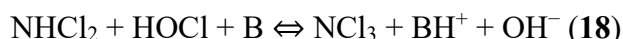
Monochloramine (NH₂Cl) has been found to be relatively stable in dilute solutions containing excess ammonia (Yiin & Margerum, 1990). However, under slightly alkaline conditions with excess chlorine, NH₂Cl has been reported to be oxidized into nitrogen gas (N₂) as per **Eq. 13** (Pressley et al., 1972). Valentine & Jafvert (1988) reported that this redox reaction resulted in the loss of NH₂Cl at pH 8. It was hypothesized that the reaction involved NHCl₂ as an intermediate that reacted rapidly with NH₂Cl to form N₂ as per **Eq. 14** (Valentine & Jafvert, 1988). The N₂-forming decomposition pathway is not specific to NH₂Cl, as it has also been observed for NHCl₂ and NCl₃ revealing the unstable nature of inorganic chloramines and the high tendency to self-decompose.



Dichloramine (NHCl₂) has been found to be relatively stable in the range of pH 3-4 but is prone to decomposition at pH above 6 (Valentine & Jafvert, 1988; Gray et al., 1978). Similar to NH₂Cl, dilute NHCl₂ solutions have been found to be relatively stable in the presence of excess ammonia at pH 6-7 (Hand & Margerum, 1983; Yiin & Margerum, 1990). Nonetheless, NHCl₂ can still slowly decompose in the presence of excess ammonia at neutral pH as shown in the equilibrium reactions (**Eq. 15**; **Eq. 16**; Hand & Margerum, 1983). In summary, at neutral pH with ammonia present in the solution, NHCl₂ undergoes a relatively slow decomposition pathway producing NH₂Cl, which is an example of how the fate of one chloramine species is related to the others via chemical equilibria.

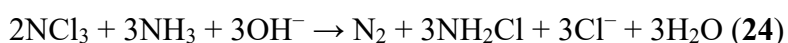
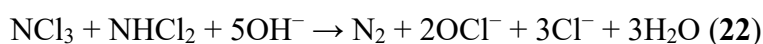
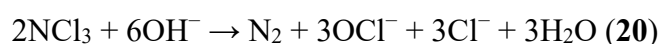


In contrast, under neutral and basic conditions in the absence of excess ammonia or in the presence of excess chlorine, decomposition of dichloramine has been found to follow a different pathway that is 5 orders of magnitude faster than that with excess ammonia at neutral pH (**Eq. 17**; Hand & Margerum, 1983). The decomposition of NHCl_2 under such conditions has been reported to consist of two steps: the general base-catalysed formation of NCl_3 from HOCl (**Eq. 18**; where $\text{B} = \text{HPO}_4^{2-}$, OCl^- , CO_3^{2-} , and OH^-) and the subsequent rapid redox reaction between NHCl_2 and the produced NCl_3 forming N_2 (**Eq. 19**; Hand & Margerum, 1983; Rayne & Forest, 2014). Although the exact mechanism of the formation of N_2 has not been reported, the reaction has been hypothesised to be base-catalysed (Hand & Margerum, 1983; Kumar et al., 1987). Although the overall reaction of NHCl_2 decomposition has been found to be autocatalysed by HOCl , it is at least 10 times slower than the reaction between HOCl and NH_3 at neutral pH (**Eq. 8**; Hand & Margerum, 1983). Hence, the presence of NH_3 in the solution will slow down decomposition of NHCl_2 as NH_3 preferentially reacts with HOCl which will become unavailable for the rapid reaction that converts NHCl_2 and NCl_3 to N_2 (**Eq. 19**). Furthermore, the reaction described by **Eq. 18** was hypothesised to be slower than **Eq. 19** so concentration of NCl_3 remained low during the reaction (Hand & Margerum, 1983). In conclusion, in the absence of ammonia, NHCl_2 decomposition proceeds much faster than that in the presence of excess ammonia and NCl_3 is involved as an intermediate in the fast redox reaction that produces N_2 . The reactions that contribute to NHCl_2 decomposition also provide insight into decomposition pathways for NCl_3 as subsequently discussed.



Different from mono- and dichloramine, trichloramine (NCl_3) is considered to be less thermodynamically stable in most conditions, though dilute NCl_3 solutions have been reported to be moderately stable in acidic conditions (Kumar et al., 1987; Yiin & Margerum, 1990). Kumar et al. (1987) proposed a mechanism for NCl_3 decomposition in basic solutions in the absence of ammonia. Under such conditions, decomposition of NCl_3 was found to follow the overall reaction (**Eq. 20**), which proceeds in two steps. First, NCl_3 produces NHCl_2 (**Eq. 21**; Saguinsin & Morris, 1975; Kumar et al., 1987; Rayne & Forest, 2014), which then rapidly reacts with an additional NCl_3 to form N_2 (**Eq. 22**), similar to **Eq. 19**. In

the presence of excess ammonia, decomposition of NCl_3 has been found to involve similar subset of reactions with an additional reaction between NCl_3 and NH_3 to form NHCl_2 and NH_2Cl (**Eq. 23**; Saguinsin & Morris, 1975; Yiin & Margerum, 1990). The NHCl_2 formed subsequently reacts with NCl_3 producing N_2 as depicted in **Eq. 19**. Summing up the reactions **Eq. 23**, **Eq. 19** and **Eq. 8** gives the overall reaction **Eq. 24** (Yiin & Margerum, 1990). With or without excess ammonia, the reactions between NHCl_2 and NCl_3 (**Eq. 22** and **Eq. 19**) were found to be a very rapid base-assisted process, involving several intermediates (Saguinsin & Morris, 1975; Yiin & Margerum, 1990), which is consistent with previous observations (Hand & Margerum, 1983; Valentine & Jafvert, 1988). Furthermore, the decomposition mechanism for NCl_3 overlaps with that for NHCl_2 in the absence of ammonia suggesting that the rapid formation of N_2 is the common pathway that drives the self-decomposition of chloramines under certain conditions. In summary, the presence of either excess ammonia or chlorine can influence the decomposition pathway for chloramines, and thus affect the decay rate and speciation of chloramines in chlorinated ammonia-containing solutions. This knowledge is important for the understanding of chemical reactions that involve formation and decomposition of volatile NCl_3 in wastewater that is dosed with free chlorine.



As the detailed kinetics of the reactions above have not been reported systematically, literature that explored the effect of pH on decomposition rates of trichloramine was reviewed. Saguinsin and Morris (1975) have reported that the decomposition of NCl_3 was first order in $[\text{NCl}_3]$. The first-order rate constants for pH 7.0, 8.25, and 9.0 were found to be $3.4 \times 10^{-5} \text{ s}^{-1}$, $6.3 \times 10^{-5} \text{ s}^{-1}$ and $2.2 \times 10^{-4} \text{ s}^{-1}$, respectively (Saguinsin & Morris, 1975). At pH 10.5 in carbonate buffer with excess OCl^- , Hand & Margerum (1983) estimated a pseudo-first-order rate constant of 0.02 s^{-1} for the decomposition of NCl_3 (**Eq. 18**; **Eq. 19**). Kumar et al. (1987) further explored the kinetics of NCl_3 decomposition via the overall reaction (**Eq. 20**), and a pseudo-first-order rate expression involving concentrations of specific base/general acid was proposed. At neutral pH with phosphate buffer, the observed first-order rate constant

ranged from 0.41×10^{-5} to $1.01 \times 10^{-5} \text{ s}^{-1}$ depending on pH and phosphate concentration (Kumar et al., 1987). In comparison, Yiin and Margerum (1990) proposed a third-order rate expression for NCl_3 decomposition with respect to the concentrations of NCl_3 , ammonia and base present in the solution, and the rate constant was found to be $4.46 \times 10^3 \text{ M}^{-2} \text{ s}^{-1}$ for OH^- according to the overall reaction **Eq. 24**. For the reaction between NHCl_2 and NCl_3 (**Eq. 19**), a second-order rate was observed to increase from $4.5 \times 10^2 \text{ M}^{-1} \text{ s}^{-1}$ to $1.1 \times 10^3 \text{ M}^{-1} \text{ s}^{-1}$ as pH increases from 6.13 to 6.88 under specified conditions (Yiin & Margerum, 1990), indicating strong pH dependence of **Eq. 19**. In summary, with various rate expressions for NCl_3 decomposition reactions proposed, a general pattern of the rate dependency was observed: the rate of NCl_3 decomposition increases with pH, base concentration and ammonia concentration. This knowledge is important when modeling aqueous NCl_3 at different pH and ammonia conditions. However, the effect of temperature on NCl_3 decomposition rate was not evaluated in these studies and is a gap in the knowledge regarding the kinetics of NCl_3 decomposition in aqueous solutions.

In summary, the previously discussed reactions describe the decomposition of inorganic chloramines and thus their availability to partition in the gas phase from the solution. The redox reactions (**Eq. 14**; **Eq. 19**; **Eq. 22**) that produce N_2 are generally believed to contribute to rapid and irreversible loss of NH_2Cl , NHCl_2 and NCl_3 . Different reaction pathways were reported to decompose chloramines under different conditions, e.g. in the presence of ammonia vs. without ammonia in solution. The rates of decomposition reactions were generally found to be controlled by pH, base concentration and concentrations of free chlorine or ammonia present in the solution. However, as a variety of kinetic rate expressions for decomposition of NCl_3 have been proposed by researchers under different conditions, there is little systematic understanding of NCl_3 decomposition under neutral conditions that are relevant to real chlorinated waters. This leads to uncertainty when modeling the decay of NCl_3 upon chlorination of ammonia-containing waters as is addressed in the current study.

2.3 Characterisation of aqueous chemistry in chlorinated waters

Chlorination has been widely used in disinfection of drinking water, wastewater and swimming pool water, hence, there is a considerable body of literature that addresses reactions between chlorine and water constituents commonly present in those systems. One of constituents of interest is ammonia as it rapidly reacts with free chlorine and forms

monochloramine (NH_2Cl), dichloramine (NHCl_2) and trichloramine (NCl_3). In those systems, formation of NH_2Cl is beneficial for maintaining stable chlorine residuals for disinfection purposes, while formation of NCl_3 is undesirable when the gas-phase concentrations of chlorinated compounds are concerned due to the high volatility of NCl_3 . As discussed in the previous section, formation and decomposition of chloramines and their relative concentrations at equilibrium are dependent on solution pH and the relative concentrations of applied chlorine and ammonia in the solution. Thus, applying that chemistry to real waters is important to characterise the fate and transport of inorganic chlorine compounds, specifically volatile species such as NCl_3 in aqueous systems with headspace. Therefore, this section reviewed literatures that have concerned about the fate of inorganic chloramines, with a focus on NCl_3 , in chlorinated ammonia-containing waters: wastewater and swimming pool water.

2.3.1 Chlorination of wastewater

In the context of water disinfection, breakpoint chlorination is a technique that has been developed to characterize the extent to which chlorine reacts with ammonia in water (Pressley et al., 1972). Hence, information from studies on breakpoint chlorination may provide insights into conditions that support formation of volatile NCl_3 . In wastewater disinfection, the mass ratio of Cl:N at the breakpoint has been reported to range between 8:1 and 9:1 (Pressley et al., 1972; Aieta & Roberts, 1983) which is higher than the stoichiometric ratio of 7.6:1 required for ammonia oxidation to N_2 . Further as previously discussed, solution pH plays a significant role in the equilibria of chloramine species and the reactions that lead to decomposition of chloramines, particularly for the case of NCl_3 . Therefore, the Cl:N ratio and pH dependency of formation and decomposition of NCl_3 during breakpoint chlorination is discussed subsequently.

The impact of solution pH on chloramine speciation was initially reviewed. Before the breakpoint stoichiometry, NH_2Cl was found to be the main species in the pH range of 7-8.5 (Pressley et al., 1972; Gray et al., 1978; Qiang & Adams, 2004). As pH decreased, NHCl_2 became favored according to the equilibrium chemistry (**Eq. 12**). At pH 4.5-5.0, NHCl_2 was the main species (Pressley et al., 1972; Gray et al., 1978). NCl_3 was the main species at pH below 4 (Pressley et al., 1972; Gray et al., 1978). However, above the breakpoint, there is little information on the pH-dependent stability of the chloramines as it has been often believed that the chloramines were completely oxidized to N_2 so the majority of total chlorine present was free chlorine (Benjamin & Lawler, 2013). In summary, a general pattern of pH-

dependent chloramine speciation was observed in chlorinated water. Lower pH tends to promote the formation of more chlorinated chloramine species ($\text{NH}_2\text{Cl} < \text{NHCl}_2 < \text{NCl}_3$), and vice versa. Thus, formation of NCl_3 can be enhanced if pH decreases.

As neutral pH conditions are relevant to sewer systems, the effect of Cl:N mass ratio on chloramine formation was reviewed. In this regard, as Cl:N was increased the NH_2Cl concentration was found to reach a maximum at a ratio of 5:1 and then decreased to near zero at the breakpoint ratio of 7.6 (Pressley et al., 1972; Qiang & Adams, 2004; Benjamin & Lawler, 2013; Devi & Dalai, 2021). Conversely, when the Cl:N mass ratio exceeded 5:1, formation of NHCl_2 was found to become significant and reached a maximum concentration at a ratio of about 7.5:1 beyond which it rapidly decomposed at the breakpoint (Pressley et al., 1972; Benjamin & Lawler, 2013). Formation of NCl_3 was found to be favoured at and above the breakpoint (Pressley et al., 1972). However, there is limited information on quantifying the extent of NCl_3 formation at and after the breakpoint stoichiometry as it has not been of significant interest in most water chlorination contexts due to its instability (Benjamin & Lawler, 2013). In summary, the general pattern in breakpoint chlorination tests is that formation of more highly chlorinated chloramines is favored as Cl:N ratio increases.

The dependency of NCl_3 responses at and beyond the breakpoint during chlorination of wastewater was specifically reviewed. At the breakpoint, Pressley et al. (1972) observed that the concentration of $\text{NCl}_3\text{-N}$ formed decreased from about 0.3 mg/1 at pH 5.0 to 0.05 mg/1 at pH 7, suggesting that higher pH resulted in lower NCl_3 yield. As chlorine dosages exceeded the breakpoint stoichiometry at neutral pH, the concentrations of NCl_3 increased with Cl:N ratio until it reached 12:1 (Pressley et al., 1972). The increase in NCl_3 concentration beyond the breakpoint agreed with an observation of Hand & Margerum (1983) that the yield of NCl_3 increased from 10% to 45% of the theoretical value when hypochlorite was present at neutral pH. One of the limitations of prior studies is that, relatively long contact times (i.e. 2 hours) were employed (Pressley et al., 1972; Devi & Dalai, 2021) based on disinfection practice, thus the dependence of NCl_3 decay rates on pH and Cl:N ratio has not been thoroughly studied leading to a gap in understanding of the kinetics of NCl_3 decay in wastewater.

As there is lack of kinetic studies on NCl_3 formation and decomposition in chlorinated wastewater, literature that reported rapid free chlorine loss at the breakpoint was reviewed, which might provide insights into rapid NCl_3 decomposition in wastewater. During

breakpoint chlorination of wastewater, residual chlorine can be lost by reacting with ammonia and forming NCl_3 as an intermediate which rapidly decomposes subsequently producing N_2 . The rapid reaction was reported by Pressley et al. (1972) where breakpoint chlorination of ammonia in wastewater oxidized 95-99% of the ammonia-N to N_2 within a 1-minute reaction time at neutral pH. Haas and Karra (1984) also observed such rapid loss of chlorine during chlorination of wastewater. To quantify the extent of chlorine loss, total chlorine residual from secondary wastewater effluents upon chlorination was modeled using a two-phase parallel first-order decay of residual chlorine, where the first phase is rapid and the second one is slow (Haas & Karra, 1984). Based on the field data collected, the rates for the second-phase decay (k_2) were observed to cluster around 0.003 min^{-1} , consistent with literature values for decomposition of inorganic and organic chloramines at neutral pH (Haas & Karra, 1984). In contrast, the first-phase decay rates (k_1) varied from 0.794 to 86.6 min^{-1} at contact time of 2 minutes, which were much higher than k_2 , indicating the formation of an inherently unstable chlorine species that decomposed faster than monochloramine or simple organic chloramines (Haas & Karra, 1984). This suggested that NCl_3 had formed and decomposed resulting in the observed chlorine loss at a first order rate of approximately 1.0 min^{-1} within 2 minutes of breakpoint chlorination, which is higher than the rates reported for NCl_3 in the previous section. In summary, the rapid initial phase of the chlorine decay implied the rapid formation and subsequent decomposition of NCl_3 upon chlorination of the ammonia-containing water. The reported initial rates spanned a large range of values, suggesting there was uncertainty in quantifying the rapid loss of free chlorine within 2 min of chlorination.

The impact of other constituents present in wastewater that react with free chlorine was reviewed as they may compete with ammonia to react with free chlorine resulting in a chlorine demand during chlorination of wastewater. Common inorganic substances that react quickly with chlorine in wastewater include nitrite, sulfide, ferrous iron and manganous manganese (Taras et al., 1950; Chen et al., 2001; Vikesland & Valentine, 2002; Deborde & von Gunten, 2008). Among those compounds, nitrite has received most attention in studies concerning chlorine demand in wastewater (Dhaliwal & Baker, 1983; Haas & Karra, 1984; Gasser, 1984; Gordon, 1985; Chen et al., 2001), as it is often present in nitrified effluents and reacts with free chlorine at a rate comparable to that of ammonia. Small organic compounds, such as amino acids, also exert chlorine demand, though they generally require longer reaction time (Taras et al., 1950). In addition to reactions with free chlorine, the chlorine-

demanding compounds can also react with monochloramine formed from free chlorine and ammonia, though monochloramine reactions with these compounds have been found to be much slower than with free chlorine (Dhaliwal & Baker, 1983; Chen et al., 2001). The implication of these reactions on the formation of volatile chlorine species is that a higher dose of free chlorine is required to achieve breakpoint chlorination than that in the absence of chlorine-demanding compounds. This information may help in modeling NCl_3 response in wastewater that contain chlorine-demanding constituents.

In summary, the literature on breakpoint chlorination reveals that NCl_3 is formed at the breakpoint stoichiometry and the extent of formation increases with the relative dose of free chlorine to ammonia (i.e. Cl:N ratio). The stability of NCl_3 formed in the chlorinated water decreases with pH, which is consistent with the base-catalysed decomposition pathway discussed previously (Hand & Margerum, 1983; Valentine & Jafvert, 1988; Yiin & Margerum, 1990). While breakpoint chlorination has been well-studied in laboratory tests, the formation and decomposition of NCl_3 has rarely been studied in practice of wastewater chlorination. Further, the dependence of the decomposition rate on pH and Cl:N ratio has not been quantified in wastewater chlorination. Thus, the lack of information on the kinetics of formation and decomposition of NCl_3 is a knowledge gap that will need to be addressed to successfully model its presence in sewer systems receiving chlorine discharges. Moreover, including chlorine demand exertion in models may increase their accuracy.

2.3.2 Chlorination of swimming pool water

Trichloramine (NCl_3) has been identified as a volatile chlorinated by-product found in the air of indoor swimming pools that use chlorine as a disinfectant for the pool water (Li & Blatchley, 2007; Schmalz et al., 2011; Chowdhury et al., 2014). Because of the concern about the health impact of exposure to NCl_3 on swimming pool users, previous studies have addressed the temporal pattern of NCl_3 concentration and its association with concentrations of NCl_3 -forming precursors in pool water. In swimming pool water, NCl_3 is formed from the chlorination of ammonia and nitrogenous organic precursors introduced by swimmers (Schmalz et al., 2011; Chowdhury et al., 2014). The applied chlorine dose is often higher than the breakpoint stoichiometry in order to maintain a certain level of free chlorine residual in pool water as required by regulations (Schmalz et al., 2011; Chowdhury et al., 2014). This may be relevant to conditions in sewers that receive high doses of chlorine discharge. Thus, the literature on the formation of NCl_3 in swimming pool water was reviewed.

The formation of NCl_3 from chlorination of swimming pool water has been found to largely depend on pH, Cl:N ratio and nitrogen precursors present in the water (Schmalz et al., 2011). Schmalz et al. (2011) evaluated the effect of pH on the yield of NCl_3 from ammonia in aqueous solution at a Cl:N molar ratio of 5:1 (equivalent to a Cl:N mass ratio of 12.7:1). The average yield of NCl_3 , expressed as a percentage of ammonia-N present in the solution after a reaction time of 30 minutes, decreased from 55.0% to 20.4% as pH increased from 6.7 to 7.7. Further, an increase in NCl_3 yield was observed as the Cl:N molar ratio increased from 1:1 to 5:1 at pH 6.8 (Schmalz et al., 2011). These results were consistent with the pH and Cl:N ratio dependency of NCl_3 concentration observed in wastewater chlorination (Pressley et al., 1972). Similar observations were made when chlorinating urea, which has been identified as an important source of organic-N introduced to swimming pool water by swimmers (Judd & Black, 2000) and an effective precursor contributing to NCl_3 formation in swimming pool water (Blatchley & Cheng, 2010; Weng & Blatchley, 2011; Weng et al., 2012; Gérardin et al., 2015). However, the reaction between urea and free chlorine has been observed to be slow compared to that with ammonia (Li & Blatchley, 2007; Blatchley & Cheng, 2010). According to Blatchley and Cheng (2010), the aqueous concentration of NCl_3 appeared to peak at between 5 to 10 hours after chlorination of urea with an initial concentration of 0.05 mM. The majority of urea present in solution remained unreacted after 24 hours of chlorination (Blatchley & Cheng, 2010). Similarly, De Laat et al. (2011) observed that urea with a concentration of 0.05 mM reacted with 0.05 mM free chlorine very slowly at pH 7.3 so that approximately 70% of the urea was not degraded by chlorine after a 48-hour reaction time. In summary, in the context of chlorinating swimming pool water, ammonia and urea have been found to be precursors for NCl_3 formation with the yield of NCl_3 dependent on water pH and Cl:N ratio. As an important organic-N precursor, urea slowly reacts with free chlorine, while ammonia reacts rapidly under the condition of swimming pool water. The relative slow formation of NCl_3 from urea may also provide insight in modeling NCl_3 in wastewater systems where urea is present.

2.3.3 Summary

The formation and decomposition of inorganic chloramines have been studied in chlorination of wastewater and swimming pool water, with the latter having a greater emphasis on formation of NCl_3 which is a volatile chlorinated product from ammonia and organic-N compounds. The kinetics of reactions between free chlorine and ammonia have been found to be fast with subsequent rapid decomposition of NCl_3 that produce N_2 and Cl^- at

neutral conditions. Although there is no systematic study on the kinetics of NCl_3 formation and decomposition in chlorinated water, the literature reviewed may provide insights in designing mechanistic models that describe the temporal response of NCl_3 under different pH and Cl:N ratios in chlorinated water. The understanding of NCl_3 response in aqueous solutions would be helpful for the prediction of gas phase NCl_3 in sewer headspace. This may also be helpful in making simple and effective assumptions for modeling NCl_3 in aqueous and gas phase and reducing mathematical complexity when solving the modeled system.

2.4 Models for liquid-gas partitioning of volatile compounds

As volatile chlorine compounds in the headspace of sewer systems have not been modeled before, information on mass transfer models of other volatile contaminants was deemed important for providing insights in understanding the transport of chlorine compounds in the gas and liquid phase of a sewer system. Corsi et al. (1992) developed a dynamic model for volatile organic compounds (VOCs) in gas and liquid phase of sewers, where sewer reaches were treated as a series of continuous stirred tank reactors (CSTRs) in both phases. In this model, the liquid-gas mass transfer of VOCs at the liquid-gas interface coupled the mass balance of VOC in the liquid and in the gas phase according to the two-film theory. This model has been adapted by Parker and Yu (2001) where the effects of drop structures and VOC-free tributary flows on gas phase VOC concentration were incorporated in the model. Drop structures in sewer systems have been found to enhance the emission of VOC to the air, while the VOC-free tributary flows decreased VOC gas concentration downstream (Parker & Yu, 2001; Roghani et al. 2021). In summary, the dynamic two-phase models available on transport of VOCs in sewer system can serve as a basis for modeling volatile chlorine compounds. One limitation of these models is that they did not take account of degradation of VOCs or any relevant chemical reactions that involved VOCs in either the liquid or gas phase of the sewers. This leads to a gap when incorporating the reactivity and instability of volatile chlorine compounds in mass transfer models.

Mass transfer models for trichloramine (NCl_3) in swimming pool systems were reviewed, as they might provide insights into modeling of NCl_3 in sewer systems. At conditions of swimming pool water, partitioning of NCl_3 to the air has been found to be limited by liquid-gas mass transfer process (Weng et al., 2011; Wu et al., 2021; Lee & Blatchley, 2022; Lee et al., 2023; Schmalz et al., 2011). Thus, to predict NCl_3 concentration

in indoor swimming pool air, a good estimation of the mass transfer coefficient for NCl_3 was found to be important. Lee et al. (2023) developed a dynamic model where the change in NCl_3 gas phase concentration over time was characterised by air flows and the mass transfer from the liquid phase, which was described by an overall mass transfer coefficient under baseline conditions (K_l) and an effective mass transfer coefficient that was proportional to number of swimmers (nK_l'). Under baseline conditions with no swimmers, field data were employed to estimate K_l at steady state, which was found to be in the range of 6.1×10^{-5} - 6.7×10^{-5} cm s^{-1} . In comparison, Schmalz et al. (2011) developed a simple mass transfer model and estimated the overall mass transfer coefficients for NCl_3 with a reference to carbon dioxide (CO_2), which were found to be 0.6×10^{-3} cm s^{-1} for a quiescent water surface and 2.4×10^{-3} cm s^{-1} for a rippled surface. The value of the mass transfer coefficient for a quiescent surface reported in Schmalz et al. (2011) was roughly 10 times higher than that reported by Lee et al. (2023) under baseline conditions, indicating uncertainty existed when estimating the value of mass transfer coefficient for NCl_3 under swimming pool-like conditions using different methods. Moreover, although it is important to account for the dynamic impact of swimmers on the mass transfer coefficient, the model developed by Lee et al. (2023) did not consider the formation and decomposition of NCl_3 in the aqueous phase, which will need to be addressed in the current study.

As there is lack of information on modeling the decay of volatile compounds in sewers, literature on mass transfer models that incorporated the formation and decay of NCl_3 was reviewed. The mass transfer model developed by Schmalz et al. (2011) accounted for the formation of NCl_3 from the reaction between urea and free chlorine (first-order decay rate of 4.58×10^{-6} s^{-1}) and the first-order decomposition of aqueous NCl_3 . For NCl_3 decomposition, Schmalz et al. (2011) used first-order rate constants of 3.4×10^{-5} s^{-1} and 2.96×10^{-6} s^{-1} , which were retrieved directly from literature sources. In comparison, Gérardin et al. (2015) incorporated multiple key reactions that involves the formation (e.g. **Eq. 10**) and decomposition (e.g. **Eq. 19**) of NCl_3 to their mass transfer model. The values of rate constants used in Gérardin et al. (2015) were derived from the kinetic model developed by Jafvert & Valentine (1992), where one of the decomposition reactions was third-order in NCl_3 with a rate constant of 5.6×10^{10} $\text{M}^{-2} \text{s}^{-1}$. Thus, only theoretical rate constants were used in these models but no observed rates of NCl_3 decomposition in the actual swimming pool water were characterised, leading to a gap when applying the literature values to water with more complex matrix. Therefore, it is important to accurately estimate the decay rate constant of

NCl_3 in water with specific conditions so that it can be incorporated in mass transfer models that predict the gas-phase concentration at real conditions.

In summary, mass transfer models that address the concentration of NCl_3 in indoor swimming pool air were reviewed as models of NCl_3 have not been established in the sewer environment. In prior studies, a range of values of mass transfer coefficients for NCl_3 under swimming pool conditions have been reported, but there is little information on the decomposition rate of NCl_3 in real waters under relevant conditions. Nevertheless, these mass transfer models may provide important information for modeling NCl_3 in the gas and liquid phase of similar systems, such as sewer environments.

2.5 Summary

This chapter reviewed the physio-chemical properties and the chemical transformations of a series of inorganic chlorine substances that are potentially volatile and are commonly present in aqueous solutions. Among these substances, trichloramine (NCl_3) has been identified to be the most volatile chlorine species besides chlorine gas, and its formation from reactions between free chlorine species and ammonia is rapid. However, NCl_3 is subject to rapid decomposition and thus, its rates of decomposition and pathways have not been well characterised in real waters at relevant environmental conditions, e.g. in wastewater. Moreover, little information was available on the mass transfer of NCl_3 at the liquid-gas interface in relevant environments, which leads to a knowledge gap on predicting gas concentrations of NCl_3 in sewer headspaces. Therefore, the current study was conducted to bridge these gaps and to understand the fate and transport of NCl_3 in a sewer environment.

Chapter 3: Methodology

3.1 Experimental plan

This study sought to investigate the underlying mechanisms leading to the apparent detection of gaseous chlorine (Cl_2) by a commercially available sensor in the headspace of a full scale operating pumping station of a large municipal sewer system. Based upon traditional aqueous chlorine chemistry it was hypothesized that the detections were due to cross-sensitivity of the detector to chlorine-containing compounds that had not been tested by the manufacturer. Hence, one of the purposes of the experimental plan was to evaluate the potential for cross-detection with chlorine compounds that might exist in a sewer system receiving chlorine discharges. In addition, the impact of aqueous chemistry on the gas phase responses was assessed using a three-phase experimental design. In Phase I, a clean water matrix that was buffered by phosphate was used to evaluate responses as a function of pH, free chlorine dose and temperature. In Phase II, the same clean water matrix was used with a fixed chlorine dosage but ammonium chloride was added in different concentrations for a range of pH and temperature conditions. In Phase III, raw wastewater was used and buffered with phosphate to evaluate responses over a range of pH and temperature values. Furthermore, a contaminant mass balance model was developed and calibrated with the experimental data to assist with data interpretation and to allow the lab results to be extended to full-scale applications.

3.2 Reactor setup and operation

A reactor setup was developed to house an ULTIMA® X5000 Gas Monitor with MSA XCell Chlorine Gas Sensor for the purposes of exploring the impacts of aqueous chemistry conditions on the gas phase response. The chlorine gas sensor employs the same Cl_2 detection mechanism (i.e. electrochemical) as installed at the full scale pumping station and has a detection range of 0 - 20 ppm and a sensitivity of 0.1 ppm. Electrochemical gas sensors employ the oxidation-reduction reactions between the sensing electrode of the sensor and the ambient gas molecules, which produces an electric current proportional to the concentration of the gas (Yi et al., 2015). Depending on the gas to be detected, some electrochemical gas sensors can have poor selectivity (Chou, 2000). For the chlorine gas sensor used in this study,

its cross-sensitivity to a variety of gases has been documented by the manufacturer which is included in Appendices (A. 9).

A column-style reactor with an inner diameter of 15 cm and a height of 25 cm was designed and built to house the chlorine gas sensor. To imitate a sewer environment, the reactor was wrapped with foil to minimize contributions from photochemical processes to the decay of chlorine compounds in the reactor. The headspace of the reactor was mixed by and by an air-circulation pump (LABOPORT® UN 86 KTP) while the liquid contents were mixed with a stir bar/plate (Corning Laboratory Stirrer PC-310) as described in **Figure 1**. There were two ports included for introducing the reacting solutions: sodium hypochlorite (NaOCl or free chlorine) solution and a “background solution”, whose composition was controlled according to the phase of the experiments. In addition, a sampling port, that was submerged in the mixed solution and which was opened/closed periodically to sample volumes of the solution for analysis was included. The reactor was maintained gas-tight during experiment runs.

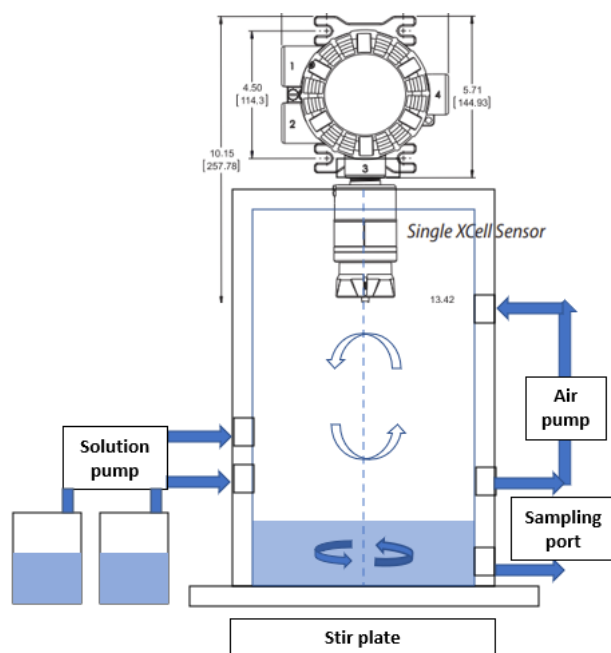


Figure 1 Schematics of the batch reactor.

To initiate an experimental run, the background solution (0.25 L) was pumped into the reactor first and this was followed by injection of the NaOCl solution (0.25 L) with a known concentration. The two solutions were mixed by the stir bar and the headspace was mixed by the air-circulation pump at constant rates for all experiments. The output signal (Volts) from

the sensor meter was calibrated into concentration (ppm), which was monitored in real time and recorded by a computer program developed using LabVIEW™. Prior to each experiment, the reading from the program was calibrated by the reading from the sensor meter screen, i.e. 0 ppm. In between runs, the reactor was emptied and the inside of the reactor was rinsed with deionized (DI) water to remove any contents left from previous runs.

3.3 Experimental procedures

Reacting solutions, stock solutions and analytical reagents were prepared and stored using glassware that was chlorine demand-free (soaked in NaOCl solution overnight and then rinsed with DI water). All chemicals used were analytical grade. Procedures for the preparation and storage of stock solutions are included in Appendices (A. 1).

The experiments evaluated gas and liquid phase responses from three different aqueous matrices: phosphate-buffered DI water without ammonia, buffered DI water with ammonia, and buffered wastewater, to which an NaOCl solution was added. Thus, the experiments were conducted in three phases: Phase I Chlorine alone, Phase II Chlorine-Ammonia, and Phase III Chlorine-Wastewater.

3.3.1 Phase I

The first phase of experiments investigated the effect of reaction conditions on gas and liquid phase responses in the absence of ammonia. The Phase I experiments provided baseline information that could be compared with that of Phase II to discern the composition of gaseous chlorine compounds detected by the gas sensor. The experimental variables included the NaOCl concentration in solution (400, 200 and 40 mg/L as Cl₂), pH (6.5, 7.0 and 7.5), and water temperature (15 and 20 °C). The selected levels of pH and temperature were believed to be relevant to the conditions that might be present in a real wastewater system receiving a concentrated bleach solution discharge. At each condition, two to three replicate tests were conducted.

Free chlorine solutions were prepared by diluting a NaOCl stock solution to the target concentrations and were standardized prior to experiments using DPD/FAS titration (APHA, 2021) to ensure the titrated concentration was within 2.5% of the target concentration. Buffer solutions (250 mL) at pH 6.5, 7.0 and 7.5 were prepared by diluting 100 mL of corresponding phosphate stock solutions with 150 mL DI water (A. 1). The total phosphate concentration in

the buffer solution was 80 mM. The water temperature was controlled by a PolyScience® MM Series Chiller that circulated a refrigerant through tubing with an inner diameter of 5/16 inch which was wrapped around the reactor column.

3.3.2 Phase II

The second phase of experiments introduced the presence of ammonia as an experimental factor that was anticipated to affect the gas-phase response due to the formation of chloramines from reactions between chlorine and ammonia. Hence, the effect of ammonia presence in the buffer solution on the gas and liquid phase responses was evaluated under different pH (6.5, 7.0 and 7.5) and temperatures (15 and 20 °C). At each condition, two to four replicate tests were conducted.

The NaOCl concentration was maintained at 400 mg/L as Cl₂ for all experiments in Phase II but the concentration of ammonia in the buffer solution was varied. The relative concentration of free chlorine to ammonia in each solution was expressed by the Cl:N ratio (**Table 3**). Six Cl:N ratios were selected to reflect different compositions of chlorine species based on knowledge of breakpoint stoichiometry (Chapter 2). To prepare a buffered ammonia solution at the target concentration and pH, 100 mL of phosphate stock solution and a selected volume of the ammonium chloride stock solution were mixed together and diluted to 250 mL by DI water (**A. 1**). The procedures for the preparation of the free chlorine solutions and temperature control were the same as described in Phase I.

Table 3 Chlorine to ammonia ratios used in Phase II experiments.

Molar ratio Cl:N	Mass ratio Cl:N	Solution concentrations (mg/L): Free chlorine to Ammonium Cl ₂ :NH ₄
6.31:1	400:25.0 (16:1)	400:32.2
5.53:1	400:28.5 (14:1)	400:36.7
4.74:1	400:33.3 (12:1)	400:42.8
3.94:1	400:40.0 (10:1)	400:51.5
3.15:1	400:50.1 (8.0:1)	400:64.4
1.79:1	400:87.9 (4.6:1)	400:113

3.3.3 Phase III

Phase III of the experiments explored gas and liquid phase responses when pH-buffered wastewater was employed such that the impact of wastewater constituents on system behaviour could be assessed by comparison with Phase II. Raw wastewater was sampled from the raw sewage line entering the wastewater laboratory at the University of Waterloo. Samples were centrifuged at 3000 rpm for 45 minutes using SORVALL® RC 5B Plus to remove the majority of the particulate content. The supernatant was portioned into 250 mL bottles and stored in refrigerator at 4 °C. Each batch of wastewater samples was used within one week. After centrifugation, samples were analysed for pH, alkalinity, total organic carbon (TOC), anions (chloride, nitrate, phosphate, sulfate), and cations (ammonium, potassium, sodium). Prior to each experiment, one bottle of processed wastewater was taken from the refrigerator and warmed in a water bath. After the sample was warmed to the target temperature, pH and ammonia nitrogen (NH₄-N) were measured prior to conducting tests.

In the tests, the concentration of the NaOCl solution was maintained at 400 mg/L as Cl₂ for all experiments. The pH of the wastewater prior to experiments was adjusted to 6.5 or 7.5 by diluting 150 mL with 100 mL phosphate stock solution. Temperature (15 and 20 °C) was controlled as described in Phase I. At each condition, two replicate tests were conducted.

3.4 Analytical methods

During each run, the solution in the reactor was periodically sampled for analysis of pH, temperature, free/total chlorine, mono-, di-, and trichloramine if applicable. In Phase I, free chlorine and total chlorine were determined using a spectrophotometer (Hach DR1900) and commercial reagent packs that corresponded to each method (**Table 4**). A calibration curve of absorbance for free/total chlorine was developed (**A. 2**). The detection range was 0.1-4.0 mg/L as Cl₂. In Phase II, free chlorine and inorganic chloramines were determined by DPD/FAS titration following Standard Method 4500 F (APHA, 2021; Palin, 1957; Palin, 1968). The detection range was 0.1-5.0 mg/L as Cl₂. In Phase III, free chlorine and chloramines were analysed using the same method as in Phase II.

Wastewater samples were analysed for common anions and cations. The anions, including chloride, nitrate, phosphate, and sulfate, were analysed using an IC (Dionex ICS-1100) following Standard Method 4110 B (APHA, 2021). The cations, including ammonium,

potassium, and sodium, were analysed using an IC (Dionex AQUION) following the method D6919-17 (ASTM International, 2017). Total organic carbon (TOC) was analysed using a TOC analyser (TOC-L SHIMADZU) following Standard Method 5310 B (APHA, 2021). Ammonia nitrogen (NH₄-N) was analysed by the HACH Salicylate Method (**Table 4**). Alkalinity was analysed following Standard Method 2320 B (APHA, 2021). Water pH and temperature were measured by a probe (ORION 9107BN) connected with a pH meter (ORION STAR A111).

Table 4 HACH methods used for determination of free chlorine, total chlorine and ammonia-N. (Retrieved from HACH manuals accessed at <https://www.hach.com/resources/water-analysis-handbook#C>).

Parameter	Method	Detection range	Document ID
Chlorine, Free	USEPA DPD Method (Method 8021)	0.02 to 2.00 mg/L Cl ₂	DOC316.53.0 1023
Chlorine, Total	USEPA DPD Method (Method 10070)	0.1 to 10.0 mg/L Cl ₂	DOC316.53.0 1029
Nitrogen, Ammonia	Salicylate Method (Method 10031)	0.4 to 50.0 mg/L N	DOC316.53.0 1079

3.5 Model description

A model that incorporated liquid-gas mass transfer and first-order decay of volatile inorganic chlorine compounds in the liquid and gas phases of the completely mixed batch reactor was developed to assist with interpretation of the experimental data. The ordinary differential equations that describe the mass balances in the liquid and gas phases are described in **Eq. 25-26**:

$$V_l \frac{dC_l}{dt} = -V_l k_{dl} C_l - V_l K_L a (C_l - \frac{C_g}{H}) \quad (25)$$

$$V_g \frac{dC_g}{dt} = -V_g k_{dg} C_g + V_l K_L a (C_l - \frac{C_g}{H}) \quad (26)$$

where

V_l and V_g = volume of liquid and gas phases, respectively, L;

C_l and C_g = concentration of compound in liquid and gas phases, mg L⁻¹;

k_{dl} and k_{dg} = first-order decay constants for compound in liquid and gas phases, hr^{-1} ;

$K_L a$ = lumped overall mass transfer coefficient for compound, hr^{-1} ;

H = dimensionless Henry's Law constant for compound, which is defined as $\frac{C_g}{C_l}$ at equilibrium.

It was assumed that (1) the headspace and aqueous solution were well-mixed, thus, they were spatially uniform in composition in each phase; (2) the formation of the volatile chlorine compound was instantaneous, thus could be represented by an initial concentration at time zero; and, (3) the rate of decomposition of the volatile chlorine compound in each phase was first-order with respect to its concentration.

The parameters employed in the models were obtained independently. The Henry's Law constants (H) were obtained from the literature (Holzwarth et al., 1984a; **Table 1**; Chapter 2). The conversion of the reported H in the original units to its dimensionless form and the temperature correction for adjusting the H values are described in the following section. The overall mass transfer coefficient ($K_L a$) for the volatile chlorine compounds was estimated from the oxygen mass transfer coefficient for the batch reactor ($K_L a^{O_2}$) that was estimated from oxygen transfer tests that were conducted in this study. The first-order decay constants, k_{dl} and k_{dg} , were obtained by iteratively fitting of the model to the experimental data generated in this study, which will be described in detail in Chapter 4.

3.6 Calculation of Henry's law constants (H)

3.6.1 Unit conversion

As dimensionless concentration-based Henry's law constants were required for the mass balance model (**Eq. 25-26**), there was a need to convert literature values of Henry's law constants that were reported in a variety of unit conventions. The Henry's constants reported by Holzwarth et al. (1984a) were mole fraction-based (H_{xx}) and defined as,

$$H_{xx} = X_G/X_L \quad (27)$$

where X_G is the mole fraction of the gas in the air and X_L is the mole fraction of the gas in the water. The mole fraction of a compound in an aqueous solution is the ratio of moles of the

dissolved compound to the sum of moles of the compound and moles of water. H_{xx} was converted to dimensionless molar concentration-based constant at 20 °C by dividing it by $(24.1 \text{ L mol}^{-1} \times 55.5 \text{ mol L}^{-1})$ as described in **Eq. 28**, assuming (1) the amount of the dissolved compound is negligible compared to the number of water molecules per litre of aqueous solution (55.5 mol L^{-1}), and (2) the volatile compound follows the ideal gas law (**A. 3**). The converted Henry's constants from Holzwarth et al. (1984a) are shown in the **Table 1** (Chapter 2), **Table 5** and **Table 6** (Chapter 4).

$$H = \frac{H_{xx}}{24.1 \frac{\text{L}}{\text{mol}} \times 55.5 \frac{\text{mol}}{\text{L}}} \quad (28)$$

3.6.2 pH dependency for effective H

The effective Henry's law constant for HOCl at pH 6.5, 7.0 and 7.5 was calculated following the method in Blatchley III et al. (1992) using equilibrium data from **Table 2** (Chapter 2) at 20°C. It was assumed that the concentration of aqueous Cl_2 was negligible at pH above 5, so the only free chlorine species in the solution were HOCl and OCl^- . As OCl^- was expected to be non-volatile (Blatchley III et al., 1992; Judd & Black, 2000), the chlorine species present in the headspace of the buffered free chlorine solution was considered to be mainly HOCl. In contrast, NCl_3 was considered to be a neutral species that does not undergo speciation in aqueous solutions. Thus, its Henry's law constant was assumed to be independent of pH.

3.6.3 Temperature correction

The values of Henry's law constants are a function of temperature. As data for Henry's law constants for HOCl and NCl_3 were available at 20°C and 40°C (Holzwarth et al., 1984a), linear extrapolation was used to estimate their Henry's constants at 15°C following the method used in Sander (2023).

3.7 Estimation of overall mass transfer coefficients (K_L)

The values of K_L for volatile chlorine compounds were estimated from that of oxygen (O_2) using the following sequence of operations.

3.7.1 K_L estimation for oxygen

The K_L for oxygen at 20°C was estimated following the procedure described in Chaturvedi et al. (2014) that involved batch tests where the rate of transfer of oxygen into solution was quantified using a dissolved oxygen (DO) probe. Before each test started, the DO present in the solution was depleted by adding an excess amount of solid sodium dithionite (30-40 mg per 500 mL). After the DO was completely depleted, air circulation was initiated. At time zero, DO started to increase until equilibrium was reached and this value was assumed to indicate the solubility of oxygen under the experimental condition.

Using the data generated from each lab test, the overall mass transfer coefficient ($K_L^{O_2}$ or $K_L a^{O_2}$) was estimated by two-parameter non-linear regression of the oxygen transfer model (**Eq. 29a; 29b**; Tchobanoglous et al., 2014). As the interfacial area (A) for mass transfer was reasonably defined in the reactor, $K_L^{O_2}$ was estimated by multiplying $K_L a^{O_2}$ by $\frac{V}{A}$.

$$V \frac{dC}{dt} = K_L^{O_2} A (C_s - C) \quad (29a)$$

or

$$V \frac{dC}{dt} = V K_L a^{O_2} (C_s - C) \quad (29b)$$

where V = volume of aqueous solution, L;

A = area of liquid-gas interface, which was approximately equal to the cross-sectional area of the reactor ($1.77 \times 10^{-2} \text{ m}^2$);

C = concentration of O_2 in the solution, mg L^{-1} ;

C_s = solubility of O_2 in water, mg L^{-1} ;

$K_L^{O_2}$ = overall mass transfer coefficient for O_2 , cm s^{-1} ;

$K_L a^{O_2}$ = the lumped mass transfer coefficient for O_2 , h^{-1} .

The $K_L a^{O_2}$ at 15°C was corrected by applying a factor of 0.89 that was calculated from **Eq. 30** (Rittmann et al., 1983). Subsequently, $K_L a$ for the volatile chlorine compounds at 15°C were corrected accordingly.

$$K_L a^{O_2(T)} = \theta^{(T-20)} K_L a^{O_2(20)} \quad (30)$$

where T = temperature, °C;

$K_L a^{O_2(20)}$ and $K_L a^{O_2(T)}$ = the lumped mass transfer coefficient for O₂ at temperature 20 °C and T °C, h⁻¹;

$\theta = 1.024$, which is a commonly used value as a temperature correction factor (Rittmann et al., 1983).

3.7.2 K_L estimation for chlorine compounds

To obtain K_L values for the volatile chlorine compounds, the measured overall mass transfer coefficient for oxygen ($K_L^{O_2}$) was corrected following **Eq. 31-33**. The liquid phase mass transfer coefficient for a chlorine compound was computed from the value of $K_L^{O_2}$ by multiplying with the ratio of the diffusion coefficients of the two compounds (Munz & Roberts, 1989; Corsi et al., 1992). This approach assumes that $k_L^{O_2} \approx K_L^{O_2}$ as the liquid phase resistance of O₂ accounts for more than 95% of the total resistance (with a dimensionless Henry's Law constant of 29.92 at 20°C; Munz & Roberts, 1989).

$$k_L^c = K_L^{O_2} \times \frac{D_L^c}{D_L^{O_2}} \quad (31)$$

where k_L^c = the liquid phase mass transfer coefficient for compound, cm s⁻¹;

$K_L^{O_2}$ = the overall mass transfer coefficient for O₂, cm s⁻¹;

$D_L^{O_2}$ = the liquid diffusion coefficient of oxygen in water, cm² s⁻¹;

D_L^c = the liquid diffusion coefficient of compound in water, cm² s⁻¹.

As HOCl, Cl₂ and NCl₃ are less volatile than O₂, a value of $k_G/k_L = 40$ was used to estimate the relative importance of gas and liquid phase mass transfer resistances in the constantly mixed batch system (Munz & Roberts, 1989). Thus,

$$k_G^c = 40k_L^c \quad (32)$$

where k_G^c is the gas phase mass transfer coefficient for compound, cm s⁻¹.

The overall mass transfer coefficient (K_L^c) for the chlorine compounds was calculated based on two-film theory (Benjamin & Lawler, 2013),

$$\frac{1}{K_L^c} = \frac{1}{k_L^c} + \frac{1}{k_G^c H} \quad (33)$$

where H is the dimensionless Henry's Law constant for compound c.

The values of the liquid diffusion coefficients (D_L^c) that were employed to estimate the mass transfer coefficients (**Eq. 31**) were estimated using the Wilke and Chang (1955) correlation,

$$D = 7.4 \times 10^{-8} \frac{(xM)^{0.5} T}{\eta V^{0.6}} \quad (34)$$

where, x = an association parameter which equals to 2.6 for water as solvent;

M = molecular weight of solvent, which is 18.015 g mol⁻¹ for water;

T = temperature, °C;

V = molar volume of solute at normal boiling point, cm³ mol⁻¹;

η = viscosity of solution, centipoise (cP).

Molar volumes (V) were required to estimate the diffusion coefficients (D_s) but, except for O₂ and Cl₂ (Wilke & Chang, 1955), were not available for the target compounds. Thus, values of V for HOCl, NH₂Cl, NHCl₂ and NCl₃ were estimated from various sources as summarised in **Table A-3** in Appendices. The values of viscosity of water (η) were retrieved from the sources described in Appendices (**A. 4**). Therefore, values of D at 15°C and 20°C were calculated and the results are included in Appendices (**A. 4**).

Chapter 4: Results and Discussion

This chapter presents the results obtained from batch tests that were conducted in three phases with increasingly complex water matrices. The mass balance model outlined in the previous chapter was employed to understand the underlying mechanisms leading to the observed experimental responses.

The results from batch tests were compared between conditions to assess the effect of experimental factors on the response from the chlorine gas sensor. Peak gas concentration (C_p) and the time to peak (t_p), were analysed quantitatively as they were deemed to be important characteristics of gas-phase response, and thus, were discussed subsequently in detail. Time series data for aqueous phase chlorine species present in the solution were also analysed to assist with interpretation of the gas-phase response.

To model the gas- and aqueous phase responses, five parameters were quantified. Two of the parameters, Henry's law constants (H) and overall mass transfer coefficients ($K_L a$) for HOCl and NCl₃, were estimated following the methods described in Chapter 3 and their values are presented as the first section of this chapter. The remaining parameters (first-order decay constant for either HOCl or NCl₃ in the gas- (k_{dg}) and aqueous (k_{dl}) phases, and initial concentration (C_{0l})) depended upon the test conditions and were fit from the observed data. The fit model predictions were compared with experimental results to evaluate the effectiveness of model fitting and to make overall conclusions regarding the factors leading to gas-phase responses. Finally, a sensitivity analysis was performed on the five model parameters to identify the most influential parameters on the gas-phase response.

4.1 Model parameters

This section presents the estimated values of the model parameters influencing liquid-gas mass transfer: Henry's law constants (H) and overall mass transfer coefficients (K_L) for hypochlorous acid (HOCl) and trichloramine (NCl₃) at 15°C and 20°C. These values were used as model inputs in later sections.

4.1.1 Henry's law constants (H)

As the effective Henry's law constant for HOCl is dependent on pH (Holzwarth et al., 1984a; Blatchley III et al., 1992), effective H for HOCl was calculated at pH values of 6.5, 7.0 and 7.5 at 20°C (**Table 5**) as described in Chapter 3. **Figure 2** plots the pH dependency for effective H for HOCl and was produced using data from Holzwarth et al. (1984a) following the method described by Blatchley III et al. (1992). The plot shows good agreement between the predicted result and the observed data reported by Holzwarth et al. (1984a). Thus, the method for predicting effective Henry's law constants for HOCl at different pH (Blatchley III et al., 1992) was considered to be effective. Therefore, the predicted values at pH 6.5, 7.0 and 7.5 were used for the model as listed in **Table 5**.

The Henry's law constants for HOCl and NCl₃ at 15°C and 20°C were estimated using available literature data as described in Chapter 3 (**Table 6**). As the Henry's law constant depends on temperature, H values for HOCl and NCl₃ at 15°C and 20°C were estimated following the method used in Sander (2023). The resulting values are listed in **Table 6**. The values of Henry's law constants for HOCl are 4 orders of magnitude lower than that of NCl₃, indicating that when HOCl and NCl₃ are present in solution at the same molar concentration, there would be considerably higher concentrations of NCl₃ in the headspace than HOCl at equilibrium. As temperature decreases, this equilibrium shifts towards producing lower concentrations of HOCl or NCl₃ in the headspace for the same aqueous concentrations. Thus, H values at 15°C for HOCl and NCl₃ were extrapolated from the 20°C data and were used for modeling. The concentration-based dimensionless constants for HOCl and NCl₃ at 15°C and 20°C were used directly in the model and for estimating the overall mass transfer coefficients (K_L) as subsequently discussed.

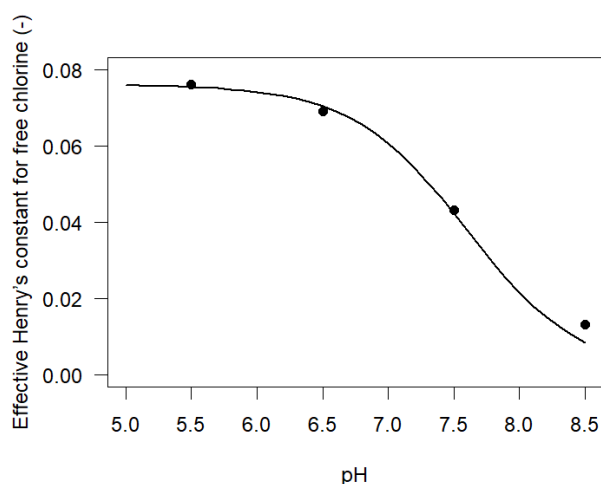


Figure 2 Effective Henry's law constant (H_{xx}) for free chlorine (HOCl) vs pH. The line is the predicted result. The points are measured data reported in Holzwarth et al. (1984a).

Table 5 Values of dimensionless effective Henry's law constant and corresponding mass transfer coefficient for HOCl at 20°C used for modeling.

pH	Predicted H (-)	Estimated $K_L a$ (h^{-1})
6.5	5.26×10^{-5}	3.3×10^{-4}
7.0	4.54×10^{-5}	2.9×10^{-4}
7.5	3.15×10^{-5}	2.0×10^{-4}

Table 6 Values of dimensionless Henry's law constant calculated at 15°C for HOCl and NCl_3 according to Sander (2023), along with values at 20°C for comparison.

Substance	15°C	20°C
HOCl	$*4.21 \times 10^{-5}$	$*5.26 \times 10^{-5}$
NCl_3	0.267	0.326

*Value was calculated using effective Henry's law constant at pH 6.5.

4.1.2 Mass transfer coefficients (K_L)

To estimate values of K_L^c for HOCl and NCl_3 , the $K_L^{O_2}$ for oxygen was first estimated from batch tests as described in Chapter 3 (**Table A-2; Figure A-2**). A mean $K_L a^{O_2}$ value from 4 replicates was estimated to be 5.9 h^{-1} with a standard deviation of 1.4 h^{-1} at 20°C.

Hence, the $K_L^{O_2}$ for O₂ was estimated to be $4.6 \pm 1.1 \times 10^{-3}$ cm s⁻¹ by multiplying $K_L a^{O_2}$ by the ratio of solution volume to the interfacial area as described in Chapter 3. The relative standard deviation (RSD) for the estimated $K_L a^{O_2}$ or $K_L^{O_2}$ value was approximately 24%. As the value of $K_L^{O_2}$ is mostly influenced by the specific characteristics of the liquid-gas mass transfer system, the high RSD value might suggest there is a level of uncertainty regarding the mixing condition in the batch reactor as the solution volume or the interfacial area were not likely to vary between tests. Nonetheless, the average value of $K_L^{O_2}$ was used to estimate K_L^c for HOCl and NCl₃ as discussed subsequently.

To estimate K_L^c values for HOCl and NCl₃ from the $K_L^{O_2}$ values, liquid diffusion coefficients (D) were estimated for O₂, HOCl and NCl₃. The value of D for O₂ was estimated to be 2.12×10^{-5} cm² s⁻¹ at 20°C (**Table A-4**) and was similar to the values that have been reported in the literature (Holmén & Liss, 1984; Munz & Roberts, 1989). The D value for NCl₃ was estimated to be 1.22×10^{-5} cm² s⁻¹ at 20°C, comparable to the value of 1.26×10^{-5} cm² s⁻¹ reported at 28°C (Schmalz et al., 2011). In contrast, the value for HOCl was estimated to be 2.05×10^{-5} cm² s⁻¹ at 20°C but no literature has reported its value.

Values of K_L^c and $K_L a$ for HOCl and NCl₃ were calculated following methods described in Chapter 3. The values of $K_L a$ for HOCl and NCl₃ are included in **Table 5** and **Table 7** at corresponding conditions. Overall, under the same condition, the estimated $K_L a$ value for HOCl was roughly 2 orders of magnitude lower than that of NCl₃, meaning the mass transfer rate for HOCl would be much slower when the concentration gradient of the two substances was the same. In summary, the values of Henry's law constant and overall mass transfer coefficients for HOCl and NCl₃ were estimated at 15°C and 20°C and were employed in the following section for simulating experimental results.

Table 7 Values of mass transfer coefficients ($K_L a$, h⁻¹) at 15°C and 20°C for HOCl and NCl₃.

Substance	15°C	20°C
HOCl	* 2.4×10^{-4}	* 3.3×10^{-4}
NCl ₃	0.076	0.088

*Value was calculated using effective Henry's law constant at pH 6.5.

4.2 Experimental and model results

This section presents the results obtained from batch experiments that were conducted to assess the impact of water matrix/composition, pH and temperature on the response obtained from a commercial chlorine gas sensor. The results of the application of a mass balance model to simulate the experimental results are also discussed. The results are presented in subsections that follow the sequence of the experiments: Phase I Chlorine alone, Phase II Chlorine-Ammonia, and Phase III Chlorine-Wastewater.

4.2.1 Phase I

In the chlorine-alone tests, a gas was detected by the chlorine sensor when free chlorine doses of 400 and 200 mg/L as Cl₂ were employed at 20°C and pH values in the range 6.5-7.5. The actual composition of the gas could not be ascertained with the available analytical equipment but was hypothesised to be HOCl as this represents a major fraction of the free chlorine at pH 6.5-7.5 and has been reported to volatilize in previous studies (Holzwarth et al., 1984a; Holzwarth et al., 1984b; Blatchley III et al., 1992). The patterns of the gas- and aqueous phase responses observed in this phase were employed as a baseline condition for comparison with the results from Phases II and III where the water composition more closely reflected that of real wastewater. To understand the mechanism leading to the observed gas-phase response, a mass balance model was employed and the effect of pH on the gas-phase response at 20°C was analysed in depth. Besides, the effect of free chlorine dose and temperature were also assessed and the results are included in the appendices (A. 5).

To illustrate the temporal pattern of gas-phase responses observed in Phase I experiments, the time series data from a representative test that had an NaOCl dose of 400 mg/L as Cl₂ at pH 6.5 and 20°C was plotted (**Figure 3**). According to the signal reported by the gas sensor, the gas concentration started to increase shortly after dosing the NaOCl solution into the test reactor. The gas response peaked around 2 hours after the start of the test at a value of 2.0 ppm, then declined gradually to zero after 5 hours. Similar trends in the gas-phase response were observed at other conditions where measurable amount of gas was detected (**Figure A-3; Figure A-4**). The observed trends suggests that there might be at least two driving mechanisms that have opposing effects which control the concentration of the gaseous compound: one mechanism drives the flux of the compound into the headspace system and the other drives the flux of the compound out of the headspace, so that a peak gas concentration is reached when the two mechanisms are equal. To understand the mechanism

of the observed gas-phase response, a mass balance model was employed and quantitative analysis was conducted and discussed subsequently.

To help with interpretation of the gas-phase responses, the aqueous concentration of free chlorine was analysed and **Figure 3** presents the values for the test that generated the previously described gas phase response. According to **Figure 3**, the free chlorine concentration decreased from approximately 150 mg/L as Cl₂ at the first point of measurement (~0.5 hr) to 70 mg/L as Cl₂ at 5 hr of the test. Upon inspection, it appeared that the temporal trend in free chlorine concentration resembled a first-order decay process, which has been commonly employed to model the decay of chlorine residual in drinking water (Onyutha & Kwio-Tamale, 2022). Thus, a first-order decay term was included in the mass balance model to describe the time-dependent decay of free chlorine in the aqueous phase.

Since the gas-phase response appeared to be temporary with increasing and decreasing limbs as discussed previously, peak gas concentration (C_p , ppm as Cl₂) and the time to peak (t_p , hr) were used as indicators to characterise the gas-phase response quantitatively. This approach was employed because it was believed that the gas in the headspace was not Cl₂ for which the sensor had been calibrated by the supplier. However, it was assumed that the signal reported by the sensor was proportional to the concentration of the actual chlorine-based gas that was present in the sensor. Hence, the proposed metrics did not rely on the actual gas phase concentrations, but rather, the trends in the concentrations with time. The value of C_p was recorded as the maximum concentration of the chlorine substance detected in the headspace during each test. The value of t_p at each test was obtained by averaging the times associated with the start and at the end of the maximum concentration reported by the sensor. It was hypothesized that the values of both t_p and C_p were influenced by rates of chemical decay and liquid-gas mass transfer in the system, which are discussed subsequently.

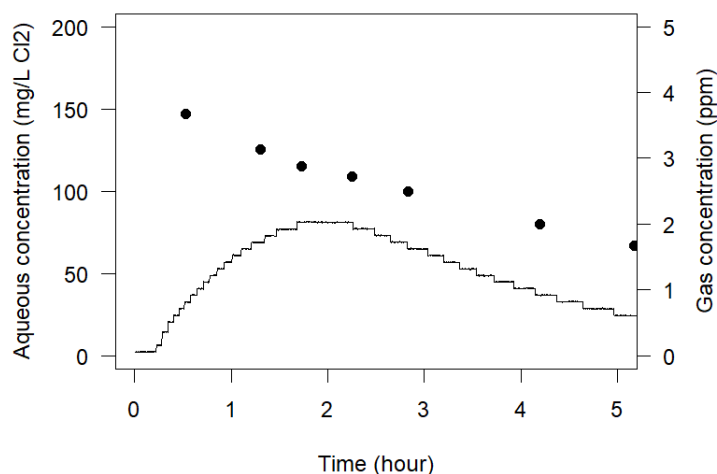


Figure 3 Time series plot for a chlorine-alone test with a NaOCl dose of 400 mg/L as Cl₂ at pH 6.5 and 20 °C. Line represents gas concentration reported by sensor. Filled circles are free chlorine concentrations.

To assess the effect of pH on the gas-phase response, tests were conducted at a free chlorine dose of 400 mg/L as Cl₂ and 20°C but at different pH values (6.5, 7.0 and 7.5), and the temporal trends reported by the gas sensor were compared (**Figure A-3; Table 8**). To quantify the pH effect, the mean values of t_p and C_p at each pH were calculated and compared between conditions. Variability in the values was quantified in terms of standard deviations (SD) and relative standard deviations (RSD) that were determined as the ratio of the SD values to the sample means. The values of sample means, SD and RSD for t_p and C_p are subsequently discussed.

The impact of pH on the magnitude of gas phase concentrations was assessed by comparing the observed results for C_p at pH 6.5, 7.0 and 7.5 and in this regard the mean values and variability in C_p between conditions were examined. The highest average C_p was observed at pH 7.0 at 4.1 ppm, while the average C_p values observed at pH 6.5 and 7.5 were similar (**Table 8**). However, the SD of C_p was also the greatest at pH 7.0. The greatest RSD in C_p was observed at pH 6.5 with an RSD value of 48%, followed by pH 7.0 (37%) and pH 7.5 (22%). When the substantial variability in C_p was considered, it was concluded that the observed C_p values did not show a distinguishable pattern with pH.

A similar analysis was completed to assess the impact of pH on t_p at pH 6.5, 7.0 and 7.5. The mean values of t_p appeared to decrease as pH increased from 6.5 to 7.5 (**Table 8**). However, the highest SD was again observed at pH 7.0. The greatest RSD in t_p was observed at pH 7.0 (15%), followed by pH 7.5 (12%) and pH 6.5 (7.5%). Thus, if the t_p data for pH 7.0 condition were not considered due to low reproducibility, the decrease in t_p as pH increased from 6.5 to 7.5 appeared to be significant. In conclusion, although t_p showed variability, it appeared that t_p decreased with pH. Furthermore, the RSD values of t_p at each pH showed that the observed t_p values were more consistent within each condition than the C_p values.

The corresponding aqueous phase responses at pH 6.5, 7.0 and 7.5 were also analysed (**Figure A-3**), and thus, the pH effect on aqueous free chlorine decay was assessed. The results from three replicate tests conducted at each pH were plotted (**Figure 4**). According to **Figure 4**, the rate of decay at pH 6.5 appears to have been distinctly lower than that at pH 7.0 or 7.5. The differences in decay rates resulted in great differences in chlorine concentration at 5 hr of the tests, where the concentration from tests at pH 6.5 were substantially higher than the other two pH levels. As results from three replicates were plotted under each condition, it appeared that the data points at pH 7.0 seemed to be more scattered than pH 6.5 and 7.5, which was consistent with the large variability observed in the gas-phase response under the same pH. In conclusion, pH appeared to influence the decay of free chlorine in the batch system, and thus affect the gas-phase response. The time series data for aqueous free chlorine concentration were subsequently used for model fitting (**Figure 5**) that related the gas- and aqueous responses.

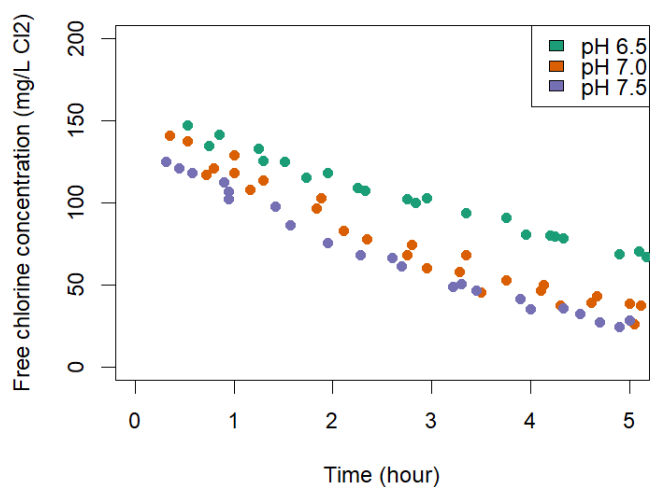


Figure 4 Time series plot for aqueous free chlorine concentrations from chlorine-alone tests at a NaOCl dose of 400 mg/L as Cl₂, 20 °C and pH 6.5 (green), 7.0 (orange) and 7.5 (purple).

The values of the parameters in the mass balance model were estimated by adjusting them until the model predictions matched the experimental results. In Phase I, it was assumed the observed gas consisted of only HOCl and hence the model was configured for this compound. Thus, the model was run with pre-determined values of Henry's law constants (H) and mass transfer coefficients ($K_L a$) for HOCl at 20°C. The first-order decay constant for aqueous free chlorine (k_{dl}) and the initial free chlorine concentration (C_{0l}) were estimated from the observed time series data of aqueous free chlorine concentrations that were previously described. It was assumed that the gas phase compound underwent decay in the headspace, and a first-order decay constant for the gas-phase free chlorine (k_{dg}) was estimated. Based on the previously discussed conceptual model, t_p was found to be a function of $K_L a$, k_{dl} , and k_{dg} as they collectively influenced the temporal trend of the gas-phase responses. Since the values of H , $K_L a$ and k_{dl} for HOCl were already obtained, k_{dg} was estimated by varying it until the model-predicted values for t_p fell within the range of values observed in the replicate experiments. In this approach, a single k_{dg} value was fit for all of the experiments that were conducted at a given chlorine dose as the pH of the aqueous solution was not expected to influence the gas phase decay. Following the model fitting procedures, the fit values of model parameters and the predicted values of t_p and C_p were obtained and are discussed subsequently.

Table 8 Fit model parameters along with observed and predicted gas-phase response characteristics at chlorine dose of 400 mg/L as Cl₂ and 20°C at pH 6.5, 7.0 and 7.5.

Model	Parameters/Characteristics	pH 6.5	pH 7.0	pH 7.5
Fit parameters	k_{dg} , hr ⁻¹	0.55	0.55	0.55
	k_{dl} , hr ⁻¹	0.17	0.30	0.33
	C_{0l} , mg/L as Cl ₂	160	160	145
Predicted	t_p , hr	1.75	1.43	1.37
	C_p , ppm as HOCl	2.5	1.9	1.2
Observed	t_p , hr	1.89±0.142	1.66±0.254	1.44±0.166
	C_p , ppm as Cl ₂	1.3±0.6	4.1±1.5	1.4±0.3
Predicted vs Observed	Ratio of predicted t_p vs observed mean t_p	0.93	0.86	0.95

Note: The observed data presented in the table are in the form of Sample Mean ± Sample Standard Deviation. Three replicates were run at each pH level.

The values of t_p that were predicted by the calibrated model were compared with the observed values to assess the quality of the model fit. From **Table 8**, it can be seen that the calibrated model predicted a decreasing trend in t_p with pH that was consistent with the observed values from the batch tests indicating that the model was able to capture the effect of pH on the gas-phase response. The predicted values of t_p were on average 91% of the observed values and were consistently above the lower bound of the standard deviation observed at each pH. Inspection of the fit parameters revealed that the decrease in t_p with pH was due to the combined effect of the increase in k_{dl} (**Table 8**) and decrease in $K_L a$ with pH for HOCl (**Table 5**). Therefore, as previously observed, pH had an effect on the chemical decay of free chlorine as well as the mass transfer process for HOCl as it undergoes speciation in aqueous solutions.

The predicted values of C_p were examined as an indicator of how the magnitude of the gas-phase response varied with pH values ranging 6.5-7.5 and 20°C. As pH increased from 6.5 to 7.5, the model revealed a decrease in C_p with pH where C_p decreased from 2.5 ppm to 1.2 ppm as HOCl (**Table 8; Figure 5**). It should be noted that this trend was not observed in the experimental data due to the large variability in gas-phase response reported by the sensor. The predicted values of C_p reasonably fell in the range of the observed values

at pH 6.5-7.5, though the model predicted a single substance that was assumed to be HOCl while the sensor interpreted the gas signal as Cl₂. Nonetheless, the temporal trend reported by the sensor was considered to be reliable. Thus, the magnitude of the gas concentration is not discussed in great detail in Phase I as the predicted C_p spanned a narrow range at values of 1.2 to 2.5 ppm as HOCl at pH 6.5-7.5 and 20°C, suggesting C_p might not be greatly sensitive to pH.

The values of the fit k_{dl} parameter were compared between pH conditions as they appeared to vary between pH 6.5, 7.0 and 7.5 (**Table 8**), which might provide insights into the chemical decay of free chlorine. As seen in **Figure 5**, the fit curves for aqueous phase response matched the observed response well. According to **Table 8**, the k_{dl} values increased from 0.17 to 0.33 hr⁻¹ as pH increased from 6.5 to 7.5. The k_{dl} value at pH 6.5 was particularly lower than that at pH 7.0 and 7.5, which was consistent with the previously described experimental observations (**Figure 4**). The fit k_{dl} values were comparable to the values of first-order chlorine decay coefficients observed in drinking water systems, where the water matrix is simple (Onyutha & Kwio-Tamale, 2022). However, the impact of pH on the first-order decay constants for free chlorine has been previously found to be minimal in drinking water (Liu et al., 2014). The impacts of pH observed in the current study may be associated with the high chlorine doses studied. Thus, the impact of pH on decay at elevated chlorine doses should be further examined as k_{dl} values were found to be a major factor influencing the temporal trend in gas-phase response at pH 6.5-7.5.

In summary, this analysis of results from the mechanistic model showed that pH was found to have an effect on the gas-phase response in the chlorine-alone batch system by acting on the values of k_{dl} , H and $K_L a$ for HOCl in Phase I. The model returned results that showed the same pH-dependent trend in t_p as the observed. While the pH-dependent trend in C_p was not observed according to the experimental data, the model revealed that C_p would decrease as pH increased from 6.5 to 7.5, though the extent of the decrease was found to be minimal. According to the model, the pH effect on the gas-phase response observed in Phase I was attribute to both mass transfer process for HOCl (H and $K_L a$) and chemical decay in solution (k_{dl}) as initially hypothesized. This suggests that the model was sufficient to reflect the difference in gas-phase responses at pH 6.5-7.5 and 20°C and hence was employed in Phase II and III.

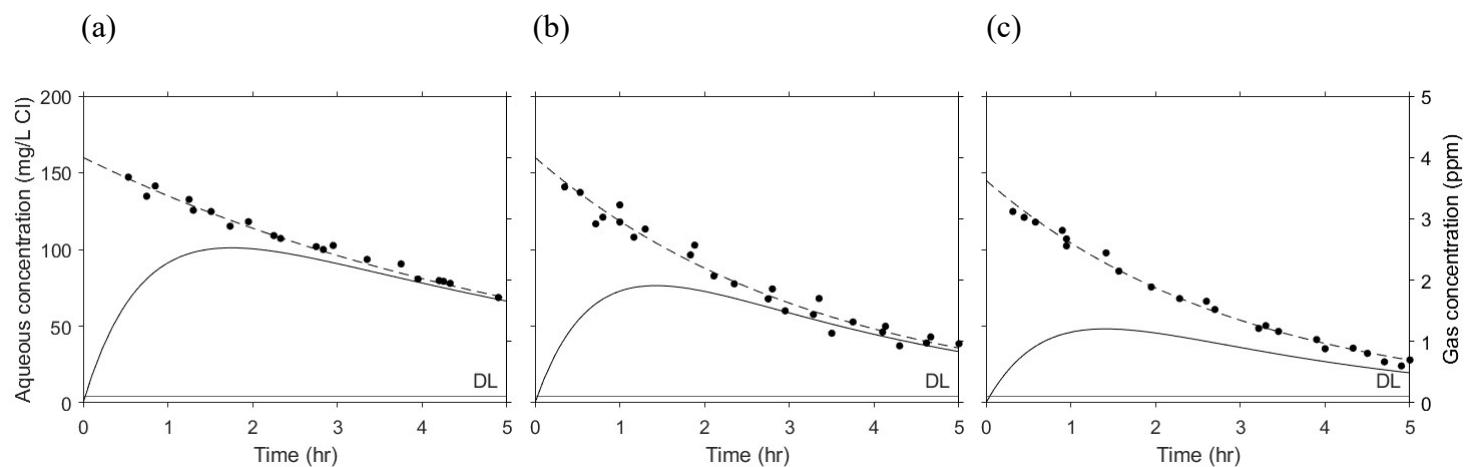


Figure 5 Model results for the temporal change of free chlorine concentrations in the headspace of the reactor and in the solution at 20°C and (a) pH 6.5, (b) pH 7.0, and (c) pH 7.5. Lines are modelled gas-phase concentration. Dashed lines are modelled aqueous concentration. Filled circles are observed aqueous free chlorine concentration from three replicates at each condition. Detection limit (DL) for the gas sensor is indicated as a horizontal line in each plot.

4.2.2 Phase II

In the chlorine-ammonia tests, the gas phase sensor reported detectable signals when the chlorine to ammonia-nitrogen mass ratio (Cl:N) was in the range of 8:1 to 16:1 at pH 6.5 and 20°C. As the temporal responses in both gas and aqueous phases were substantially different from those in Phase I, it was hypothesized that the detected gas consisted of NCl_3 , which is the most volatile product formed from the reaction between chlorine and ammonia (Holzwarth et al., 1984a). To understand the mechanisms leading to the observed gas-phase responses, the mass balance model used in Phase I was employed with a different set of parameter values for NCl_3 . The effect of Cl:N ratio was assessed in depth as it was believed to be a major factor affecting the gas-phase response. The effects of pH and temperature are also discussed in this section.

To illustrate the temporal pattern of gas-phase response observed in Phase II experiments and compare with Phase I observations, sensor data obtained from a representative test at a free chlorine dose of 400 mg/L as Cl_2 , pH 6.5 and 20°C with ammonia present at Cl:N mass ratio of 12:1 was plotted in **Figure 6**. From this figure, it can be seen that the gas concentration increased almost instantaneously and rapidly upon dosing the free chlorine solution, and it peaked before 0.5 hour of the batch test at a value of 8.7 ppm. After the peak concentration was reached, it dissipated rapidly and became undetectable after ~1.5 hour. Similar patterns in the gas-phase responses were observed at other conditions where measurable amounts of gas were detected (**Figure A-7**; **Figure A-8**). Compared to the temporal trends observed in Phase I (**Figure 3**), the gas-phase responses in Phase II were much more rapid and less persistent during the test. This suggested that, in Phase II where ammonia was present, the substance(s) that contributed to the pattern of sensor gas response were different from that in Phase I.

To investigate the chlorine substance(s) that contributed to the observed gas-phase responses, the aqueous concentrations of free chlorine, monochloramine (NH_2Cl), dichloramine (NHCl_2) and trichloramine (NCl_3) were analysed as they have previously been established to be the products of the reactions between free chlorine and ammonia (Chapter 2). The sum of all of the chlorine species analysed was used to estimate the total chlorine concentration (**Figure 6**). **Figure 6** shows that the concentration of total chlorine at 1 hr of the test was ~20 mg/L as Cl_2 , which was much lower than that observed in Phase I at the same condition in the absence of ammonia. Under this condition (**Figure 6**), NH_2Cl was the

dominant fraction of total chlorine, and this was followed by NHCl_2 . The concentrations of NH_2Cl and NHCl_2 appeared to slowly decrease over time after 1 hour, and within 4 hours of the test, the NHCl_2 concentration did not change substantially. In contrast, the concentration of NCl_3 decreased more rapidly after the first measurement and became undetectable at 1 hour of the test. Free chlorine was not detected after the first measurement. Based on the analysis of the aqueous phase responses for the various chlorine species, it was concluded that the corresponding gas phase response was not likely from free chlorine (as in Phase I) since there was relatively little present. Hence, the gas phase response was attributed to the presence of chloramines.

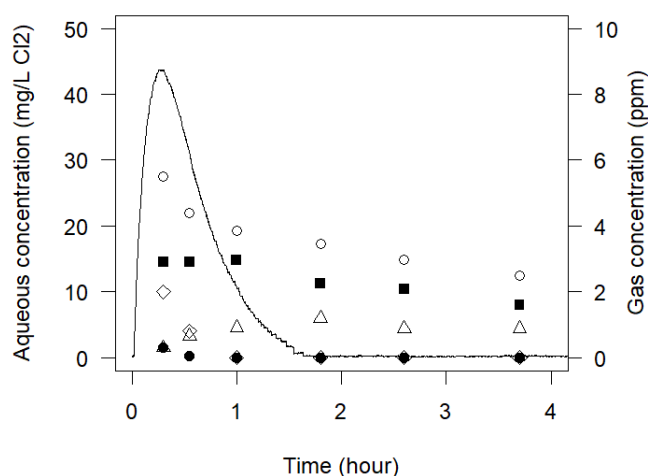


Figure 6 Time series plot for a chlorine-ammonia test with a NaOCl dose of 400 mg/L as Cl_2 at 20 °C, pH 6.5, and Cl:N mass ratio of 12:1. Open circles are total chlorine; squares are monochloramine; triangles are dichloramine; diamonds are trichloramine; filled circles are free chlorine.

To assess the effect of Cl:N mass ratio on the gas-phase response, a similar approach that was used in Phase I was employed to characterise gas-phase responses in Phase II. The peak gas concentration (C_p) was highly influenced by the Cl:N mass ratio (**Figure A-7**; **Figure A-8**). At Cl:N ratios of 4.6:1 and 8.0:1 and pH 6.5, little gas was detected by the gas sensor. Thus, these two conditions were excluded from the following discussion. As the Cl:N ratio increased from 10:1 to 16:1 at pH 6.5 (**Table 9**), the mean value of C_p increased until a value of 12:1, after which it decreased as the Cl:N ratio further increased. Under these conditions, the values of C_p ranged from 2.3 ppm to 13.8 ppm, where the highest C_p value

was observed at the Cl:N ratio of 12:1. However, the highest standard deviations (SD) of C_p was also observed at the Cl:N ratio of 12:1. Thus, to compare the variability in C_p values between the different Cl:N ratios, relative standard deviations (RSD) were calculated and found to be highest at a Cl:N ratio of 14:1 (52%), followed by 12:1 (40%), 16:1 (16%), and 10:1 (7.9%). The RSD values were comparable to those observed in the Phase I tests, indicating that the variability in C_p values was inherent to the test apparatus. Nonetheless, the trend in the mean values of C_p appeared to be affected by to the Cl:N mass ratio, as the values increased as Cl:N ratio increased from 8.0:1 to 12:1 and decreased as Cl:N ratio further increased to 16:1.

Table 9 Fit model parameters along with observed and predicted gas-phase response characteristics at pH 6.5 and 20°C with Cl:N mass ratios 10:1, 12:1, 14:1 and 16:1 applied.

Model	Parameters /Characteristics	Cl:N 10:1	Cl:N 12:1	Cl:N 14:1	Cl:N 16:1
Fit parameters	k_{dg} , hr ⁻¹	4.0	4.0	4.0	-
	k_{dl} , hr ⁻¹	6.0	3.7	3.0	-
	C_{0l} , mg/L as Cl ₂	15	30	23	-
Predicted	t_p , hr	0.200	0.256	0.282	-
	C_p , ppm as NCl ₃	2.8	7.1	6.0	-
Observed	t_p , hr	0.20±0.013 (3)	0.26±0.046 (3)	0.28±0.040 (4)	0.37±0.057 (2)
	C_p , ppm as Cl ₂	2.9±0.2 (3)	9.6±3.9 (3)	5.1±2.7 (4)	2.6±0.4 (2)

Note: The observed data presented in the table are in the form of Sample Mean ± Sample Standard Deviation (Number of replicates).

The time to peak (t_p) was calculated from the observed data as an additional characteristics of the gas-phase response, and its values were compared with the Cl:N mass ratios (**Table 9**). **Table 9** shows that the mean t_p value appeared to increase from 0.20 to 0.37 hr as the Cl:N mass ratio increased from 10:1 to 16:1. The RSD values for t_p at Cl:N ratios of 16:1, 14:1, 12:1 and 10:1 were relatively consistent with values of 15%, 14%, 18% and 6.7%, respectively. Considering the variability between each condition, it appeared that at Cl:N ratios of 12:1 and 14:1, there was little difference in the observed t_p values. Nonetheless, the t_p value at a Cl:N ratio of 10:1 appeared to be substantially lower than that at Cl:N 12:1 or 14:1. Similarly, the t_p at a Cl:N ratio of 16:1 appeared to be substantially higher than that at

Cl:N 12:1 or 14:1. Overall, it appeared that there was an increase in t_p values with increasing Cl:N mass ratio, though the difference between the Cl:N ratios 12:1 and 14:1 appeared to be insignificant.

The aqueous concentrations of NH_2Cl , NHCl_2 and NCl_3 at the different Cl:N mass ratios were examined to infer the aqueous chlorine species that may have contributed to the gas-phase responses observed in Phase II (**Figure A-7**; **Figure A-8**). At relatively low Cl:N ratios, i.e. 4.6:1 and 8.0:1 at pH 6.5, no free chlorine or NCl_3 was detected in solution. At a Cl:N ratio of 4.6:1, NH_2Cl appeared to be the main species and this was followed by NHCl_2 , which became the main species as the Cl:N ratio increased to 8.0:1. At these two ratios, the concentrations of either NH_2Cl or NHCl_2 were above 50 mg/L as Cl_2 in first hour of the test. However, the sensor barely reported little gas at these ratios. Only a small peak of gas-phase response was captured by the sensor in a short period of time at the ratio of 8.0:1 with a peak concentration less than 1 ppm. This suggests that both NH_2Cl and NHCl_2 were not detected by the sensor in the headspace of the batch system even though they have been reported to be more volatile than HOCl (**Table 1**).

When relating the aqueous and gas-phase responses in Phase II, the gas reported by the sensor was hypothesised to be NCl_3 at Cl:N mass ratios of 10:1, 12:1 and 14:1. At Cl:N mass ratios ranging from 10:1 to 16:1, NCl_3 along with free chlorine were detected in the solution within 1 hour of the tests at relatively low concentrations (**Figure A-7**; **Figure A-8**). The contribution of free chlorine to the gas-phase response at these ratios was considered to be negligible since in Phase I no measurable gas was reported by the sensor when the free chlorine concentration in the solution was below 10 mg/L as Cl_2 (**Figure A-5**), which was the case at Cl:N ratios of 10:1, 12:1 and 14:1. However, at a Cl:N ratio of 16:1, the temporal pattern of the gas-phase response appeared to be different from those at other ratios with higher t_p values (**Table 9**), which could be due to the relatively high concentrations of free chlorine (~ 20 mg/L as Cl_2 at the first measurement) in the solution that contributed to the reported gas signal. This suggests that the contribution of free chlorine to the gas signal reported by the sensor could not be excluded at the Cl:N ratio of 16:1 and potentially at higher ratios due to increasing excess of free chlorine in the solution. In conclusion, the measurable gas that was reported at Cl:N ratios of 10:1, 12:1 and 14:1 was attributed to NCl_3 instead of other chlorine species investigated in the study. Thus, a mass balance model was employed in the subsequent analysis with parameters that were estimated for NCl_3 .

The data on aqueous NCl_3 concentrations and the characteristics of the gas phase responses obtained from Phase II experiments were used to estimate the parameters of the mass balance model. The model fitting procedure previously described in Phase I was employed in Phase II. The values of first-order decay constant for NCl_3 (k_{dl}) and the initial NCl_3 concentration in the solution (C_{l0}) were estimated from the time series data for aqueous NCl_3 at each condition. The value of the first-order decay constant for the gas-phase NCl_3 (k_{dg}) was then estimated by adjusting it until the model-predicted values for t_p fell within the range of values observed in the replicate experiments. The value of k_{dg} was expected to be independent of pH and the Cl:N mass ratio applied in the solution. Thus, the values of fit parameters were obtained and are discussed subsequently.

To assess the quality of the model fit, the predicted values of t_p were compared with the observed values and the values of fit parameters estimated at each Cl:N mass ratio are discussed. According to **Table 9**, the model-predicted values of t_p fell within the range of the observed values and they increased with the Cl:N ratio. The trend in predicted values of t_p corresponded to a decrease in the k_{dl} values with Cl:N ratio as the values of k_{dg} did not change with Cl:N ratio. In conclusion, with the estimated k_{dl} , k_{dg} values and previously estimated $K_L a$ and H for NCl_3 , the predicted values of t_p fit reasonably well with the observed data.

Since the value of k_{dl} appeared to substantially impact the predicted values of t_p , the values of k_{dl} were examined relative to the Cl:N mass ratio. According to the model, the predicted values k_{dl} ranged from 3.0 to 6.0 hr^{-1} as the Cl:N mass ratio increased from 10:1 to 14:1 at pH 6.5 and 20°C (**Table 9**). The estimated k_{dl} values are more than 10 times higher than the first-order decay constants reported by Saguinsin and Morris (1975) and may have been due to the higher initial concentrations employed in the current tests. However, given the limited data on aqueous NCl_3 concentration in replicate tests, there was uncertainty associated with the estimation of the decay constants from the measured concentrations for NCl_3 in the solution (**Figure 7**). Thus, future investigations should further examine the impact of the Cl:N mass ratio on the rate of NCl_3 decay.

The predicted values of C_p were examined to assess the effect of Cl:N mass ratio on the magnitude of the gas-phase response and the corresponding initial concentration of NCl_3 in the solution (C_{l0}). The trend in predicted values of C_p with Cl:N ratio was consistent with

the observed trend with the greatest C_p value predicted at a Cl:N mass ratio of 12:1 (**Table 9**). Meanwhile, the fit values of C_{l0} followed the same trend with the greatest C_{l0} value also estimated at Cl:N 12:1. This suggests that C_{l0} was an important factor affecting the magnitude of the gas-phase response, though there was uncertainty when estimating C_{l0} due to the limited availability of data on aqueous NCl_3 concentration at the very beginning of the tests. Viewed collectively, the predicted values of C_p followed the same trend as reported by the sensor and appeared to be substantially affected by the Cl:N mass ratio which impacted on C_{l0} values. As will be subsequently demonstrated in a sensitivity analysis, C_{l0} was the most influential factor in the value of C_p that was employed as an indicator of the magnitude of the gas-phase response.

The effect of pH on the gas-phase response was assessed at a Cl:N mass ratio of 10:1 over a range of pH values including 6.5, 7.0 and 7.5. Compared to the mean C_p value of 2.9 ppm that was observed at a pH 6.5 (**Table 9**), the mean C_p observed at pH 7.0 was 1.6 ppm (**Figure A-9**) and no measurable gas was reported by the sensor at pH 7.5 (**Figure A-10**). While the mean t_p was 0.20 hr at pH 6.5, a lower mean t_p value (0.13 hr) was observed at pH 7.0. As the aqueous NCl_3 concentration was below detection at neither pH 7.0 or 7.5, it was speculated that the observed decrease in the values of C_p and t_p with pH was due to an increase in the decay rate of NCl_3 at elevated pH values. The increase in rates of NCl_3 decomposition with pH has been reported in previous studies as discussed in Chapter 2. In conclusion, the effect of pH over values ranging from 6.5-7.5, on the gas-phase response was substantial at a Cl:N mass ratio of 10:1. When compared with the Phase I results, the gas-phase response observed in Phase II appeared to be more sensitive to pH which was consistent with the unstable nature of NCl_3 .

The effect of temperature (15°C and 20°C) on the gas-phase response was assessed at a Cl:N mass ratio of 12:1 and pH 6.5. At 15°C, the mean C_p value (5.6 ± 2.5 ppm; **Figure A-11**) was lower than that observed at 20°C (**Table 9**), while the mean t_p value (0.29 ± 0.043 hr) was greater than that observed at 20°C. The delay in the time to peak was attributed to decreases in decay rate constants in both gaseous and aqueous phases as well as the mass transfer rate. Thus, with the temperature-corrected $K_L a$ for NCl_3 at 20°C, the same model was run with lowered values of k_{dg} (3.6 hr^{-1}) and k_{dl} (3.3 hr^{-1}). The model-predicted C_p and t_p values were 6.7 ppm and 0.285 hr, respectively, which fell in the range of observed values. According to **Figure 7**, temperature appeared to have a minor impact on the liquid-phase

concentrations, though there is a lack of studies on the impact of temperature on the rate of NCl_3 decay. Overall, temperature was observed to impact the gas-phase response and the model parameters needed to be adjusted to predict the observed trends.

In summary, the gas-phase responses observed in Phase II were distinctly different from those in Phase I. As a result, the values of the fit parameters k_{dg} , k_{dl} , H and $K_L a$ for the mechanistic model were substantially different from those estimated in Phase I. Thus, the substance that contributed to the gas-phase responses was concluded to be NCl_3 , which was cross-detected by the chlorine gas sensor. Model analysis showed that the gas-phase response was affected by the Cl:N mass ratio, pH and temperature, with the greatest gas-phase response observed at a Cl:N ratio of 12:1 pH 6.5 and 20°C. The results from Phase II provided a reference for Phase III that evaluated the effect of water matrix on the gas-phase response.

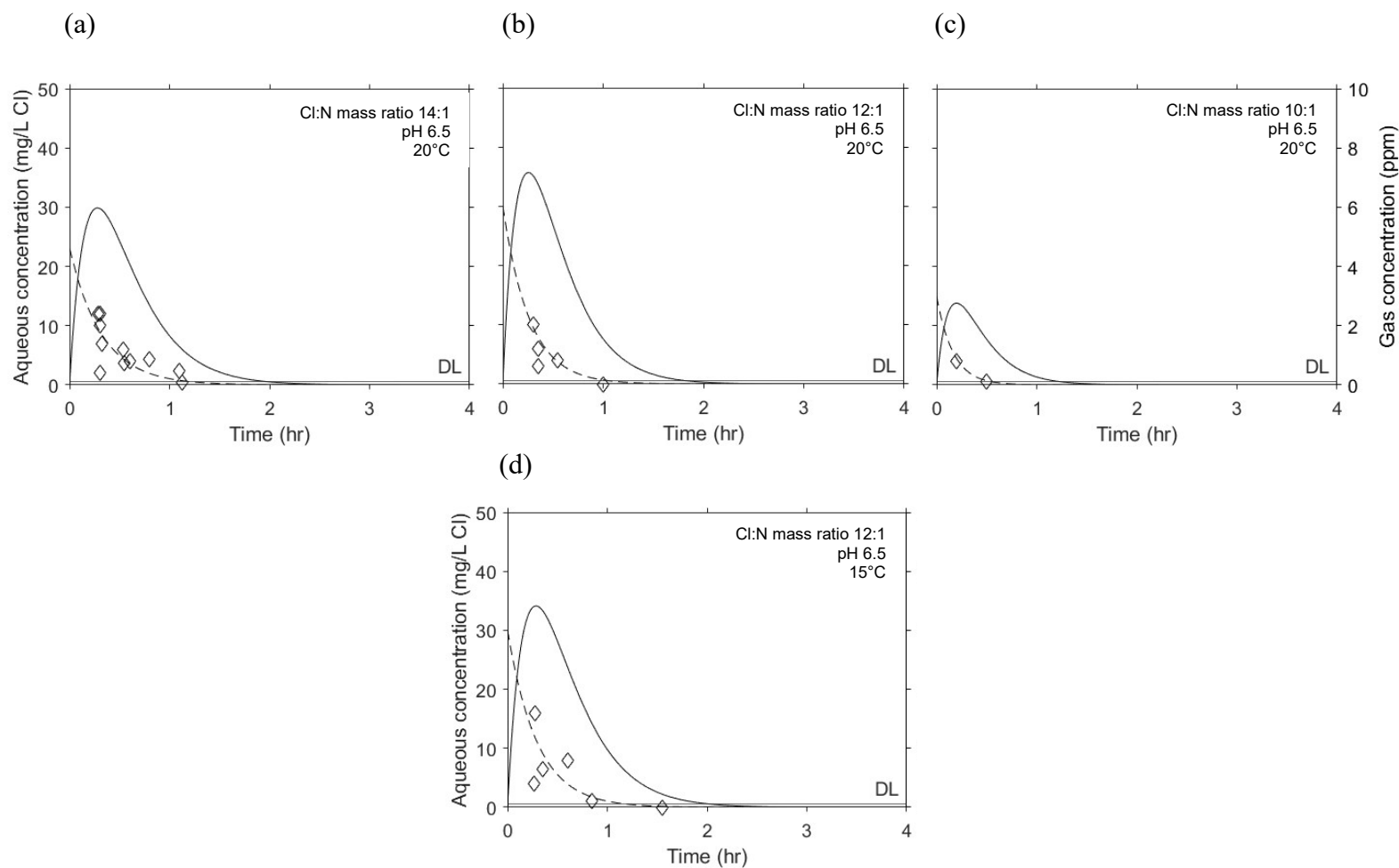


Figure 7 Model results for the temporal change of trichloramine concentrations in the headspace of the reactor and in the solution at Cl:N mass ratios of 14:1 (a), 12:1 (b, d) and 10:1 (c). Plots (a), (b) and (c) are at pH 6.5 20°C; (d) at pH 6.5 15°C. Lines are modelled gas-phase concentration. Dashed lines are modelled aqueous concentration. Diamonds are observed aqueous trichloramine concentration. Detection limit (DL) for the gas sensor is indicated as a horizontal line in each plot.

4.2.3 Phase III

In the chlorine-wastewater tests, a detectable gas was consistently reported by the chlorine gas sensor through a range of conditions: ammonia concentrations of 28-38 mg/L NH₄-N, pH values of 6.5-7.5 and temperatures of 15 and 20°C. The composition of the gas was considered to be similar to that in Phase II, though the gas concentrations were in lower magnitude. Thus, to understand the difference in the gas-phase responses between Phase II and III, tests were conducted at similar conditions so that the effect of the water matrix on the gas-phase responses was directly assessed. The same mass balance model used in Phase II was employed to simulate the gas-phase responses in Phase III with altered values of fit parameters. The effects of pH and temperature were examined and discussed in this section. The characteristics of the wastewater used for the tests are presented in Appendix (A. 8).

To illustrate the temporal pattern of gas-phase responses observed in Phase III experiments, sensor data obtained from a representative test at a free chlorine dose of 400 mg/L as Cl₂, pH 6.5 and 20°C with ammonia present at a Cl:N mass ratio of 11.6:1 is presented (**Figure 8**). **Figure 8** shows that the gas concentration increased shortly after dosing the free chlorine solution and peaked around 0.5 hour of the test at a value of 2.2 ppm. Then, it declined to zero at 3 hours of the test. Similar to the temporal trends observed in Phase II, the gas-phase response was not as persistent as observed in Phase I. However, different from the results in Phase II, the gas-phase response observed in Phase III appeared to be less rapid and lower in the magnitude of the gas concentration which was attributed to differences in the water matrix.

To help interpret the gas-phase response, the aqueous concentrations of free chlorine, monochloramine (NH₂Cl), dichloramine (NHCl₂) and trichloramine (NCl₃) were analysed following the same procedure used in Phase II (**Figure 8**). As seen in **Figure 8**, the concentrations of NH₂Cl and NHCl₂ were close to the detection limit, which was 1.0 mg/L as Cl₂. Hence, the main fraction of total chlorine was free chlorine, and this was followed by NCl₃, indicating that the breakpoint stoichiometry had been reached (Pressley et al, 1972). During the test period, the total chlorine concentration decreased from ~40 mg/L as Cl₂ at the time of the first measurement to ~10 mg/L as Cl₂ at 4 hours of the test, similar to the observed trend at a Cl:N mass ratio of 14:1 in Phase II. Moreover, the concentration of NCl₃ appeared to be at a similar level at the start of the test as observed in Phase II but it declined at a lower rate. This suggested that, in the wastewater, the decay of NCl₃ was reduced by the presence of

free chlorine, which reacted faster with other reducing constituents (Soltermann et al., 2015). Another reason might be that NCl_3 had partially and slowly formed from the reaction between free chlorine and urea and/or other organic precursors in wastewater during the test. In conclusion, considering the relative concentrations of chlorine species in the solution and relatively high volatility of NCl_3 , it was believed that NCl_3 was the main contributor to the gas-phase response in Phase III when the Cl:N mass ratio was 11.6:1.

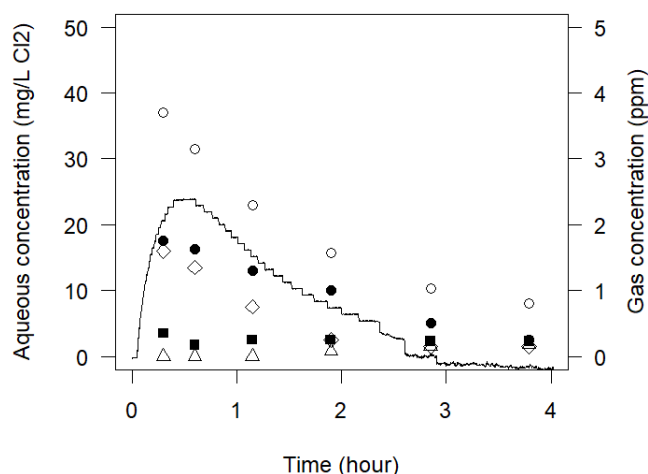


Figure 8 Time series plot for a chlorine-wastewater test with a NaOCl dose of 400 mg/L as Cl_2 to yield a Cl:N mass ratio of $\sim 11.6:1$ at pH 6.5 and 20°C. Open circles are total chlorine; squares are monochloramine; triangles are dichloramine; diamonds are trichloramine; filled circles are free chlorine.

In addition to the effect of the water matrix, the effects of pH and temperature on the gas-phase response were also assessed in Phase III. The wastewater tests were conducted at three conditions: pH 6.5 20°C, pH 7.5 20°C, and pH 6.5 15°C (**Figure A-12; Table 10**). According to **Table 10**, the mean t_p values ranged from 0.52 to 0.59 hr among the three conditions, which was a relatively narrow range. When considering the standard deviation (SD) values that were calculated from the replicate tests, it appeared that the t_p values were consistent across the three conditions, and therefore, pH and temperature had little impact on t_p though the number of data was limited. Nonetheless, when compared with the Phase II results at the corresponding conditions, the t_p values observed in Phase III were about two times higher, indicating the rates of change in gas-phase concentrations were lower in Phase III considering the low magnitude of the gas concentrations reported.

The values of C_p were compared between the three conditions to assess the effect of pH and temperature on the magnitude of the gas-phase responses. Compared to the mean value of C_p at pH 6.5 and 20°C, the mean values of C_p at conditions of pH 7.5 and 20°C and pH 6.5 and 15°C were lower (**Table 10**). However, the relative standard deviations (RSD) were found to be highest at pH 6.5 and 20°C (52%), followed by pH 6.5 and 15°C (37%), and pH 7.5 and 20°C (11%). Thus, considering the high RSD values observed at 20°C and 15°C at pH 6.5, the 5°C of change in temperature appeared to have minimal impact on C_p . In contrast, because of the relatively low RSD value observed at pH 7.5 and 20°C, the mean C_p was lower than that at pH 6.5 at the same temperature. Therefore, elevation in pH from 6.5 to 7.5 resulted in lower C_p values, while increasing temperature from 15°C to 20°C had relatively small impact on C_p value. These trends were consistent with the Phase II observations under equivalent conditions.

Table 10 Fit model parameters along with observed and predicted gas-phase response characteristics at pH 6.5 20°C, pH 7.5 20°C, and pH 6.5 15°C.

Model	Parameters /Characteristics	pH 6.5 20°C	pH 7.5 20°C	pH 6.5 15°C
Fit parameters	k_{dg} , hr ⁻¹	4.0	4.0	3.6
	k_{dl} , hr ⁻¹	0.85	0.90	0.75
	C_{0l} , mg/L as Cl ₂	25	6	25
Predicted	t_p , hr	0.487	0.477	0.533
	C_p , ppm as NCl ₃	2.1	0.5	1.9
Observed	t_p , hr	0.52±0.088 (3)	0.59±0.085 (2)	0.59±0.021 (2)
	C_p , ppm as Cl ₂	2.1±1.1 (3)	0.65±0.07 (2)	0.95±0.35 (2)

Note: The observed data presented in the table are in the form of Sample Mean ± Sample Standard Deviation (Number of replicates).

As the gas phase responses from the wastewater tests generally had lower peaks that persisted longer than those in Phase II and the aqueous concentrations of NCl₃ were similar, it was hypothesized that the lower magnitude of the gas-phase response was due to the reduction in the mass transfer rate for NCl₃ in wastewater. The reduction of the overall mass transfer coefficient for oxygen in wastewater is typically described by an “alpha-factor” (α) (Gilbert, 1979; as cited in Munz & Roberts, 1989). A typical value of 0.79 has been reported for α when filtered wastewater was compared to MQ-water (Munz & Roberts, 1989).

However, information on the liquid-gas transfer of NCl_3 in wastewater was not available in the literature. Hence, to model the gas-phase response of NCl_3 which was formed in the wastewater phase, the α value for NCl_3 was adjusted when matching model predictions to observed data.

To model the gas-phase response observed in Phase III, values of the model parameters were estimated following a similar procedure as described in Phase II. The gas-phase response reported by the sensor was attributed to NCl_3 , as determined in Phase II. The values of the decay constant for NCl_3 (k_{dl}) and the initial NCl_3 concentration in the solution (C_{l0}) were estimated from the time series data for aqueous NCl_3 at each condition. The values of first-order decay constant for the gas-phase NCl_3 (k_{dg}) were maintained the same as in Phase II as the k_{dg} values were not expected to change in the gas above a different water matrix in the batch reactor. To account for the effect of water matrix on the mass transfer process, an α value was applied to correct the value of the mass transfer coefficient ($K_L a$) for NCl_3 and was estimated from the model fit to the data.

The model predicted values of t_p were compared with the observed to assess the fit of the model. The predicted values of t_p among the three test conditions ranged from 0.48 to 0.53 hr, which was a narrower range than the observed values considering the variability (**Table 10**). Consistent with the observed values, the predicted t_p observed values did not vary substantially among the three conditions. This suggests that t_p might not be highly sensitive to changes in pH over the range of 6.5-7.5 or temperature over 15-20°C in the wastewater at a Cl:N mass ratio of 11.6:1.

The model-predicted values of C_p and the corresponding initial concentration of NCl_3 in the solution (C_{l0}) were examined to assess the effect of pH (6.5 and 7.5) on the gas-phase response at 20°C. Consistent with the observed results, the predicted value of C_p was lower at pH 7.5 than pH 6.5, corresponding to the lower value of C_{l0} fit from the aqueous phase data (**Table 10; Figure 9**). The decrease in the value of C_p with pH was consistent with the trend observed in Phase II, suggesting that pH (6.5 and 7.5) impacted on the magnitude of the gas-phase response as a result of reducing initial NCl_3 concentration in the solution with either a simple or complex matrix. Furthermore, the fit value of C_{l0} at pH 6.5 was at a similar level to that in Phase II, suggesting the overall reduction in C_p was due to the lower rate of mass transfer process.

A similar analysis was conducted to assess the effect of temperature (15°C and 20°C) on the gas-phase response at pH 6.5. When comparing C_p values at 15°C and 20°C, a difference of 0.2 ppm was observed (**Table 10**). This suggested that temperature had limited impact on C_p as it was expected to not affect C_{l0} which appeared to be a major factor affecting the magnitude of the gas-phase response as discussed previously. Nonetheless, the model-predicted decrease in C_p at 15°C was consistent with the temperature dependency as predicted in Phase II.

The values of the fit parameters were examined to understand how the gas- and aqueous phase responses were affected by the water matrix. As previously mentioned, the lower magnitudes in gas-phase responses were attributed to the reduction in mass transfer rates from the wastewater matrix. An α value of 0.2 was estimated from the model fitting and applied to the mass transfer coefficient ($K_L a$), which is lower than the values that have been reported for oxygen in raw wastewater (0.55-0.56; Hebrard et al., 2000). The values of k_{dl} were found to be lower than the values estimated in Phase II and were not distinctly different across the test conditions (**Table 10; Figure 9**). Thus, the decay of NCl_3 in wastewater does not appear to be as sensitive to changes in wastewater condition as observed in Phase II. Overall, the difference in the gas-phase responses between Phase II and III was primarily attributed to the decrease in $K_L a$ by a factor of 0.2, which limited the amount of gas that was volatilized in the headspace of the batch system. As the values k_{dl} were lower in wastewater and relatively insensitive to changes in pH and temperature, the persistence of NCl_3 in raw wastewater potentially allows the presence of aqueous NCl_3 as a source of the volatilization in sewer systems for a long period of time.

In summary, the magnitude of the gas-phase responses observed in Phase III were substantially lower than those in Phase II when similar conditions were compared. The difference in the gas-phase responses between the two Phases was mainly attributed to the reduction in the rate of the liquid-gas mass transfer process, where the overall mass transfer coefficient ($K_L a$) was lowered by a factor of 0.2 to match the observed results. Fitting of the models to the observed data showed that the magnitude of the gas-phase response was largely affected by pH in the range of 6.5-7.5 but less affected by temperature, which was consistent with the findings in Phase II.

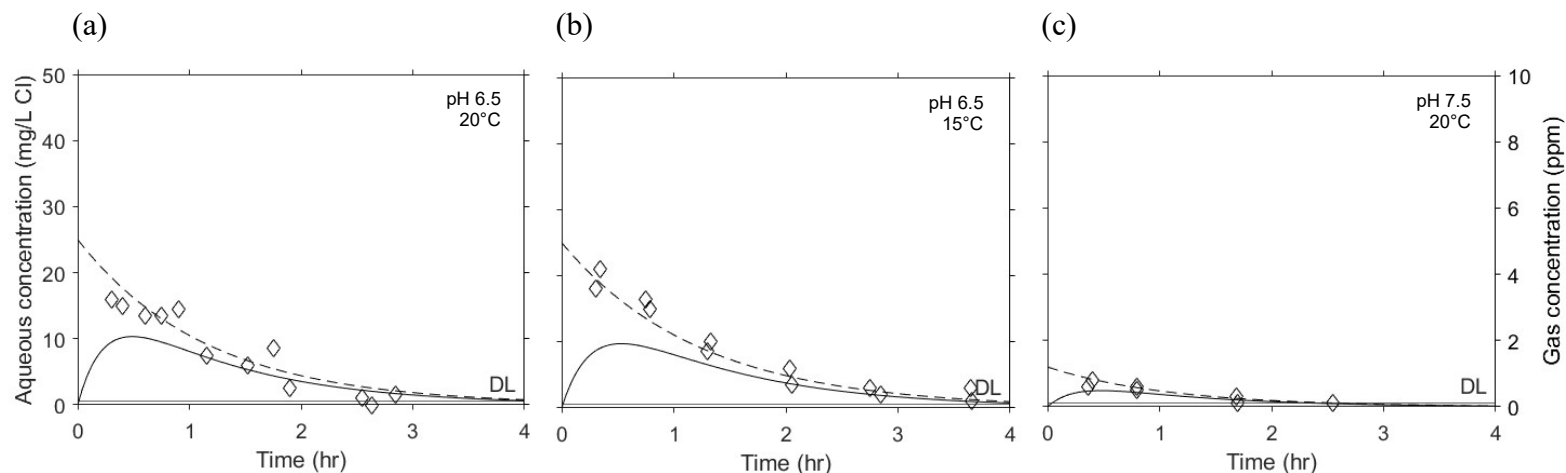


Figure 9 Model results for the temporal change of trichloramine concentrations in the headspace of the reactor and in the solution at a Cl:N mass ratio of $\sim 11.6:1$ at (a) pH 6.5 20°C, (b) pH 6.5 15°C, and (c) pH 7.5 20°C. Lines are modelled gas-phase concentration. Dashed lines are modelled aqueous concentration. Diamonds are observed aqueous trichloramine concentration. Detection limit (DL) for the gas sensor is indicated as a horizontal line in each plot.

4.3 Sensitivity analysis

A sensitivity analysis of the mass balance model was performed to assess the relative impacts of the model parameters on the characteristics of the gas-phase response, i.e., t_p and C_p . The five model parameters, H , $K_L a$, k_{dg} , k_{dl} and C_{0l} , were analysed one at a time, while other parameters were held constant. The analysis was conducted at one test condition as the base case, where the greatest peak gas-phase concentrations were observed (at Cl:N ratio of 12:1, pH 6.5 and 20°C). The values of the five parameters at the condition were varied $\pm 10\%$ from their base values (**Table 9**). For each parameter, changes in the values of the model outputs, i.e., t_p and C_p , were obtained by running the model with the varied parameter value (**Table 11**). The slope of the change in the value of either t_p or C_p with respect to the change in the value of the parameter was calculated and referred to as sensitivity coefficient (S). To allow better comparisons between parameters, the sensitivity coefficient was normalized by multiplying it by the base value of the model parameter over the model output (S_n). Hence, the relative impacts of the model parameters on output values of t_p and C_p are discussed subsequently.

The values of the sensitivity coefficient and the normalized values were compared between the five parameters to assess their impacts on the base model output values of C_p (**Table 11**). According to **Table 11**, the values of C_{0l} , $K_L a$, and H had positive impacts on the value of C_p , while k_{dl} and k_{dg} had negative impacts. When comparing the values of sensitivity coefficients, $K_L a$ had the greatest impact on C_p . When comparing the values of normalized sensitivity coefficients, the value for C_{0l} was 1.00, indicating C_p was linearly related to C_{0l} in the base model. Followed by C_{0l} , the value of normalized sensitivity coefficient for $K_L a$ was close to 1, which confirmed its substantial impact on C_p . The values of normalized sensitivity coefficients for k_{dl} and k_{dg} were similar, suggesting their impacts on C_p were comparable as their base values were similar (**Table 9**). In contrast, H had the lowest value of normalized sensitivity coefficient, suggesting the model value of C_p was least sensitive to H . In conclusion, with the interpretation of sensitivity coefficients for the five model parameters, the response of the base model in term of C_p was most sensitive to C_{0l} and $K_L a$, moderately sensitive to k_{dl} and k_{dg} but relatively insensitive to H .

A similar analysis was completed to assess the relative impact of the five parameters on the base model output values of t_p (**Table 11**). According to **Table 11**, the values of $K_L a$,

k_{dl} and k_{dg} had negative impacts on t_p , while H had a positive impact. C_{0l} did not have an effect on the value of t_p as it only affected the magnitude of the gas-phase response. When comparing the values of the normalized sensitivity coefficients, k_{dl} and k_{dg} had similar and moderate impacts on t_p . In contrast, $K_L a$ had a relatively minor impact on t_p , while H again had the least impact. Therefore, the response of the base model t_p was most sensitive to k_{dl} and k_{dg} followed by $K_L a$ and H , and it was unaffected by C_{0l} .

Table 11 Estimated values of sensitivity coefficient (S) and normalized sensitivity coefficient (S_n).

Response/ Parameter	C_p		t_p	
	S^a	S_n	S^b	S_n
C_{0l}	0.238	1.00	0.0000	0.000
$K_L a$	80.2	0.984	-0.0457	-0.016
k_{dl}	-0.926	-0.480	-0.0335	-0.484
k_{dg}	-0.907	-0.508	-0.0321	-0.502
H	0.094	0.004	0.0031	0.004

Notes:

$$\text{Sensitivity coefficient: } S = \frac{C(P_{base+10\%}) - C(P_{base-10\%})}{20\% \cdot P_{base}}$$

$$\text{Normalized sensitivity coefficient: } S_n = S \cdot \frac{P_{base}}{C(P_{base})}$$

^a The units of sensitivity coefficient are ppm/(mg/L as Cl₂) for C_{0l} ; ppm hr for $K_L a$, k_{dl} and k_{dg} ; ppm for H .

^b The units of sensitivity coefficient are hr/(mg/L as Cl₂) for C_{0l} ; hr² for $K_L a$, k_{dl} and k_{dg} ; hr for H .

The significance of the most influential parameters in the base model and their impacts on the responses of t_p and C_p are discussed relative to the methods that were employed for estimating the values of the parameters. According to the above analysis, the value of C_p was highly sensitive to C_{0l} and $K_L a$ in the base model. High variability in C_p was consistently observed in all phases of experiments, which could be due to the uncertainty in the values of C_{0l} and $K_L a$. While C_{0l} was estimated from the limited aqueous phase data for NCl₃, $K_L a$ for NCl₃ was estimated from empirical correlations of the experiment data that had a relative standard deviation of 24%, though the method was believed to best approximate the

true value of $K_L a$ in the batch system. In contrast, the value of t_p was less sensitive to $K_L a$ but more sensitive to k_{dl} and k_{dg} . The former was estimated from the limited aqueous phase data for NCl_3 , while the latter was estimated from model fitting to the data on gas-phase responses. However, the uncertainty in the estimated values of k_{dg} was not able to be quantified due to the absence of analytical methods for gas-phase NCl_3 . Therefore, considering the limitations in NCl_3 analysis, the current methods employed for model calibration were believed to produce the accurate results for the influential parameters.

In summary, the sensitivity analysis revealed that C_p was most sensitive to C_{0l} and $K_L a$, while t_p was sensitive to k_{dl} and k_{dg} in the base model. Both t_p and C_p were insensitive to H . This suggests that, when the magnitude of the gas-phase response was concerned in a similar system, accurate characterisation of C_{0l} and $K_L a$ for modeling the gas-phase response would be of critical importance. If the timing of the peak gas-phase response was concerned, the rate constants of the first-order decay reactions in both aqueous and gas phases would be important parameters to be quantified.

Chapter 5: Conclusions and Recommendations

The current study investigated the chlorine substances that were produced from aqueous solutions and caused a commercial chlorine gas sensor to generate measurable signals across a range of experimental conditions. To evaluate the effect of water matrix and composition on the gas-phase response reported by the sensor, experiments were conducted in three phases. In Phase I where only free chlorine was present in the solution at neutral pH, the gas-phase responses were attributed to HOCl, which is an uncharged free chlorine species that was present in the solution in measurable concentrations. In Phase II where ammonia was present in the solution at neutral pH, NCl_3 formed and contributed to the gas-phase responses at Cl:N ratios between 10:1 and 14:1. Similar trends in gas-phase responses were observed in Phase III where wastewater was used, but the responses were lower in magnitude and more persistent compared to Phase II. The mass transfer of NCl_3 from the liquid to the gas was greatly reduced due to the wastewater matrix employed. Thus, a major finding from the experimental observations is that the chlorine gas sensor employed at the sewer system were able to cross-detect NCl_3 , which was formed from the fast reactions between chlorine and ammonia in the aqueous solution and subsequently volatilized into the headspace of the system. The gas-phase responses were found to be influenced by Cl:N ratio, pH, temperature and water matrix.

To support the findings from the batch experiments, a mass balance model that included the processes of liquid-gas mass transfer at the interface and chemical decay at the bulk phases was developed and employed for analysis. Model parameters were estimated either using empirical correlations or by fitting to the observed data. The model-predicted outputs fell within the range of observed variability. It was found that the magnitude of the gas-phase response for NCl_3 was substantially sensitive to its overall mass transfer coefficient ($K_L a$) in the system, compared to its first-order decay constants for both aqueous and gas phases (k_{dl} and k_{dg}). Thus, to extend the current batch model to a sewer reach model, an accurate estimate of $K_L a$ for flowing wastewater should be a priority as the gas phase model responses were found to be sensitive to this parameter.

To reduce the uncertainty and improve the accuracy of the model predictions, the following recommendations are proposed:

- Develop robust methods to quantify the Henry's law constant for NCl_3 at controlled conditions as the current knowledge on the physico-chemical properties of NCl_3 is limited.
- Improve experimental reproducibility and develop/employ a more robust analytical method for the determination of NCl_3 in aqueous solutions and in wastewater.
- Design and conduct experiments to explore the chemical kinetics of NCl_3 in similar systems as there is lack of knowledge on NCl_3 formation and decomposition in real waters.

The existence of trichloramine (NCl_3) in sewer systems may pose health impacts on workers and may cause corrosion to metal structures. In a swimming pool environment, exposure to NCl_3 has been associated with increasing risks of respiratory symptoms and may promote the development of asthma in children (Chu et al., 2013; Wastensson & Eriksson, 2020). WHO recommended a provisional value of 0.5 mg m^{-3} (approx. 0.1 ppm) for NCl_3 in the atmosphere of swimming pools and similar environments (WHO, 2006), and even lower exposure limits have been proposed in previous studies (Parrat et al., 2012; Chu et al., 2013). However, there is little knowledge on the corrosivity of gaseous NCl_3 , though a previous investigation has reported severe corrosion of stainless steel air strippers caused by NCl_3 (Lowry & Saindon, 2013). To address potential corrosion by NCl_3 , further investigations need to be conducted.

Considering known health impacts of working exposure to NCl_3 and its potential corrosion impact on metal structures, it is recommended that municipalities develop bylaws to control chlorine-bearing wastewaters that are discharged to the sewer systems. Furthermore, on-site treatment of chlorine-based wastewater prior to discharge is recommended.

Considering the cross-sensitivity of the chlorine gas sensor employed in the municipal sewer system, it should be made aware that the gas concentrations reported by the sensor do not likely represent the true concentrations of NCl_3 or free chlorine species (e.g. HOCl) in the headspace. In some conditions, the mixture of both groups of chlorine substances may be present especially when the chlorine-containing wastewater is mixed with an existing water at a Cl:N mass ratio that exceeded 14:1.

Overall, this research was the first to model the temporal response of NCl_3 in a wastewater-air system with values of model parameters estimated empirically and experimentally under controlled conditions. The model successfully incorporated the liquid-gas mass transfer process for NCl_3 and its chemical decay process in both liquid and gas phases. Since there is a lack of knowledge on the chemical kinetics of NCl_3 in wastewater and in the air, the data collected in this study provides a reference for future studies.

References

- Adam, L. C., Gordon, G. 1999. Hypochlorite Ion Decomposition: Effects of Temperature, Ionic Strength, and Chloride Ion. *Inorganic Chemistry* 38 (6), 1299-1304.
- Adam, L.C., Fabian, I., Suzuki, K., Gordon, G. 1992. Hypochlorous Acid Decomposition in the pH 5-8 Region. *Inorganic Chemistry*. 31 (17), 3534–41.
- Afifi, M. Z. and Blatchley, E. R. 2015. Seasonal dynamics of water and air chemistry in an indoor chlorinated swimming pool. *Water research* 68, 771-783.
- Aieta, E. M. and Roberts, P. V. 1983. Disinfection with Chlorine and Chlorine Dioxide. *Journal of Environmental Engineering* 109 (4), 783-799.
- Aieta, E. M. and Roberts, P. V. 1986. Application of mass-transfer theory to the kinetics of a fast gas-liquid reaction: chlorine hydrolysis. *Environmental science & technology* 20 (1), 44-50.
- American Public Health Association (APHA). 2021. *Standard Methods for the Examination of Water and Wastewater* (23rd ed.). American Water Works Association, Water Environment Federation, Washington, D.C.
- ASTM International. 2017. Standard Test Method for Determination of Dissolved Alkali and Alkaline Earth Cations and Ammonium in Water and Wastewater by Ion Chromatography. <https://www.astm.org/d6919-17.html>
- Benjamin, M. M. and Lawler, D. F. 2013. *Water quality engineering physical/chemical treatment processes*. John Wiley & Sons, Hoboken, N.J.
- Blatchley III, E.R., Johnson, R.W., Alleman, J.E., McCoy, W.F. 1992. Effective Henry's Law Constants for Free Chlorine and Free Bromine. *Water Research (Oxford)*. 26, 99–106.
- Busch, M., Simic, N., Ahlberg, E. 2019. Exploring the mechanism of hypochlorous acid decomposition in aqueous solutions. *Physical Chemistry Chemical Physics* 21 (35), 19342-19348.
- Chaturvedi, M. K. M., Langote, S. D., Kumar, D., Asolekar, S. R. 2014. Significance and estimation of oxygen mass transfer coefficient in simulated waste stabilization pond. *Ecological engineering*. 73, 331-334.
- Chen, W. and Jensen, J. N. 2001. Effect of Chlorine Demand on the Ammonia Breakpoint Curve: Model Development, Validation with Nitrite, and Application to Municipal Wastewater. *Water Environment Research* 73 (6), 721-731.
- Chou, J. 2000. A practical guide to hazardous gas monitors. *Occupational Hazards* 62 (9), 61-66.
- Chowdhury, S., Alhooshani, K., Karanfil, T. 2014. Disinfection byproducts in swimming pool: Occurrences, implications and future needs. *Water research* 53, 68-109.
- Chu, T., Cheng, S., Wang, G., Tsai, S. 2013. Occupational exposures of airborne trichloramine at indoor swimming pools in Taipei. *Science of The Total Environment* 461-462, 317-322.

- Corsi, R. L., Chang, D. P. Y., Schroeder, E. D. 1992. A modeling approach for VOC emissions from sewers. *Water Environment Research* 64 (5), 734-741.
- De Laat, J., Feng, W., Freyfer, D. A., Dossier-Berne, F. 2011. Concentration levels of urea in swimming pool water and reactivity of chlorine with urea. *Water research* 45 (3), 1139-1146.
- Deacon, E. L. 1977. Gas transfer to and across an air-water interface. *Tellus* 29 (4), 363-374.
- Deborde, M. and von Gunten, U. 2008. Reactions of chlorine with inorganic and organic compounds during water treatment—Kinetics and mechanisms: A critical review. *Water research* 42 (1), 13-51.
- Devi, P. and Dalai, A. K. 2021. Implications of breakpoint chlorination on chloramines decay and disinfection by-products formation in brine solution. *Desalination* 504, 114961.
- Dhaliwal, B. S. and Baker, R. A. 1983. Role of Ammonia-N in Secondary Effluent Chlorination. *Water Pollution Control Federation* 55 (5), 454-456.
- Gasser, J. A. 1984. Disinfection of Nitrified Effluents. *Water Pollution Control Federation* 56 (4), 386-387.
- Gérardin, F., Cloteaux, A., Guillemot, M., Faure, M., André, J.,C. 2013. Photocatalytic Conversion of Gaseous Nitrogen Trichloride into Available Chlorine - Experimental and Modeling Study. *Environmental science & technology* 47 (9), 4628-4635.
- Gérardin, F., Cloteaux, A., Midoux, N. 2015. Modeling of variations in nitrogen trichloride concentration over time in swimming pool water. *Process Safety and Environmental Protection* 94, 452-462.
- Gordon, J. H. 1985. The Effect of Ammonia in Effluent Chlorination. *Water Pollution Control Federation* 57 (1), 101-102.
- Gray, E. T. J., Margerum, D. W., Huffman, R. P. 1978. Chloramine Equilibria and the Kinetics of Disproportionation in Aqueous Solution. In: *Organometals and Organometalloids*, American Chemical Society, 264-277.
- Haas, B. S. and Herrmann, R. 1996. Transport of chlorinated hydrocarbons between sewage and sewer atmosphere. *Water Science and Technology* 34(3-4), 557-564.
- Haas, C. N. and Karra, S. B. 1984. Kinetics of Wastewater Chlorine Demand Exertion. *Water Pollution Control Federation* 56 (2), 170-173.
- Hand, V. C. and Margerum, D. W. 1983. Kinetics and mechanisms of the decomposition of dichloramine in aqueous solution. *Inorganic chemistry* 22 (10), 1449-1456.
- Hebrard, G., Destrac, P., Roustan, M., Huyard, A., Audic, J. M. 2000. Determination of the water quality correction factor α using a tracer gas method. *Water research* 34 (2), 684-689.
- Holmén, K. and Liss, P. 1984. Models for air-water gas transfer: an experimental investigation. *Tellus B: Chemical and Physical Meteorology*.
- Holzwarth, G., Balmer, R. G., Soni, L. 1984b. The fate of chlorine in recirculating cooling towers Field results. *Water research* 18 (11), 1429-1435.

- Holzwarth, G., Balmer, R.G. and Soni, L. 1984a. The fate of chlorine and chloramines in cooling tower: Henry's law constants for flashoff. *Water Research*. 18, 1421–27,
- Jafvert, C.T., Valentine, R.L., 1987. Dichloramine decomposition in the presence of excess ammonia. *Environ. Sci. Technol.* 26, 577-586.
- Jafvert, C.T., Valentine, R.L., 1992. Reaction Scheme for the Chlorination of Ammoniacal Water. *Water Res.* 21, 967-973.
- Judd, S. J. and Black, S. H. 2000. Disinfection by-product formation in swimming pool waters: a simple mass balance. *Water research* 34 (5), 1611-1619.
- Kumar, K., Shinness, R. W., Margerum, D. W. 1987. Kinetics and mechanisms of the base decomposition of nitrogen trichloride in aqueous solution. *Inorg. Chem.* 26 (21), 3430-3434.
- Leaist, D. G. 1986. Absorption of chlorine into water. *Journal of solution chemistry.* 15 (10), 827-838.
- Lee, J. W., Lee, D., Lee, H., Shim, S., Kim, J. H., Lee, C. 2023. Enhanced oxidation of urea by pH swing during chlorination: pH-dependent reaction mechanism. *Water research* 242, 120183.
- Lee, L. T., Wu, T., Boor, B. E., Blatchley, E. R. 2023. Dynamic behavior of gas-phase NCl_3 and CO_2 in indoor pool facilities. *Building and Environment* 233, 110088.
- Li, J. and Blatchley, E. R. 2007. Volatile Disinfection Byproduct Formation Resulting from Chlorination of Organic–Nitrogen Precursors in Swimming Pools. *Environmental science & technology* 41 (19), 6732-6739.
- Lin, C. and Pehkonen, S. O. 1998. Oxidation of elemental mercury by aqueous chlorine (HOCl/OCl^-): Implications for tropospheric mercury chemistry. *Journal of Geophysical Research*, Washington, DC 103, 28093-28102.
- Liu, B., Reckhow, D. A., Li, Y. 2014. A two-site chlorine decay model for the combined effects of pH, water distribution temperature and in-home heating profiles using differential evolution. *Water research* 53, 47-57.
- Lowry, J. and Saindon, L. 2013. Rapid Corrosion of a Stainless Steel Air Stripper by Trichloramine [PowerPoint slides]. Retrieved from <https://static1.squarespace.com/static/65ce67133ff86731b6e969f0/t/663bcf5124839b2dbef50468/1715195732621/ntc-presentation.pdf>
- Mishalanie, E. A., Rutkowski, C. J., Hutte, R. S., Birks, J. W. 1986. Ultraviolet absorption spectrum of gaseous HOCl . *The Journal of physical chemistry* 90 (22), 5578-5584.
- Munz, C. and Roberts, P. V. 1989. Gas- and liquid-phase mass transfer resistances of organic compounds during mechanical surface aeration. *Water research* 23 (5), 589-601.
- Onyutha, C. and Kwio-Tamale, J. 2022. Modelling chlorine residuals in drinking water: a review. *International Journal of Environmental Science and Technology* 19 (11), 11613-11630.

- Palin, A. T. 1957. The Determination of Free and Combined Chlorine in Water by the Use of Diethyl-p-phenylene Diamine. *Journal AWWA* 49 (7), 873-880.
- Palin, A. T. 1968. Determination of Nitrogen Trichloride in Water. *Journal AWWA* 60 (7), 847-851.
- Palin, A. T. 1975. Water disinfection - chemical aspects and analytical control. In: Johnson, J.D. (Ed.), *Disinfection Water and Wastewater*. Ann Arbor Science, Michigan, 67-89.
- Parker, W. J. and Yu, J. 2001. Dynamic Modeling to Assess Worker Exposure to Gas-Phase Volatile Organic Compounds in Collector Sewers. *Water Environment Research* 73 (4), 450-460.
- Parrat, J., Donzé, G., Iseli, C., Perret, D., Tomicic, C., Schenk, O. 2012. Assessment of occupational and public exposure to trichloramine in Swiss indoor swimming pools: A proposal for an occupational exposure limit. *Annals of Occupational Hygiene* 56 (3), 264–277.
- Pressley, T. A., Bishop, D. F., Roan, S. G. 1972. Ammonia-nitrogen removal by breakpoint chlorination. *Environmental science & technology* 6 (7), 622-628.
- Qiang, Z. and Adams, C. D. 2004. Determination of Monochloramine Formation Rate Constants with Stopped-Flow Spectrophotometry. *Environmental science & technology* 38 (5), 1435-1444.
- Rittmann, B.E., Suozzo, R.J., & Romero, B. 1983. Temperature effects on oxygen transfer to rotating biological contactors. *Journal of Water Pollution Control Federation* 55 (3), 270-277.
- Roghani, M., Li, Y., Rezaei, N., Robinson, A., Shirazi, E., Pennell, K. G. 2021. Modeling Fate and Transport of Volatile Organic Compounds (VOCs) Inside Sewer Systems. *Groundwater Monitoring & Remediation* 41 (2), 112-121.
- Saguinsin, L.S., Morris, C.J. 1975. The chemistry of aqueous nitrogen trichloride. In: Johnson, J.D. (Ed.), *Disinfection Water and Wastewater*. Ann Arbor Science, Michigan, 277-299.
- Sander, R. 2023. Compilation of Henry's law constants (version 5.0.0) for water as solvent. *Atmospheric chemistry and physics : ACP*. 23 (19), 10901-12440.
- Schwarzenbach, R. P., Gschwend, P. M., Imboden, D. M. (2017) *Environmental organic chemistry*. Wiley, Hoboken, N.J.
- Sivey, J. D., McCullough, C. E., Roberts, A. L. 2010. Chlorine Monoxide (Cl₂O) and Molecular Chlorine (Cl₂) as Active Chlorinating Agents in Reaction of Dimethenamid with Aqueous Free Chlorine. *Environmental science & technology* 44 (9), 3357-3362.
- Snoeyink, V.L., Jenkins, D., 1980. *Water chemistry*. Wiley, New York.
- Soltermann, F., Canonica, S., von Gunten, U. 2015. Trichloramine reactions with nitrogenous and carbonaceous compounds: Kinetics, products and chloroform formation. *Water research (Oxford)* 71, 318-329.

- Sondossi, M. 2000. Biocides. In Alexander M, Bloom BR, Hopwood DA, Hull R, Iglewski B, Laskin AI, Oliver SG, Schaechter M, Summers WC (eds.). *Encyclopedia of Microbiology, Four-Volume Set* (2 ed.). Academic Press.
- Taras, M. J., Hedgepeth, L. L., Faber, H. A. 1950. Preliminary Studies on the Chlorine Demand of Specific Chemical Compounds. *American Water Works Association* 42 (5), 462-474.
- Tchobanoglous, G., Stensel, H. D., Tsuchihashi, R., Burton, F. L. 2014. *Wastewater engineering: treatment and resource recovery*. Fifth edition. McGraw-Hill Education, New York.
- Valentine, R. L. and Jafvert, C. T. 1988. General acid catalysis of monochloramine disproportionation. *Environmental science & technology* 22 (6), 691-696.
- Valentine, R. L., Brandt, K. I., Jafvert, C. T. 1986. A spectrophotometric study of the formation of an unidentified monochloramine decomposition product. *Water research* 20 (8), 1067-1074.
- Valentine, R. L., Jafvert, C. T., Leung, S. W. 1988. Evaluation of a chloramine decomposition model incorporating general acid catalysis. *Water research* 22 (9), 1147-1153.
- Vikesland, P. J. and Valentine, R. L. 2002. Modeling the Kinetics of Ferrous Iron Oxidation by Monochloramine. *Environmental science & technology* 36 (4), 662-668.
- Vikesland, P.J., Ozekin, K., Valentine, R.L., 2001. Monochloramine Decay in Model and Distribution System Waters. *Water Res.* 35, 1766-1776.
- Wang, T. X., and Margerum, D. W. 1994. Kinetics of Reversible Chlorine Hydrolysis: Temperature Dependence and General-Acid/Base-Assisted Mechanisms. *Inorganic Chemistry*, 33(6), 1050–1055.
- Wastensson, G. and Eriksson, K. 2020. Inorganic chloramines: a critical review of the toxicological and epidemiological evidence as a basis for occupational exposure limit setting. *Critical reviews in toxicology* 50 (3), 219–271.
- Weil, I. and Morris, J. C. 1949. Kinetic Studies on the Chloramines. I. The Rates of Formation of Monochloramine, N-Chlormethylamine and N-Chlordimethylamine. *Journal of the American Chemical Society* 71 (5), 1664-1671.
- Weng, S. and Blatchley, E. R. 2011. Disinfection by-product dynamics in a chlorinated, indoor swimming pool under conditions of heavy use: National swimming competition. *Water research* 45 (16), 5241-5248.
- Weng, S., Li, J., Blatchley, E. R. 2012. Effects of UV254 irradiation on residual chlorine and DBPs in chlorination of model organic-N precursors in swimming pools. *Water research* 46 (8), 2674-2682.
- Weng, S.-C., Weaver, W.A., Zare Afifi, M., Blatchley, T.N., Cramer, J.S., Chen, J., Blatchley III, E.R., 2011. Dynamics of gas-phase trichloramine (NCl₃) in chlorinated, indoor swimming pool facilities. *Indoor Air*. 21, 391-399.

Wojtowicz, J.A. 2004. Dichlorine Monoxide, Hypochlorous Acid, and Hypochlorites. In Kirk-Othmer Encyclopedia of Chemical Technology, (Ed.).

World Health Organization (WHO). 2006. Swimming pools and similar environments. Guidelines for safe recreational water environments, vol. 2. Geneva, Switzerland.

Wu, T., Földes, T., Lee, L. T., Wagner, D. N., Jiang, J., Tasoglou, A., Boor, B. E., Blatchley, E. R. I.,II 2021. Real-Time Measurements of Gas-Phase Trichloramine (NCl₃) in an Indoor Aquatic Center. *Environmental science & technology* 55 (12), 8097-8107.

Yi, W. Y., Lo, K. M., Mak, T., Leung, K. S., Leung, Y., Meng, M. L. 2015. A survey of wireless sensor network based air pollution monitoring systems. *Sensors (Basel, Switzerland)* 15 (12), 31392-31427.

Appendices

A. 1. Procedures for preparing stock solutions

Oxygen-free reagent water:

Purge helium into ultrapure water for at least 30 minutes.

Sodium hypochlorite (NaOCl):

Dilute sodium hypochlorite (5% available chlorine) to 400 mg/L as Cl₂ and stored in aluminum foil-covered bottles. Standardize it regularly by DPD/FAS titration prior to experiments. The density of 5% NaOCl solution is 1.093 g/mL at 20 °C.

Ammonium chloride (NH₄Cl):

The target concentration is 805 mg/L NH₄. Dissolve 1196.1 mg NH₄Cl (MW 53.49 g·mol⁻¹) in 500 mL reagent water.

Use the stock solution to prepare test solutions:

Molar ratio Cl to N	Mass ratio Cl to N	Dilution time	Volume of stock required (mL) per 500 mL
6.31:1	16.0:1	25.0	20.0
5.53:1	14.0:1	21.9	22.8
4.74:1	12.0:1	18.8	26.6
3.94:1	10.0:1	15.6	32.0
3.15:1	7.98:1	12.5	40.0
1.79:1	4.6:1	7.14	70.0

Stock buffer solution at pH 6.5:

Dissolve 8.6 g anhydrous Na₂HPO₄ and 19 g anhydrous KH₂PO₄ in reagent water. Combine with 100 mL reagent water in which 400 mg disodium ethylenediamine tetraacetate dihydrate (EDTA) have been dissolved. Dilute to 1 L with reagent water, so the phosphate concentration will be around 0.2 M.

Stock buffer solution at pH 7.0:

Dissolve 18 g anhydrous Na_2HPO_4 and 10 g anhydrous KH_2PO_4 in reagent water. Combine with 100 mL reagent water in which 400 mg disodium ethylenediamine tetraacetate dihydrate (EDTA) have been dissolved. Dilute to 1 L with reagent water, so the phosphate concentration will be around 0.2 M.

Stock buffer solution at pH 7.5:

Dissolve 23 g anhydrous Na_2HPO_4 and 3.2 g anhydrous KH_2PO_4 in reagent water. Combine with 100 mL reagent water in which 400 mg disodium ethylenediamine tetraacetate dihydrate (EDTA) have been dissolved. Dilute to 1 L with reagent water, so the phosphate concentration will be around 0.2 M. When preparing for the chlorine test, dilute 100 mL stock buffer into 250 mL. The final concentration will be 0.08 M.

A. 2. Calibration curve development

A calibration curve for free/total chlorine analysis for Phase I was developed by plotting absorbance read from the spectrophotometer at 515 nm against concentration measured from DPD/FAS titration (Standard Method 4500-Cl F; **Figure A-1**). Linear regression was performed in the range from 0.5-3.5 mg/L. Thus, an equation expressing the relationship between absorbance at 515 nm and chlorine concentration was obtained, as indicated in **Figure A-1**. Using the DPD spectrophotometry method reduced the duration of each analysis that would be done by DPD titration.

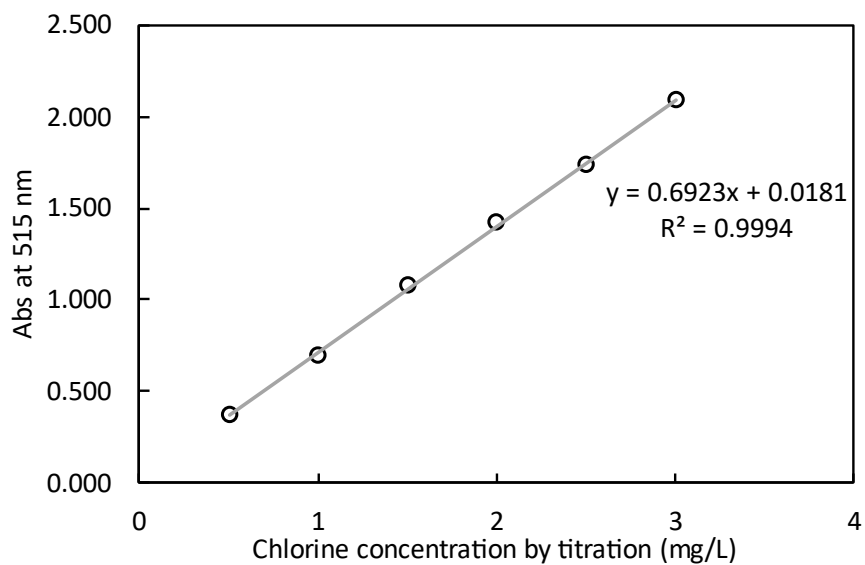


Figure A-1 Calibration curve obtained by DPD titration and DPD spectrophotometry using Hach DR1900. Circles are measured results and the grey line is resulted from linear regression of the analytical results.

A. 3. Unit conversions

According to the ideal gas law,

$$PV = nRT$$

thus,

$$V = \frac{nRT}{P}$$

solve volume per mole of gas at 1 atm, 20 °C,

$$V = \frac{1.00\text{mol} \times 0.08206 \frac{\text{L} \cdot \text{atm}}{\text{mol} \cdot \text{K}} \times 293.15\text{K}}{1.00\text{atm}} = 24.1 \text{ L}$$

At 15°C and 40°C, the volume per mole of gas is 23.6 L and 25.7 L, respectively.

To convert gas concentrations from mg/L to ppm (v/v) at 1 atm, 20 °C:

$$1 \frac{\text{mg}}{\text{L}} = 1 \frac{\text{mg}}{\text{L}} \times 10^{-3} \times \frac{24.1 \frac{\text{L}}{\text{mol}}}{35.45 \frac{\text{g}}{\text{mol}}} \times 10^6 = 678.6 \text{ ppm}$$

A. 4. Parameter estimation

Experimental results for estimating $K_L a$ for oxygen at 20°C

The lumped overall mass transfer coefficient ($K_L a^{O_2}$) was estimated from each of the four experimental runs by non-linear regression of the oxygen transfer model (**Figure A-2**). The least squares method was used for the regression analysis and the test results were summarised in **Table A-2**. All the estimated values were significant at α of 0.05.

Table A-2 Regression results for the oxygen transfer model.

Experiment#	Parameter	Values
1	Cs	7.987
	KLa	7.327
2	Cs	7.580
	KLa	4.099
3	Cs	8.162
	KLa	5.434
4	Cs	8.189
	KLa	6.733

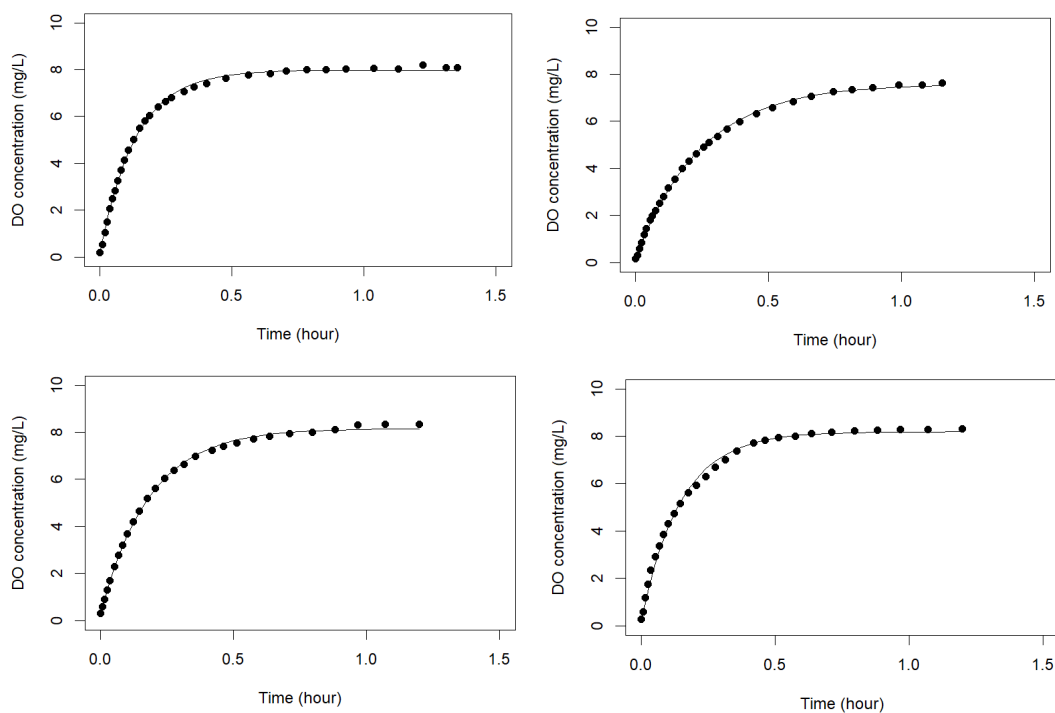


Figure A-2 Non-linear regression plots for four replicated tests estimating $K_L a^{O_2}$ at 20°C. Dots are measured data. Lines are lines of best fit from the regression model as described in Chapter 3.

Molar volumes for inorganic substances

Molar volumes (V_s) were estimated by summation of atomic volumes of all elements in a compound. The reported values of atomic volumes vary among studies resulting in different molar volumes calculated for HOCl, NH₂Cl, NHCl₂ and NCl₃ (**Table A-3**). In Wilke and Chang (1955), atomic volumes for inorganic nitrogen were absent, thus the molar volumes for inorganic chloramines were not able to be obtained. The method of Abraham and McGowan (1987) was designed for estimating molar volumes of complex organic molecules thus is unlikely to be applicable for simple inorganic substances. In contrast, although Fuller et al. (1966) provided diffusion volume increments applied to organic molecules, but “it would be possible to estimate volumes [of simple gases] by summing increments as before” (Fuller et al., 1966). Therefore, the method of Fuller et al. (1966) was selected for estimating molar volumes for the inorganic chlorine compounds. Lastly, it should be made aware of the uncertainty in estimation of molar volumes that were used for estimating diffusion coefficients and thus mass transfer coefficients for these compounds.

Table A-3 Summary of reported and calculated molar volumes (cm³ mol⁻¹) for inorganic substances from different sources and methods.

Substances	Abraham and McGowan (1987)	Wilke and Chang (1955; referred as “Le Bas volume”)	Heusler and Van Dien (1982)	Fuller, Schettler, and Giddings (1966)
O ₂	18.3 ^a	25.6	28	16.6
Cl ₂	35.34 ^a	48.4	39.8	37.7 ^b
HOCl	28.97 ^a	35.7 ^a	-	26.96 ^{a b}
NH ₂ Cl	33.08 ^a	42.5 ^{a c}	-	29.15 ^{a b}
NHCl ₂	45.32 ^a	64.9 ^{a c}	-	46.67 ^{a b}
NCl ₃	57.56 ^a	85.8 ^{a c}	-	64.19 ^{a b}

a Values calculated by summing atomic diffusion volume increments used in the corresponding study.

b Uncertain values indicated by the authors due to small numbers of data.

c Values calculated using nitrogen atomic volume for primary amines for NH₂Cl and secondary amines for NHCl₂ and NCl₃, respectively.

Dynamic viscosities of water at 15°C and 20°C

According to Rumble (2018) experimentally determined dynamic viscosity of water at 20°C is 1.0016 cP. The experimental determined value at 15°C is not available in that source, and thus, was calculated using the semi-empirical Vogel-Fulcher-Tammann equation (Viswanath et al., 2007),

$$\eta = \eta_0 \cdot e^{\frac{\alpha}{T-T_0}}$$

where η_0 and α are empirical material-dependent parameters, and T_0 is also an empirical fitting parameter. For water, η_0 is 0.02939 mPa·s; α is 507.88 K; T_0 is 149.39 K (Viswanath et al., 2007). Therefore, the value of dynamic viscosity of water at 15°C was calculated to be 1.1396 cP.

Diffusion coefficients for chlorine compounds

Table A-4 Diffusion coefficients ($\text{cm}^2 \text{s}^{-1}$) for substances of interest at 15°C and 20°C.

Substance	Molar volume, $\text{cm}^3 \text{mol}^{-1}$	Diffusion coefficient, $\text{cm}^2 \text{s}^{-1}$	
		15°C / 288.15 K	20°C / 293.15 K
O2	25.6	1.83E-05	2.12E-05
Cl2	48.4	1.25E-05	1.45E-05
HOCl	27.0	1.77E-05	2.05E-05
NH2Cl	29.2	1.69E-05	1.96E-05
NHC2	46.7	1.28E-05	1.48E-05
NCI3	64.2	1.05E-05	1.22E-05

A. 5. Test results for Phase I

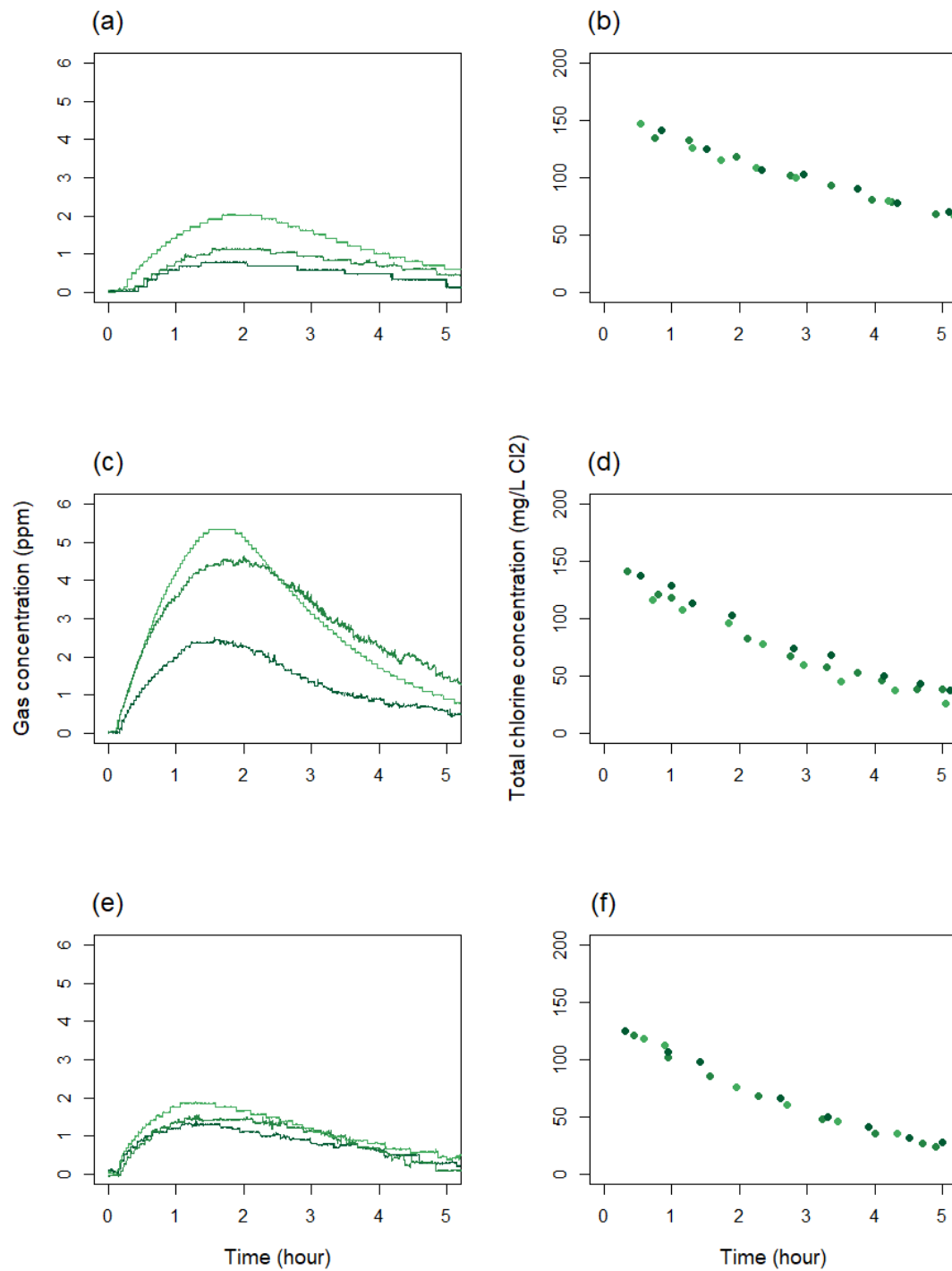


Figure A-3 Chlorine-alone test results at a dose of 400 mg/L as Cl₂ NaOCl solution at 20 °C pH 6.5 (a, b), 7.0 (c, d) and 7.5 (e, f) with three replicates at each condition.

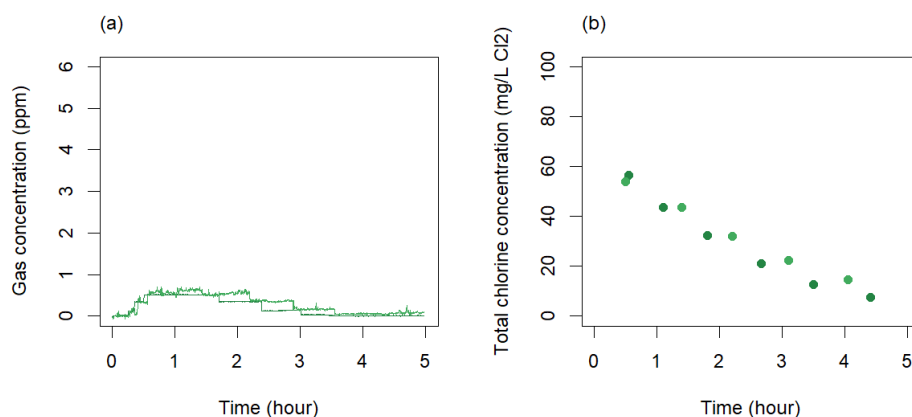


Figure A-4 Chlorine-alone test results at a dose of 200 mg/L as Cl₂ NaOCl solution at 20 °C pH 7.5 with two replicates.

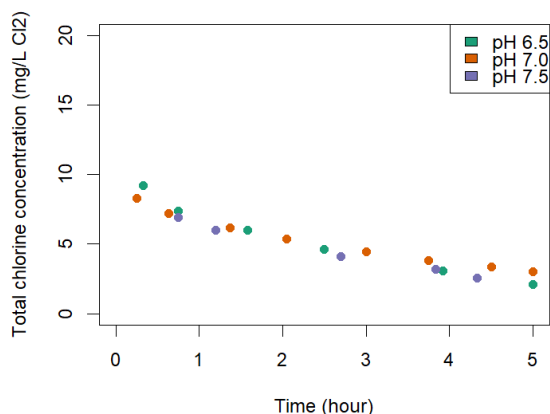


Figure A-5 Chlorine-alone test results at a dose of 40 mg/L as Cl₂ NaOCl solution at 20 °C pH 6.5, 7.0 and 7.5.

Discussion

The effect of free chlorine dose on the gas-phase responses was assessed. The gas-phase response at a free chlorine dose of 200 mg/L as Cl₂ and 20°C showed a similar trend as that at a dose of 400 mg/L as Cl₂, while at a dose of 40 mg/L as Cl₂ no measurable gas was observed. At a chlorine dose of 200 mg/L as Cl₂, 20°C and pH 7.5, the average C_p was 0.55 ppm (**Figure A-4**), versus 1.4 ppm at the dose of 400 mg/L as Cl₂. The average t_p was 1.18 hr, lower than that at the dose of 400 mg/L as Cl₂. At a free chlorine dose of 40 mg/L as Cl₂ and pH 6.5-7.5, no gas was detected and the aqueous phase data is included in **Figure A-5**. The observed free chlorine concentrations were all lower than 10 mg/L as Cl₂, suggesting at

this level of free chlorine in solution the sensor was not able to detect any gas in the headspace of the batch system. These results were in contrast with what was observed at a higher dose, i.e. 400 mg/L as Cl₂, suggesting one-time dosage of free chlorine solution might be an important factor affecting the gas phase response.

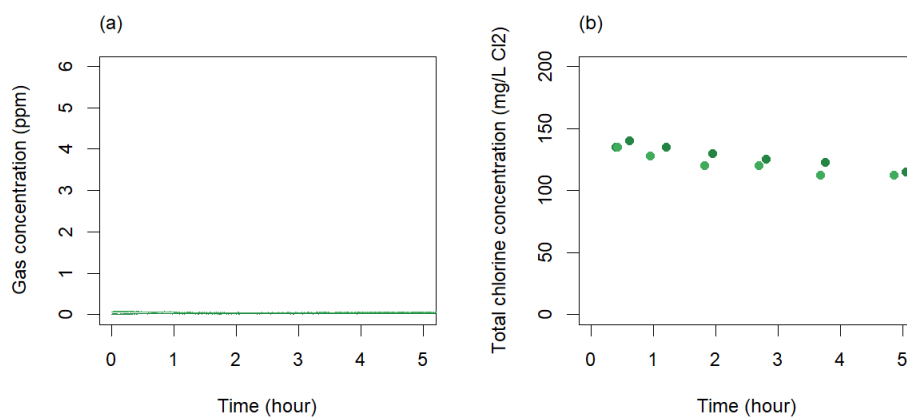


Figure A-6 Chlorine-alone test results at 15°C pH 6.5 at a dose of 400 mg/L as Cl₂ NaOCl solution.

The effect of temperature on the gas-phase responses was also assessed. At 15°C at a free chlorine dose of 400 mg/L as Cl₂ and pH 6.5, no detectable gas was reported by the gas sensor (**Figure A-6**). Upon inspection of the aqueous concentration data, the free chlorine decay process seemed to be much slower than that at 20°C under the same condition, and relatively high levels of free chlorine were available in the solution for a longer time (**Figure A-6**), which would cause higher concentration in the gas phase. However, no measurable gas was reported by the sensor, which was likely to be attributed to the decrease in mass transfer rate coefficient of the system.

A. 6. Test results for Phase II

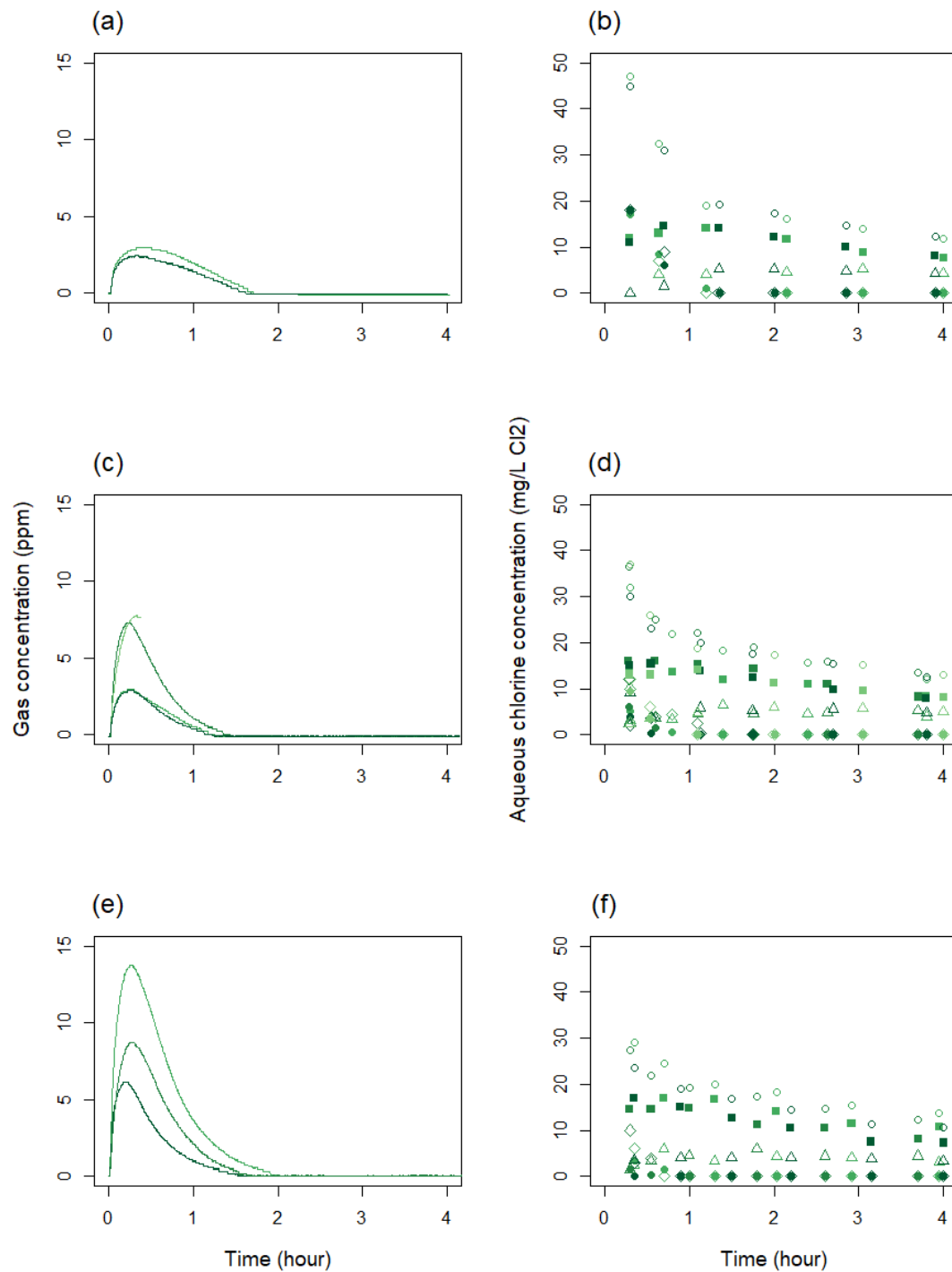


Figure A-7 Chlorine-ammonia test results at a dose of 400 mg/L as Cl₂ NaOCl solution at 20 °C and pH 6.5 with Cl:N mass ratios of 16:1 (a, b), 14:1 (c, d) and 12:1 (e, f). Replicates at each condition were indicated as a series of green colours. Circles are total chlorine; squares are monochloramine; triangles are dichloramine; diamonds are trichloramine; filled circles are free chlorine.

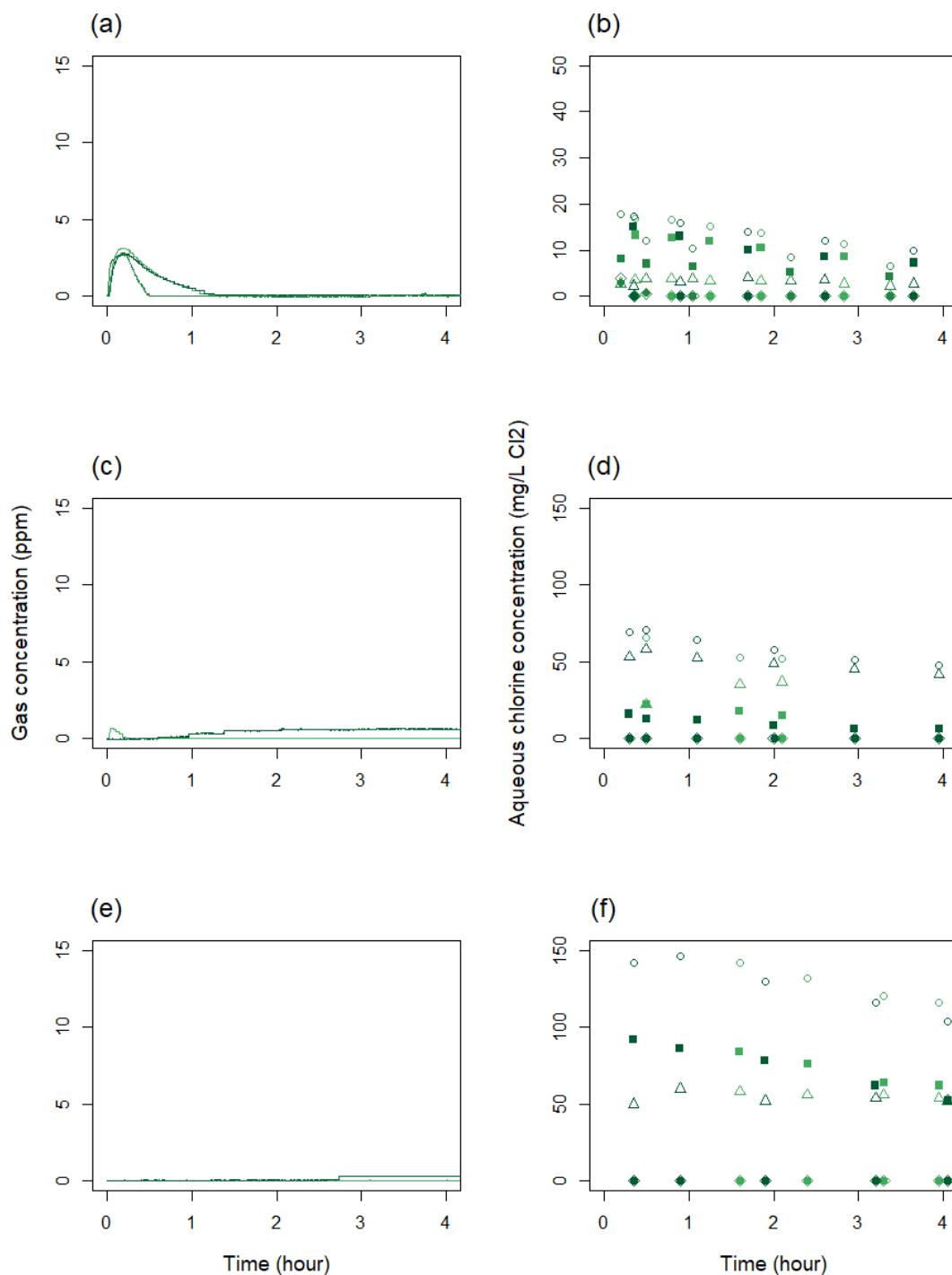


Figure A-8 Chlorine-ammonia test results at a dose of 400 mg/L as Cl₂ NaOCl solution at 20 °C and pH 6.5 with Cl:N mass ratios of 10:1 (a, b), 8.0:1 (c, d) and 4.6:1 (e, f). Replicates at each condition were indicated as a series of green colours. Circles are total chlorine; squares are monochloramine; triangles are dichloramine; diamonds are trichloramine; filled circles are free chlorine.

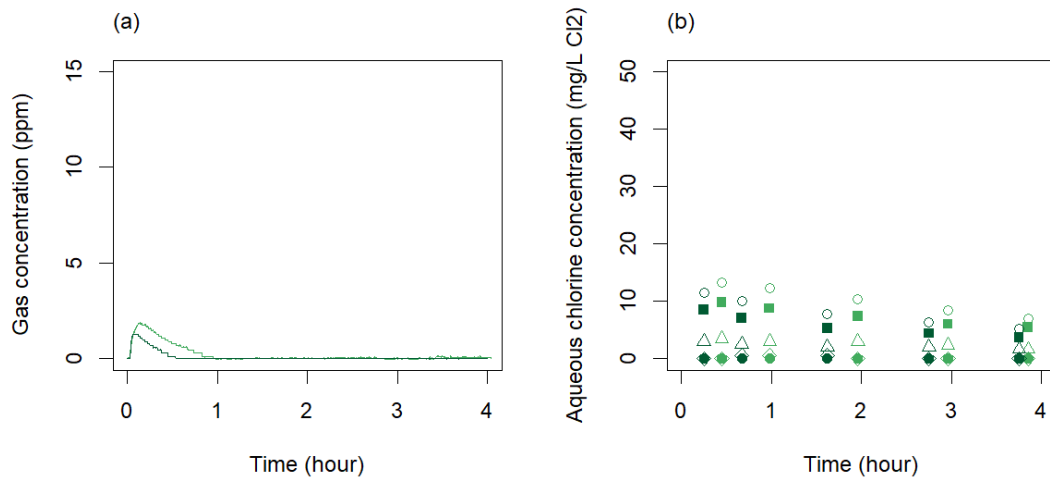


Figure A-9 Chlorine-ammonia test results at a dose of 400 mg/L as Cl₂ NaOCl solution at a Cl:N mass ratio of 10:1 at pH 7.0 and 20 °C with two replicates. Circles are total chlorine; squares are monochloramine; triangles are dichloramine; diamonds are trichloramine; filled circles are free chlorine.

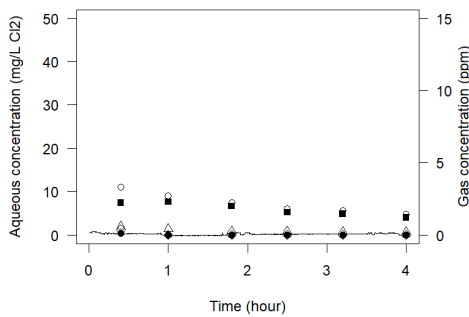


Figure A-10 Chlorine-ammonia test results at a dose of 400 mg/L as Cl₂ NaOCl solution at a Cl:N mass ratio of 10:1, pH 7.5 and 20 °C. Circles are total chlorine; squares are monochloramine; triangles are dichloramine; diamonds are trichloramine; filled circles are free chlorine.

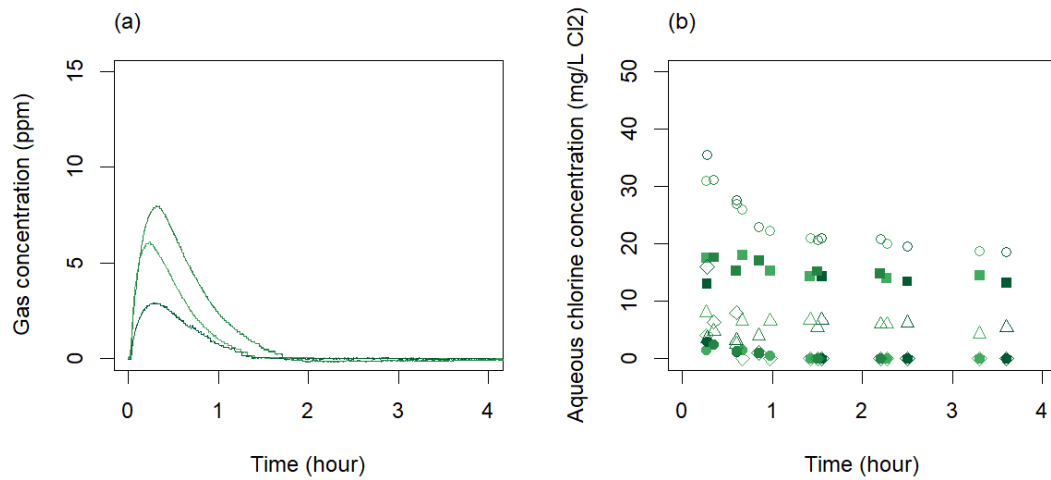


Figure A-11 Chlorine-ammonia test results at a dose of 400 mg/L as Cl₂ NaOCl solution at a Cl:N mass ratio of 12:1, 15 °C and pH 6.5 with two replicates. Circles are total chlorine; squares are monochloramine; triangles are dichloramine; diamonds are trichloramine; filled circles are free chlorine.

A. 7. Test results for Phase III

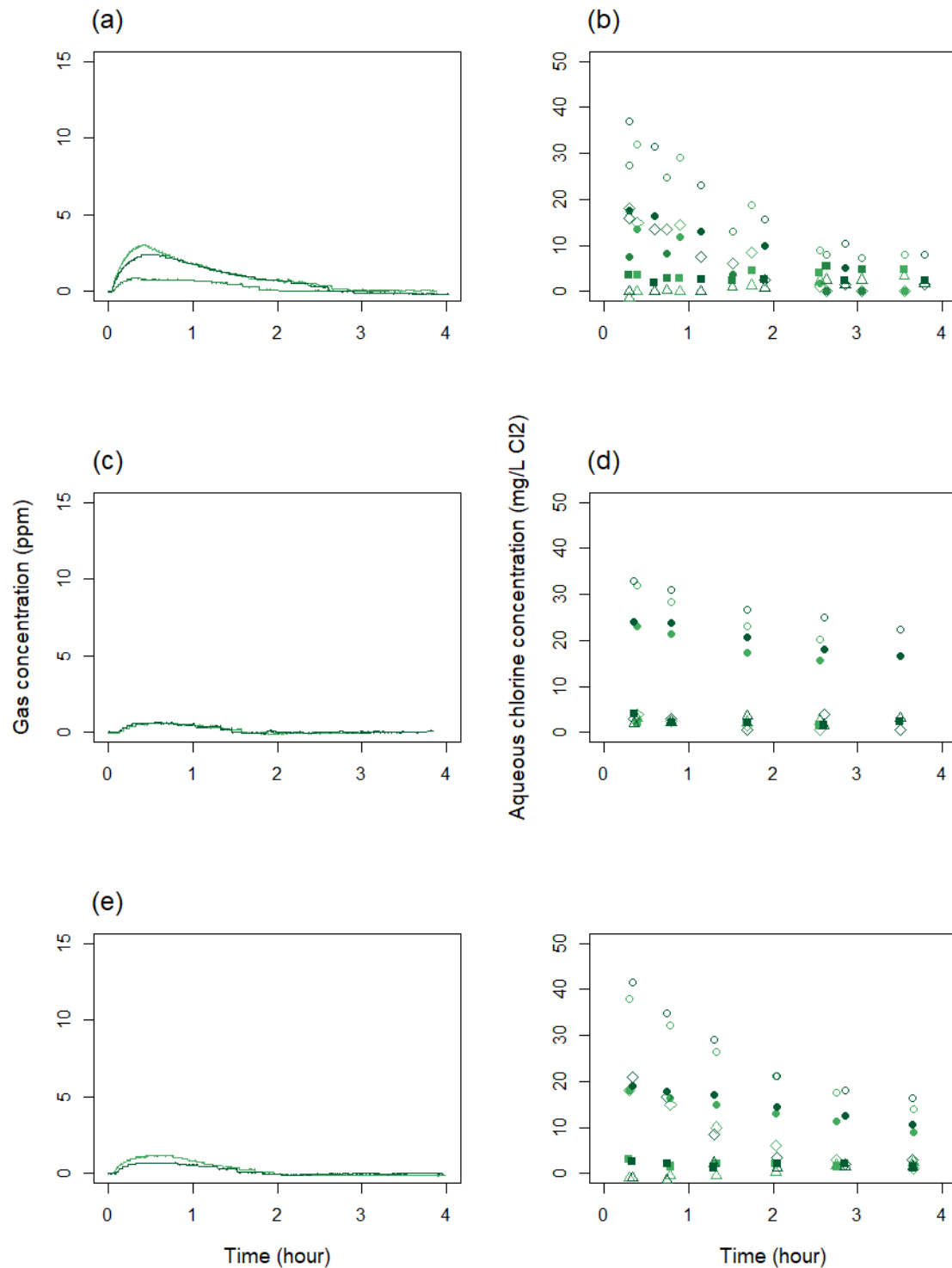


Figure A-12 Chlorine-wastewater test results at a dose of 400 mg/L as Cl₂NaOCl solution with the Cl:N mass ratio of ~12:1 at (a, b) pH 6.5 and 20°C, (c, d) pH 7.5 and 20°C, and (e, f) pH 6.5 and 15°C. Circles are total chlorine; squares are monochloramine; triangles are dichloramine; diamonds are trichloramine; filled circles are free chlorine

A. 8 Wastewater characterization in Phase III

Test results presented in Chapter 4 Phase III were produced from one batch of sampled wastewater whose characteristics are included in **Table A-5**. As the ammonia concentration in the raw wastewater was too high to expect measurable gas reported from the sensor when dosing the same amount of free chlorine as in Phase II, the wastewater was diluted prior to testing. In the diluted wastewater, the ammonia concentration was 34.4 ± 0.5 mg/L $\text{NH}_4\text{-N}$, yielding a Cl:N ratio of 11.6:1 when a free chlorine dose of 400 mg/L as Cl_2 was employed, which was within the range of Cl:N ratios tested in Phase II where a measurable gas were reported. Thus, all the results presented in Chapter 4 Phase III are around a Cl:N ratio of 11.6:1.

Table A-5 Characteristics of filtered raw wastewater.

Water parameter, Unit	Value
Total organic carbon, mg/L	63.7
Alkalinity, mg/L as CaCO_3	470
Ammonia, mg/L N	57.4
Nitrate, mg/L N	1.47
Chloride, mg/L Cl	352

A. 9 Sensor cross-sensitivity data

A data sheet of cross-sensitivity with other gases has been provided by the sensor manufacturer:

Cross Sensitivity Data		
Gas Applied	Concentration Applied	Cross Sensitivity
ACETONE	1,000 ppm	0 ppm
ACETYLENE	100 ppm	0 ppm
ACRYLONITRILE	1,000 ppm	0 ppm
METHYL ALCOHOL	100 ppm	0 ppm
ETHYL ALCOHOL	100 ppm	0 ppm
AMMONIA	25 ppm	-3 ppm
BENZENE	50 ppm	0 ppm
BUTADIENE	2,000 ppm	0 ppm
CARBON DIOXIDE	10,000 ppm	0 ppm
CARBON MONOXIDE	100 ppm	0 ppm
CARBONYL SULFIDE	50 ppm	0 ppm
ETHYLENE	20 ppm	0 ppm
ETHYLENE OXIDE	100 ppm	0 ppm
ETHYL ETHER	100 ppm	0 ppm
FREON 22	1000 ppm	0 ppm
FREON 404A	2000 ppm	0 ppm
HEXANE	10,000 ppm	0 ppm
HYDROGEN	500 ppm	0 ppm
HYDROGEN CHLORIDE	40 ppm	4 ppm
HYDROGEN CYANIDE	35 ppm	0 ppm
HYDROGEN SULFIDE	40 ppm	-1 ppm
ISOBUTANE	100 ppm	0 ppm
ISOBUTYLENE	100 ppm	1 ppm
METHANE	10,000 ppm	0 ppm
METHYL MERCAPTAN	50 ppm	-0.4 ppm
ETHYL MERCAPTAN	30 ppm	3 ppm
NITROGEN OXIDE	5 ppm	0 ppm
NITROGEN DIOXIDE	5 ppm	7 ppm
NITRIC OXIDE	100 ppm	0 ppm
SULFUR DIOXIDE	10 ppm	-0.2 ppm

Retrieved [September 11, 2024] from

<https://us.msasafety.com/p/000070001800001133?locale=en§ion=literature#>

A. 10 References

Abraham, M.H. and McGowan, J.C. 1987. The use of characteristic volumes to measure cavity terms in reversed phase liquid chromatography. *Chromatographia* 23 (4), 243–246.

Heusler, K. E. and Van Dien, N. 1982. Partial molal volumes of halogens in aqueous electrolyte solutions. *Electrochimica Acta* 27 (1), 79-82.

Rumble, John R., ed. (2018). *CRC Handbook of Chemistry and Physics* (99th ed.). Boca Raton, FL: CRC Press. ISBN 978-1-138-56163-2.

Sander, R. 2023. Compilation of Henry's law constants (version 5.0.0) for water as solvent. *Atmospheric chemistry and physics : ACP*. 23 (19), 10901-12440.

Viswanath, D. S., Dutt, N. V. K., Ghosh, T. K., Prasad, D. H. L., Rani, K. Y. 2007. *Viscosity of Liquids: Theory, Estimation, Experiment, and Data*. Springer-Verlag, Dordrecht.

Wilke, C. R. and Chang, P. 1955. Correlation of diffusion coefficients in dilute solutions. *AIChE Journal* 1 (2), 264-270.